THE ROLE OF MITOCHONDRIAL ANTIOXIDANT ENZYME SUPEROXIDE DISMUTASE 2 (SOD2) IN PLURIPOTENCY AND DIFFERENTIATION

by

Emma L. Martell

Submitted in partial fulfillment of the requirements
for the degree of Master of Science

at

Dalhousie University
Halifax, Nova Scotia
July 2019

TABLE OF CONTENTS

LIST OF TABLES

LIST OF FIGURES

ABSTRACT

The mitochondrial antioxidant enzyme superoxide dismutase 2 (SOD2) is important for maintaining mitochondrial integrity and keeping the levels of reactive oxygen species (ROS) low. Small populations of poorly-differentiated cells with stem-like properties, termed cancer stem-like cells (CSLCs), have been identified in tumor masses and play an important role in chemoresistance and cancer recurrence. The purpose of this study was to examine the role of SOD2 in CSLCs. Using several models of CSLCs including: embryonal CSLCs, breast CSLCs (BCSLCs), and patient-derived brain tumor-initiating cells (BTICs), it was found that silencing of SOD2 inhibits the expression of stemness-maintaining pluripotency factors. Furthermore, the comparison of CSLCs with their non-stem like counterparts revealed that CSLCs harbor drastically higher levels of SOD2. Further mechanistic analysis demonstrated that SOD2 depletion promotes apoptosis and induces differentiation in CSLCs. In conclusion, CSLCs appear to rely on SOD2 expression for maintaining their stem-like features.

LIST OF ABBREVIATIONS AND SYMBOLS USED

ADP	Adenosine diphosphate
Anti-Anti	Antibiotic-Antimycotic
APAF-1	Apoptotic protease activating factor
APL	Acute promyelocytic leukemia
ATCC	American Type Culture Collection
ATP	Adenosine triphosphate
ATRA	All-trans retinoic acid
BCSLCs	Breast cancer stem-like cells
bFGF	Basic transforming growth factor
BMP	Bone morphogenic protein
BrPA	Bromopyruvic acid
BSA	Bovine serum albumin
BTICs	Brain tumor-initiating ells
CO_2	Carbon dioxide
CQ	Chloroquine
CSLCs	Cancer stem-like cells
Cu-Zn	Copper-Zinc
DMEM	Dulbecco's Modified Eagle's Medium
DCF	2',7'-dichlorofluorescein
ECCs	Embryonal carcinoma cells
ECL	Electrochemiluminescence
ECM	Extracellular matrix
EGF	Epidermal growth factor
EMT	Epithelial-to-mesenchymal transition
ECSLC	Embryonal carcinoma stem-like cells
ETC	Electron transport chain
$FADH_2$	Flavin adenine dinucleotide
FBS	Fetal bovine serum
GBM	Glioblastoma
GPx	Glutathione peroxidase

GSH	Glutathione
H^+	Hydrogen proton
H2-DCFDA	2',7'-dichlorodihydrofluorescein
H_2O_2	Hydrogen peroxide
HCQ	Hydroxychloroquine
HEPES	4-(2-hydroxyethyl)-1-piperazineethanesulfonic acid
HMLE	Human mammary epithelial cells
HMLER	HMLE-Ras transformed
$HMLER^{shECad}$	HMLER shRNA silencing of E-Cadherin
HRP	Horse radish peroxidase
iPSC	Induced pluripotent stem cells
LC3-II	LC3-PE
MAP1/LC3	Microtubule-associated protein 3 light chain 1
MAPK	Mitogen-activated protein kinase
MFI	Mean fluorescent intensity
Mn	Manganese
MOMP	Mitochondria outer membrane pore
MS	Mass spectrometry
MTOR	Mammalian target of rapamycin
NAD^+	Nicotinamide adenine dinucleotide
NADH	Nicotinamide adenine dinucleotide-Hydrogen
NEAAs	Non-essential amino acids
$NO^{\bullet}$	Nitric oxide
$^{\bullet}OH$	Hydroxyl radical
$O_2^{\bullet-}$	Superoxide anion
$O_2^{2\cdot}$	Peroxide
PARP	Poly (ADP-ribose) polymerase
PBS	Phosphate buffered saline
PBST	Phosphate buffered saline-Tween
PE	phosphatidylethanolamine
PDAC	Pancreatic ductal adenocarcinoma

PI3K	Phosphatidylinositol kinase
PI3K-III	Phosphatidylinositol kinase class III
PML	Promyelocytic leukemia gene
PML-RARα	PML-retinoic acid receptor-α fusion gene
qRT-PCR	Quantitative real-time polymerase chain reaction
ROS	Reactive oxygen species
shRNA	Small-hairpin RNA
SOD	Superoxide dismutase
SQSTM1	Sequestosome 1/p62
TCA	Tricarboxylic acid cycle
TEMED	Tetramethylethylenediamine
TMT	Tandem mass tag
TSC	Tuberous sclerosis complex
α	Alpha
β	Beta
μL	Micro litre
μM	Micro molar
μm	Micro meter
%	Percent
ºC	Degrees Celsius

ACKNOWLEDGMENTS

I would like to thank the various funding agencies that have supported me throughout my degree, the Canadian Institute of Health Research (CIHR), the Nova Scotia Health Research Foundation (NSHRF), and the Nova Scotia Graduate Student (NSGS) Scholarship.

I would like to acknowledge Dr. Sheila Singh (McMaster University) and colleagues for their generosity in providing the patient-derived samples used in this study. A special thank you to Dr. Patrick Murphy for his help with performing the proteomics experiments.

I would like to thank my close colleagues and friends, Cathleen Dai and Saleh Ghassemi-Rad, for all of their help and support throughout the past five years. We made a wonderful team and we accomplished great things together. I am so happy and proud of their ongoing success.

To my supervisors, past and present, I would like to thank Dr. Shashi Gujar for allowing me the opportunity to complete my degree under his supervision and supporting me as a Masters student in the lab. I would also like to thank my past supervisor Dr. Patrick Lee for his ongoing support and encouragement.

Most importantly, I would like to thank my supervisor Dr. Tanveer Sharif for his extraordinary mentorship and guidance over the past five years. You introduced me to science as a young undergraduate student and taught me everything I know. I do not know where I would be today without you. You are a friend, a teacher, and a role model. I am eternally grateful for all you have done for me.

CHAPTER 1. INTRODUCTION

1.1 Cancer

Cancer is a devastating disease that affects millions of people worldwide. It is estimated that 18.1 million new cases of cancer were diagnosed in 2018 and 9.6 million people died from the disease (1). The burden of cancer is increasing across the globe and approximately half of all Canadians are expected to be diagnosed with cancer in their lifetime (1,2). Cancer is a complex disease that can involve a combination of genetic and environmental factors that triggers transforming events within one's cells which renders them malignant (3,4). Because the development of cancer involves the transformation of an individual's cells, every cancer is genetically distinct based on the unique genetic makeup of the person. This complex genetic heterogeneity can make it extremely difficult to predict how a particular patient will respond to treatment (4). Despite this, certain hallmarks have been identified which are characteristic of all cancer cells (5,6). The original 'Hallmarks of Cancer' included the ability of cancer cells to sustain proliferative growth and gain replicative immortality, induce angiogenesis and gain the capacity to invade and metastasize, while evading regulatory growth suppression mechanisms and resisting cell death signals (5). These hallmarks have since been expanded to encompass new 'Emerging Hallmarks' which include the capacity for cancer cells to deregulate cellular energetics to maintain enhanced energy requirements while avoiding recognition and destruction by immune cells (6). Traditional chemotherapies and radiation treatments aim to exploit the uncontrolled proliferation hallmark of cancer by targeting rapidly dividing cells. However, these treatments are not confined to specifically targeting cancer cells and are associated with highly toxic side effects (7-9). Furthermore, resistance and

cancer recurrence following treatment remains a common problem (10,11). Hence, the development of safer and more targeted therapies based on the increased understanding of the complex genetic heterogeneity of cancers remains a key priority in cancer research.

1.2 Cancer heterogeneity and cancer stem-like cells

Tumors consist of functionally heterogeneous populations of cancer cells that vary in their degree of differentiation and proliferation capacity (12,13). The degree of differentiation refers to how closely cancer cells resemble the structure and function of normal, non-malignant cells from the tissue of origin (14). Within tumors, there exists a small population of poorly-differentiated cancer cells that possess stem-like characteristics, termed cancer stem-like cells (CSLCs). These CSLCs are malignant cells that display properties that are attributed to normal stem cells, such as self-renewal capacity and multi-lineage differentiation potential (15,16). Self-renewal is a unique characteristic of stem cells that allows them to indefinitely divide while maintaining their undifferentiated, stem-like state. The self-renewal capacity of CSLCs allows CSLC populations to persist within the tumor (15,16). The major clinical problem with CSLCs is their contribution to chemoresistance and cancer relapse (17-21). Many conventional chemotherapies aim to target rapidly dividing cancer cells by inhibiting mitotic division or inducing DNA damage that leads to apoptosis. These chemotherapies have been demonstrated to be less effective at targeting CSLCs, as these cells may display slower cycling rates, increased DNA repair mechanisms, and higher expression of anti-apoptotic proteins (22,23). Moreover, because CSLCs typically comprise a very small proportion of tumor tissue (usually <10%), it can be difficult, if not impossible, to detect residual CSLC populations following treatment (24). These CSLCs display robust tumorigenic potential, where it has been demonstrated

that just a single CSLC could be sufficient to initiate tumor formation in immune-compromised animals (25,26). Hence, CSLCs pose a major obstacle for achieving optimal therapeutic outcomes for cancer patients. Figure 1.1 depicts a schematic representation of the model wherein poorly-differentiated cancer stem-like cells are responsible for therapy resistance and cancer recurrence. Therefore, there is considerable therapeutic interest in understanding the biological properties that regulate stemness features and chemoresistance in CSLCs.

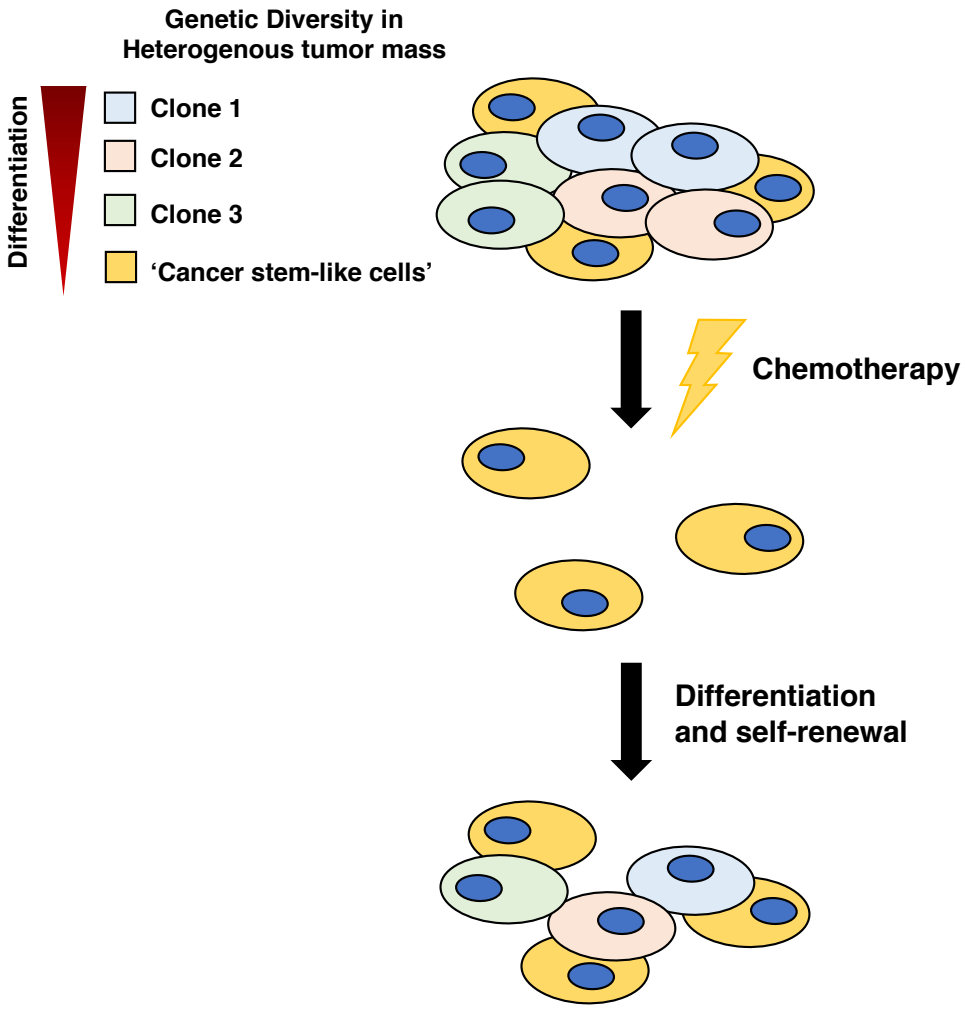

Figure 1.1

Figure 1.1. *The cancer stem cell model*. Tumor masses consist of heterogeneous populations of cells at varying degrees of differentiation. The cancer stem cell model proposes that small populations of poorly-differentiated cells with stem-like characteristics, termed 'cancer stem-like cells' exist within tumors and are more resistant to chemotherapies than more differentiated cancer cells. These cancer stem-like cells can survive chemotherapeutic assaults and can re-initiate tumor formation. These cells have the capacity to undergo multi-lineage differentiation and re-establish the clonal heterogeneity of the original tumor. Cancer stem-like cells also have the ability to self-renew and persist to maintain the cancer stem-like cell populations within the tumor mass.

1.3 Differentiation therapy for the treatment of cancer stem-like cells

Due to the clinical implications for CSLCs in chemoresistance and recurrence of cancer, there is a priority for the identification and development of specific CSLC-targeting therapies. The induction of terminal differentiation has emerged as a potential strategy to target poorly-differentiated CSLCs.

All-trans retinoic acid (ATRA) was the first widely used differentiation-inducing therapy that was approved for the treatment of acute promyelocytic leukemia (APL) patients (27,28). APL tumors are uniquely characterized by the presence of the reciprocal translocation of chromosomes 15 and 17 which results in the fusion of the promyelocytic leukemia (PML) gene and the retinoic acid receptor-α (PML-RARα). This fusion event prevents myeloid cell differentiation and leads to the accumulation of malignant, self-renewing promyeloid progenitor stem-like cells (29). Treatment with ATRA induces the differentiation of promyeloid cells in APL patients and has the potential to cure the disease when combined with other agents (29).

While differentiation therapy has been widely used for treating hematopoietic cancers, recent studies have advocated for the use of differentiation therapy as a mechanism to target poorly-differentiated cancer cells within solid tumors such as breast cancer and glioblastoma (30-33). This approach aims to suppress the stemness capacity of CSLCs

through induction of terminal differentiation, so that these cells may lose their tumorigenic potential and become more susceptible to subsequent chemotherapeutic interventions, theoretically minimizing the likelihood of cancer relapse. There is some evidence to support this theory, where it has been shown that ATRA induces the differentiation of $CD133^+$ glioma CSLCs and suppresses aggressive properties associated with invasion and therapy resistance (30). However, the addition of bone-morphogenic protein (BMP; a well-known inducer of differentiation in normal stem cells) in glioblastoma CSLCs was shown to induce some epigenetic responses but failed to induce terminal differentiation or cell cycle arrest (31). In breast cancer, salinomycin was identified in a high-throughput screen to specifically suppress $CD44^+/CD24^-$ breast CSLCs by inducing epithelial differentiation and cell cycle arrest (32,33). Although several studies have demonstrated that differentiation induction holds potential to suppress CSLCs, whether differentiation therapy can effectively be combined with additional chemotherapeutic agents to eliminate CSLCs to potentially cure patients with solid tumors remains to be determined.

1.4 The role of autophagy in cancer and cancer stem-like cells

Autophagy is a highly conserved homeostatic cellular degradation mechanism also known as 'self-eating'. Autophagy is important for maintaining cellular bioenergetics and clearance of protein aggregates, damaged organelles, and pathogens. Through autophagy, proteins and organelles are engulfed within autophagosomes (*de novo* formed vesicles) and delivered to lysosomes for degradation (34).

Autophagy is typically triggered in response to nutrient starvation such as amino acid deprivation, which is a particularly potent inducer of autophagy in mammalian cells (35). Nutrient deprivation triggers autophagy through the mammalian target of rapamycin

(MTOR)-mediated signaling. (36). MTOR is a major negative regulator of autophagy, and inhibits autophagy activation under normal conditions. Under nutrient stress or conditions lacking growth stimuli, the phosphorylation and activation of MTOR is inhibited (36). MTOR activity can be regulated by directly sensing amino acid levels, or through upstream signal transduction pathways regulated by growth factor signal transduction pathways. AKT signaling connects growth factor signaling with MTOR activation through regulation of the tuberous sclerosis complex (TSC) (37-39). AKT becomes phosphorylated and activated in response to growth factors interacting with their receptors, such as insulin receptor signaling (38). Activated AKT phosphorylates and inhibits TSC2, a negative regulator of MTOR which activates the GTPase activity of Rheb, converting Rheb-GTP to inactive Rheb-GDP (39,40). When Rheb-GTP is active following AKT-mediated suppression of TSC2, it will bind MTOR and allow it to become activated (41). Activated MTOR suppresses autophagy by directly phosphorylating and inhibiting the ULK complex, which is required for the initiation of canonical autophagy (42).

The activation of the ULK complex is the first step in canonical autophagy initiation. The ULK complex translocates to autophagy initiation sites upon activation and recruits the second autophagy initiation complex, the phosphatidylinositol kinase III (PI3K-III) complex, also known as the VSP34 complex (43). The PI3K III complex consists of PI3K-III, Beclin-1, VSP15, and ATG14L. Together, these complexes promote the *de novo* nucleation of the phagophore membrane, which will eventually expand and seal to become the autophagosome vesicle (43). The elongation of the phagophore and maturation of the autophagosome membrane involves a multistep process consisting of sequential modification of microtubule-associated protein 1 light chain 3 (MAP1/LC3)

(34,43). After synthesis, the C-terminus of LC3 is cleaved by a cysteine protease ATG4 to produce LC3-I with a molecular weight (MW) of 18 kDa. Upon activation of autophagy, a fraction of LC3-I is transferred to phosphotidylethanolamine (PE) to produce an LC3-PE conjugate (also known as LC3-II) that gets associated with autophagosomes. Thus the amount of LC3-II and the formation of LC3 puncta are used as markers of the autophagosome (34,43,44). Autophagic degradation can be unselective and engulf random portions of cytoplasmic components, or autophagy can selectively break-down proteins and organelles that have been targeted for autophagic degradation (45). Sequestosome-1/p62 (SQSTM1) is a protein involved in selective autophagic degradation, and recognizes specific ubiquitinated protein aggregates and interacts with LC3B-II to sequester these proteins to the autophagosome (45). Upon autophagosome-lysosome fusion, SQSTM1 is itself degraded in the autolysosome, therefore, degradation of SQSTM1 is commonly used as an indicator of autophagic degradation activity (46) (Fig. 1.2).

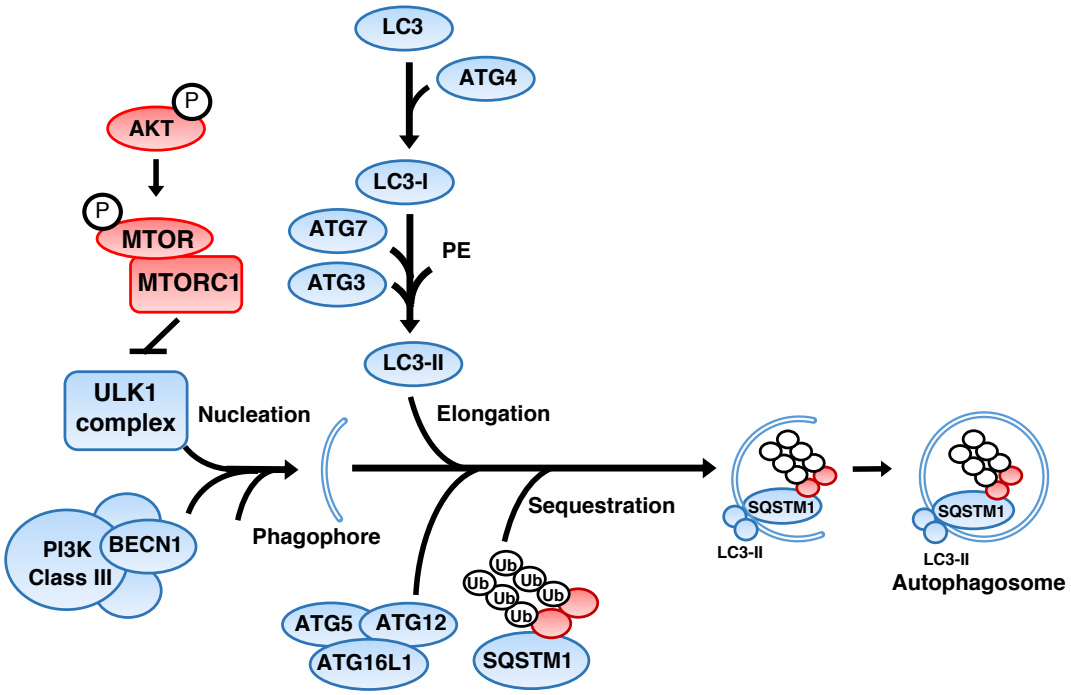

Figure 1.2. *Schematic diagram depicting the regulation of autophagy through AKT/MTOR signaling.* Activated phosphorylated AKT (Ser473) promotes the phosphorylation and activation of MTOR (Ser2448) which leads to the inhibition of the ULK1 autophagy initiation complex. Activation of the ULK1 complex leads to the recruitment of the phosphatidylinositol kinase III (PI3K-III) complex, which includes PI3 kinase class III and Beclin-1. The ULK1 and PI3K-III complex promote the *de novo* nucleation of the phagophore membrane. The elongation of the phagophore involves sequential modification of LC3, where it becomes conjugated to phosphotidylethanolamine (PE) and incorporated into the phagophore membrane with the help of autophagy-related genes (ATGs; ATG4, ATG7, ATG3, ATG5, ATG12, and ATG16L). Sequestosome-1/p62 (SQSTM1) recognizes specific ubiquitinated protein aggregates and interacts with LC3B-II to sequester these proteins to the autophagosome.

Maintaining autophagic homeostasis is required for proper cell function. As such, disorders of autophagy are associated with many pathologies, ranging from neurodegeneration to cancer (47). As autophagy is generally regarded as a pro-survival mechanism under physiological conditions to adapt to stress and nutrient deprivation, it was originally assumed that enhancing autophagy may confer a growth advantage to tumor

cells to cope with the stress associated with rapid proliferation (48). There is evidence to support this, and many cancer cells have been found to upregulate autophagy in response to metabolic stress which helps sustain their survival (49-52).

Autophagy can also play a role in mediating apoptosis resistance in cancer cells. Autophagy and apoptosis are intimately linked processes that engage in molecular cross-talks which are still poorly understood (53,54). Intrinsic apoptosis is typically triggered by signaling mechanisms mediated by the mitochondria. Under conditions of cellular or genotoxic stress, the mitochondrial membrane becomes permeabilized through activation and dimerization of BAK or BAX, which creates a mitochondrial outer membrane permeability (MOMP) pore (55). Permeabilization of the mitochondria allows for cytochrome C, which is typically confined in the mitochondria, to be released into the cytoplasm. When cytochrome C is present in the cytoplasm, it binds with the apoptosis protease activating factor-1 (APAF-1), which creates the apoptosome (56,57). The apoptosome complex will then bind and activate the protease caspase-9, which leads to a cascade of activation of other apoptosis-associated caspase proteases (56,58). Once the terminal caspase is activated in this cascade, when procaspase-3 is converted to its cleaved and activated form, the cell is committed to apoptosis and death is inevitable (59-61). Caspase-3 will directly cleave proteins required for cell function, such as the DNA repair protein poly (ADP-ribose) polymerase (PARP), and activate nucleases to degrade cellular DNA (62-64). Degraded cellular materials are then organized and packaged into vesicles that bleb off of the cell membrane so that cellular contents are not released into the microenvironment (59) (Fig. 1.3). Autophagy can prevent apoptosis activation through the clearance of damaged mitochondria before they can elicit pro-apoptotic signals (65,66).

Interestingly, Beclin-1, an essential component of canonical autophagy, is also regulated by apoptotic proteins, as it contains a BH3 domain and forms complexes with apoptotic BH3 family members, such as BCL-2 (67,68). BCL-2 can inhibit autophagy by binding with Beclin-1, making it unavailable to initiate autophagy (67,69).

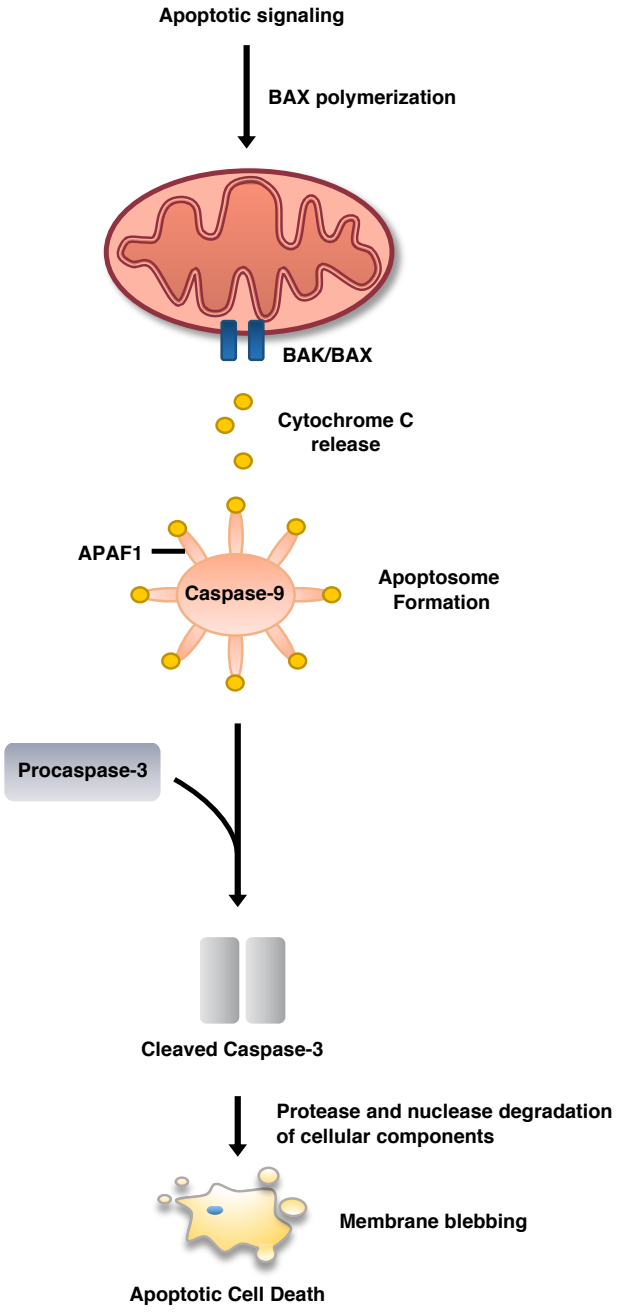

Figure 1.3

Figure 1.3. *Induction of apoptosis.* When apoptotic signals are present, the mitochondrial membrane becomes permeabilized through activation and dimerization of BAK or BAX, which leads to permeabilization of the mitochondrial outer membrane and release of cytochrome C into the cytoplasm. When cytochrome C is present in the cytoplasm, it binds with the apoptosis protease activating factor-1 (APAF-1), which creates the apoptosome. The apoptosome complex will then bind and activate the protease caspase-9, which leads to a cascade of activation of other apoptosis-associated caspase proteases. When procaspase-3 is converted to its cleaved and activated form it will directly cleave proteins required for cell function, such as the DNA repair protein PARP, and activate nucleases to degrade cellular DNA. Degraded cellular materials are then organized and packaged into vesicles that bleb off of the cell in a manner that is phenotypic of apoptotic cell death.

Recent studies have also demonstrated that autophagy can be upregulated as an adaptation mechanism in response to therapeutic interventions and helps confer resistance to cancer treatments (70-74). For this reason, the autophagy inhibitor hydroxychloroquine (HCQ) is being explored in clinical trials as a combination therapy with other chemotherapeutic agents (75-79).

Despite considerable evidence that suggests autophagy is a pro-cancer mechanism, the role of autophagy in cancer is far more complex. Deficiencies in autophagy have also been shown to enhance susceptibility to cancer development, where animals that are haplodeficient for the autophagy-related protein Beclin-$1^{+/-}$ have been shown to suffer from a high incidence of spontaneous tumor development (mice with a complete knockout of Beclin-1 do not survive through embryonic development) (80,81). Moreover, some types of cancers have been shown to possess recurrent mutations in autophagy-related genes such as ULK4 and ATG7 (82). Overactivation of autophagy can lead to autophagy-mediated programmed cell death that is independent of apoptosis. Therefore, induction of autophagy may act as a means of inducing autophagic cell death in apoptosis-resistant cancer cells (53,68).

The role of autophagy is even more complicated in the context of CSLCs. Recently, autophagy has been demonstrated to play a crucial role in maintaining the stemness characteristics of both normal stem cells and CSLCs (83-85). Our research group has shown that autophagic homeostasis is required to maintain the stemness characteristics of CSLCs and that fluctuations in the basal levels of autophagy in CSLCs (through either pharmacological inhibition or promotion of autophagy) suppresses stemness and promotes differentiation and/or senescence (85). It is possible that increased reliance on autophagy in CSLCs can be attributed to their enhanced chemoresistant properties. Our laboratory has also found that CSLCs and differentiated cancer cells respond differently to the same therapeutic interventions through differential modulation of autophagy (86). Treatment with the histone deacetylase (HDAC) inhibitor, Tubastatin A, was found to promote apoptosis in differentiated cancer cells but not CSLCs. However, Tubastatin A treatment led to the upregulation of autophagy and promoted differentiation in CSLCs (86). These findings provide a rationale for potentially combining differentiation-inducing therapies with autophagy modulating drugs as a strategy to eliminate therapy-resistant CSLCs.

1.5 Antioxidant defense system

As a result of normal cellular metabolism and energy production, cells continuously produce toxic cellular by-products that can lead to cell damage. These toxic waste products include compounds such as nitrogenous waste (e.g., urea), carbon dioxide (CO_2), lactate produced from anaerobic glycolysis, and reactive oxygen species (ROS) (87-89) (Fig. 1.4). ROS refers to highly reactive free radicals that are derived from molecular oxygen. Because oxygen consists of two unpaired electrons, it is particularly vulnerable to radical formation (90-92). When oxygen is reduced by gaining electrons, this can lead to the

formation of several ROS species such as; superoxide anion ($O_2^{\bullet-}$), peroxide ($O_2^{2\bullet}$), hydrogen peroxide (H_2O_2), hydroxyl radical ($^{\bullet}OH$), and nitric oxide ($NO^{\bullet}$). Because mammalian cells frequently uptake oxygen for energy production, this leads to the generation of vast amounts of ROS (93). ROS can cause cellular damage through multiple mechanisms (92,93). ROS can react with lipids in membranes and cause organelle and cell membrane damage (92). ROS also reacts with nucleotides and leads to DNA damage or mutations. Most often, ROS modifies guanine, leading to G→T transversions and can cause double-stranded and single-stranded DNA breaks (94,95). It is estimated that ROS production from normal cellular metabolism can modify 10,000 nucleotides per cell in one day in humans (93). For this reason, mammalian cells have evolved mechanisms called antioxidant defense systems to deal with ROS and prevent cell damage.

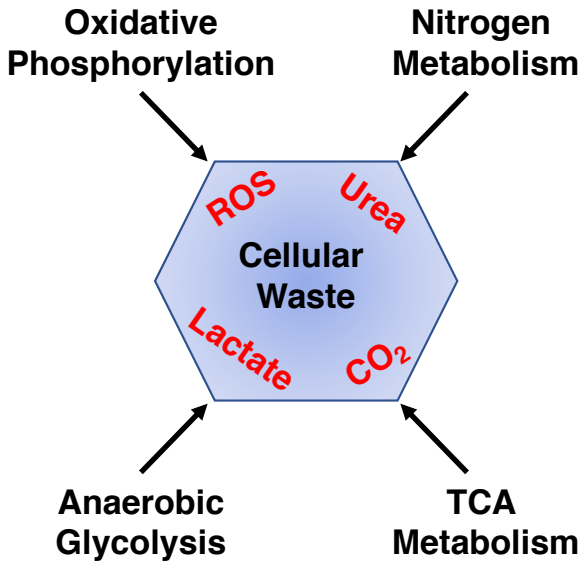

Figure 1.4. *Types of waste produced by cellular metabolism*. As a result of normal cellular metabolism and energy production, cells continuously produce toxic cellular by-products that can lead to cell damage. These toxic waste products include compounds such as nitrogenous waste (e.g. urea), carbon dioxide (CO2), lactate produced from anaerobic glycolysis, and reactive oxygen species (ROS).

Antioxidant defense systems work to scavenge and convert ROS into non-harmful products through enzymatic and non-enzymatic mechanisms (96). Enzymatic antioxidants include; the family of superoxide dismutases (SODs), catalase, and glutathione-peroxidase (GPx) (96-99). These enzymes catalyze the reduction of ROS into less harmful substances. The SOD family of antioxidant enzymes function by catalyzing the dismutation of $O_2^{\bullet-}$ into H_2O_2, where it is then converted to water by the action of catalase or GPx (96-99) (Fig. 1.5). There are three SOD enzymes that differ in their subcellular localization and metal cofactors. SOD1 is expressed in the cytoplasm and utilizes copper and zinc (Cu-Zn) as cofactors, whereas SOD2 is found in the mitochondria and depends on magnesium (Mn) for its enzymatic activity (97). SOD3, similar to SOD1, functions using Cu-Zn, but is secreted in the extracellular matrix (ECM) and protects tissues from ROS in the extracellular environment (97). Non-enzymatic antioxidants include various vitamins obtained from dietary sources such as vitamins C and E, as well as small compounds such as glutathione (GSH) or β-carotene (96,100,101).

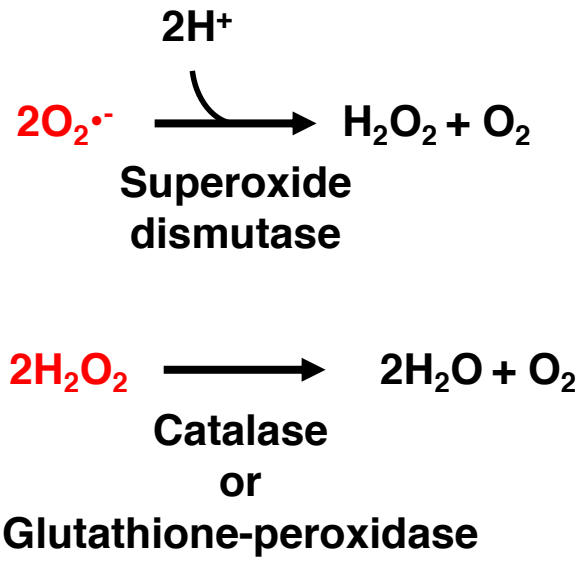

Figure 1.5. *Mechanisms of antioxidant enzymes*. Superoxide dismutases (SODs) convert superoxide anion ($O2^{\bullet-}$) into hydrogen peroxide (H_2O_2). H_2O_2 is converted to water (H_2O) by the action of catalases or glutathione peroxidases (GPx).

Although ROS can cause extensive stress and cellular damage that may be detrimental for cells, there are also physiological functions for ROS. Phagocytic immune cells utilize ROS to kill engulfed foreign bacteria (102). ROS can also modulate various signal transduction pathways such as the mitogen-activated protein kinase (MAPK) signaling pathway and the phosphoinositide-3-kinase (PI3K) pathway through oxidation of catalytic sites on regulatory enzymes (90,103). The levels of physiological ROS that can be tolerated by cells is highly cell-type dependent. Sustained exposure to pathophysiological levels of ROS, from either endogenous or environmental sources, is a major driver of oncogenic transformation (90,104,105). Cigarette smoke is a major source of environmental ROS that leads to extensive oxidative stress in cells and is a strong risk

factor for cancer development (106). Therefore, antioxidants are typically considered as tumor-suppressors associated with cancer prevention (107).

1.6 Mitochondrial antioxidant defense system

The mitochondrion is the site where the majority of energy production takes place in the cell. Mitochondria host several important metabolic pathways, such as the tricarboxylic acid cycle (TCA) and the electron transport chain (ETC) (108,109). The ETC is used for energy production under aerobic conditions, through oxidative phosphorylation. Through the ETC, electrons are passed from the electron carriers NADH and $FADH_2$, which are generated by other metabolic pathways, to either complex I or II of the ETC (109). The electrons are then passed through the complexes of the ETC, and complexes I, II and IV use this energy to pump hydrogen (H^+) protons into the mitochondrial intermembrane space, generating a proton gradient (109). Once the electrons have made their way through complexes I-IV of the ETC, they are passed to the final electron acceptor, oxygen (O_2) (109). Hence, O_2 is required for ETC function. The proton gradient generated by the ETC creates energy to drive the phosphorylation of ADP to ATP, through controlled influx back into the mitochondrial matrix through complex V of the ETC, the ATP synthase (109). The ETC is the most efficient mode of energy production in aerobic organisms and can produce up to 32 ATP molecules per metabolized molecule of glucose (108). Because mitochondria require a constant influx of O_2 to maintain oxidative phosphorylation, this also leads to the generation of a lot of ROS (110). For this reason, the mitochondria are equipped with their own antioxidant defense system. The antioxidant enzyme SOD2 is exclusively localized in the mitochondria and converts $O_2^{\bullet-}$ generated from the ETC into H_2O_2 (97). H_2O_2 must then be converted to water with the help of catalase (Fig. 1.6).

Because SOD2 is essential for preventing the accumulation of mitochondrial ROS, SOD2 is very important for maintaining both mitochondrial and overall cellular integrity (111).

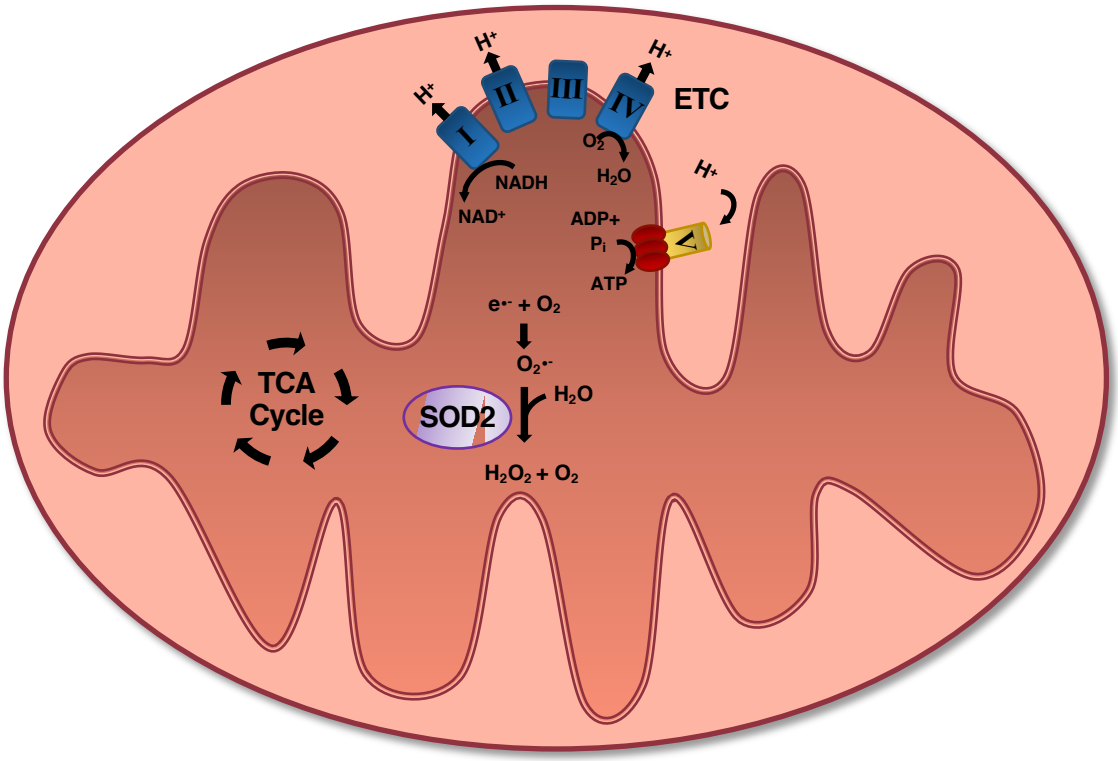

Figure 1.6. *Mitochondrial metabolism and antioxidant defense.* The mitochondria host several important metabolic pathways, such as the tricarboxylic acid cycle (TCA) and the electron transport chain (ETC). The ETC moves electrons to create a proton gradient that provides energy for the generation of ATP. The ETC requires oxygen (O_2) as a final electron acceptor and generates a lot of reactive oxygen species (ROS) such as superoxide anion ($O2^{\bullet-}$). Superoxide dismutase 2 is a mitochondrial antioxidant enzyme that converts $O2^{\bullet-}$ into H_2O_2, which is then converted to water (H_2O).

1.7 Role of mitochondrial antioxidant enzyme SOD2 in cancer

Because of the critical role of SOD2 in preventing ROS accumulation generated from ETC, SOD2 was initially regarded as a tumor suppressor that prevents ROS-induced oncogenic transformation. This notion was supported by the observations that the reduction of SOD2 expression enhances tumorigenesis by increasing ROS-dependent DNA damage that promotes the accumulation of oncogenic mutations (112,113). Moreover, it was found

that some tumors display decreased SOD2 expression compared to normal cells and that exogenous overexpression of SOD2 can delay tumor growth (114-123). Mutations that affect SOD2 function or localization to the mitochondria have been associated with an increased risk of developing pancreatic cancer and non-small cell lung carcinoma (124,125). However, recent evidence suggests that the role of SOD2 is far more complex. It was found that loss of the tumor suppressor p53, a common driving event of oncogenic transformation, actually increases the expression of SOD2 in cancer (126-128). Furthermore, the expression of wild-type SOD2 was associated with a higher risk of developing prostate, ovarian and breast cancers compared to the expression of SOD2 with the Ala16Val polymorphism that lowers SOD2 activity (129-131). During metastasis, SOD2 expression is upregulated, which can help cells cope with the oxidative stress associated with matrix detachment (132,133). In line with this, metastatic and aggressive cancers tend to have upregulated SOD2 expression (134-140). Also, the H_2O_2 produced by SOD2, if not converted to H_2O, can play a role in oncogenic signaling pathways that regulate metastasis, invasion, and angiogenesis (133,141-144). In line with this, it has been shown that some tumors will have increased SOD2 expression but decreased levels of catalase, leading to enhanced production of H_2O_2 to promote oncogenic signaling (134,141-143). Therefore, it appears that the role of SOD2 in cancer is highly context-dependent.

1.8 Mitochondrial metabolism and antioxidant defense in cancer stem-like cells

It has long been recognized that the energy demands of cancer cells are much higher than in normal cells and that cancer cells undergo so-called ‘metabolic reprogramming’ to meet these increased energy demands (145). One of the earliest demonstrations of this

concept came from experiments performed by Otto Warburg in the 1920s, which demonstrated that cancer cells preferentially utilize anaerobic glycolysis as a means of energy production, even in the presence of oxygen, as opposed to oxidative phosphorylation (146,147). This phenomenon, now famously termed the "Warburg effect", was initially quite confounding as cancer cells require more energy in order to rapidly proliferate yet, glycolysis is a far more inefficient means of ATP production as compared to oxidative phosphorylation. While this was a ground-breaking discovery, it was nonetheless only the tip of the iceberg in terms of cancer cell's ability to modulate energy metabolism. In addition to enhanced glycolytic capacity, cancer cells must also increase macromolecule biosynthesis pathways to produce proteins and nucleic acids that are needed for growth and replication (145,146). To maintain these bioenergetic demands, cancer cells will upregulate glucose transporters such as GLUT1 and GLUT3 to maximize glucose uptake (148). They also upregulate metabolic pathways that produce the cofactors required for the maintenance of continuous glycolysis, such as lactate fermentation and NAD^+ salvaging pathways (149,150). Enhancing glycolysis allows cancer cells to use glycolytic and TCA cycle intermediates in macromolecule biosynthesis pathways needed for replication (150,151).

With the emergence of new technologies such as mass spectrometry (MS)-based metabolomics, a plethora of discoveries have been made over the past decade that has shifted the paradigm of cancer metabolism (152). Early research on cancer metabolism centered around the dogma that enhanced glycolysis is the major metabolic phenotype that drives cancer growth, largely in part due to the work of Dr. Warburg. But in fact, there are many other essential metabolic pathways required for cancer, including mitochondrial

metabolic pathways (146). Mitochondria were originally hypothesized to be dispensable for cancer cells and Dr. Warburg postulated that mitochondrial dysfunction was a driver of cancer-associated aerobic glycolysis (147). However, it is now known that functional mitochondrial metabolism contributes to carcinogenesis and aggressiveness and is required for many types of cancers (153,154).

In this new era of cancer metabolism research, the focus has shifted to understanding the different metabolic phenotypes manifested by heterogeneous cell populations within the tumor and the tumor microenvironment. Through these efforts, it has been demonstrated that CSLCs display unique metabolic demands compared to their more differentiated non-stem like counterparts. Several studies have found that CSLCs often rely more heavily on mitochondrial metabolism and oxidative phosphorylation than non-stem like cancer cells (155-160). The unique metabolic phenotypes of CSLCs may contribute to their chemoresistant properties (155,156). Studies have found that cancer cells that possess the metabolic plasticity to switch between oxidative phosphorylation and glycolysis can better adapt to nutrient deprivation and therapeutic assaults (154,159).

1.9 Research rationale

Recent evidence has demonstrated that heterogeneous cell populations within the tumor and tumor microenvironment display unique metabolic phenotypes (161). CSLCs have been found to display unique growth and metabolic characteristics (18,24,155-160,162-168). Moreover, CLSCs may rely more heavily on metabolic plasticity and oxidative phosphorylation to maintain their stem-like and chemoresistant properties (154-160). ROS is a major toxic by-product generated by energy metabolism, particularly from oxidative phosphorylation in the mitochondria (110). SOD2 is an antioxidant enzyme

specifically localized in the mitochondria and is important for preventing mitochondria-associated ROS accumulation and maintaining overall cellular integrity (97,112). Since ROS accumulation is a potent inducer of differentiation (169), CSLCs should keep ROS levels low in order to maintain their poorly-differentiated, stem-like state. Therefore, CSLCs ought to possess enhanced mechanisms for dealing with oxidative stress. The purpose of this research is to explore the role of the mitochondrial antioxidant enzyme SOD2 in maintaining the stemness and the poorly-differentiated state of CSLCs. It is hypothesized that, in order to maintain their stemness features and undifferentiated state, CSLCs rely heavily on SOD2.

CHAPTER 2. MATERIALS AND METHODS

2.1 Reagents and antibodies

Dulbecco's Modified Eagle Medium (DMEM) with 25.0 mM D-Glucose, 4.0 mM L-Glutamine, and 25.0 mM 4-(2-hydroxyethyl)-1-piperazineethanesulfonic acid (HEPES) was purchased from Gibco™ (Gaithersburg, MD), Catalogue number: 12430104. KnockOut™ DMEM/Nutrient Mixture F-12 (DMEM/F-12) with low osmolality without L-Glutamine or HEPES was purchased from Gibco™ (Gaithersburg, MD), Catalogue number: 12660012. HuMEC serum-free media was purchased Gibco™ (Gaithersburg, MD), Catalogue number: 12752010 and supplemented with components from the HuMEC Supplement Kit purchased Gibco™ (Gaithersburg, MD), Catalogue number: 12755013, which includes epidermal growth factor (EGF), hydrocortisone, isoproterenol, transferrin, insulin, and 50 µg/ml of bovine pituitary extract. NeuroCult™ NS-A Proliferation Medium, serum-free, was purchased from STEMCell Technologies (Vancouver, BC), Catalogue number: 05750. Hydrocortisone, heparin solution, human recombinant basic fibroblast growth factor (bFGF) and EGF were purchased from STEMCell Technologies (Vancouver, BC). Trypsin, Fetal bovine serum (FBS), phosphate buffered saline (PBS), non-essential amino acids (NEAAs) and Antibiotic-Antimycotic (Anti-Anti) were purchased from Gibco™ (Gaithersburg, MD). Recombinant human insulin, PureLink™ HiPure Plasmid Midiprep Kit, Puromycin, 2',7'-dichlorodihydrofluorescein diacetate (H2-DCFDA), Trypan blue solution, Halt™ Protease Inhibitor Cocktail (PIC), Micro BCA™ assay kit, BCA™ assay kit, 28 cm of C18 Accucore 120 resin, TMT10 reagents, PureLink™ RNA Mini Kit, and Superscript™ II Reverse Transcriptase, were purchased from Thermo Fisher Scientific (Waltham, MA). 30% acrylamide (29:1), 2X Laemmli sample buffer,

tetramethylethylenediamine (TEMED), 0.45μm nitrocellulose membrane, Clarity™ electrochemiluminescence (ECL) substrate, and SsoAdvanced™ Universal SYBR® Green Supermix, were purchased from BioRad (Portland, ME). Carbinicillin, polybrene, phosphatase inhibitor, bovine serum albumin (BSA), β-mercaptoethanol, hydroxylamine hydrochloride, chloroquine (CQ), and Triton X-100, were purchased from Sigma-Aldrich (St. Louis, MO). MS sequencing-grade trypsin was purchased from Promega (Madison, WI). Endoproteinase Lys-C was purchased from Wako Chemicals (Richmond, VA). 50 mg and 200 mg solid phase C18 extraction cartridges were purchased from Waters (Milford, MA). 5 μm particle size C18 column was purchased from Agilent (Santa Clara, CA). MitoTEMPO was purchased from Cayman Chemical (Ann Arbor, MI). pMD2.G plasmid was a gift from Didier Trono (Addgene plasmid # 12259; http://n2t.net/addgene:12259 ; RRID:Addgene_12259), which was purchased from Addgene (Watertown, MA). psPAX2 plasmid was a gift from Didier Trono (Addgene plasmid # 12260; http://n2t.net/addgene:12260 ; RRID:Addgene_12260), which was purchased from Addgene (Watertown, MA). EGFP-LC3 plasmid was a gift from Karla Kirkegaard (Addgene plasmid # 11546; http://n2t.net/addgene:11546; RRID:Addgene_11546), which was purchased from Addgene (Watertown, MA). A full list of antibodies used for western blot and immunofluorescence, including distributor and catalog number identifier, can be found in Table 2.1.

Table 2.1. *Antibodies utilized for western blot analysis and immunofluorescence.*

Target	***Company***	***Identifier***
SOD2	Cell Signaling Technology (Danvers, MA)	13141
Oct4	Santa Cruz Biotechnology (Dallas, TX)	sc-5279
Nanog	Cell Signaling Technology (Danvers, MA)	8822
Sox-2	Cell Signaling Technology (Danvers, MA)	2748
KLF4	Cell Signaling Technology (Danvers, MA)	4038
β3-tubulin	Santa Cruz Biotechnology (Dallas, TX)	sc-80005
SQSTM1	Cell Signaling Technology (Danvers, MA)	5114
LC3A-II	Cell Signaling Technology (Danvers, MA)	4599
LC3B-II	Cell Signaling Technology (Danvers, MA)	3868
p-mTOR (Ser2448)	Cell Signaling Technology (Danvers, MA)	2971
mTOR	Cell Signaling Technology (Danvers, MA)	2983
p-AKT (Ser473)	Cell Signaling Technology (Danvers, MA)	4060
AKT	Cell Signaling Technology (Danvers, MA)	4685
Caspase-3	Cell Signaling Technology (Danvers, MA)	9662
PARP	Santa Cruz Biotechnology (Dallas, TX)	sc-8007
RIPK3	Cell Signaling Technology (Danvers, MA)	95702
E-Cadherin	Cell Signaling Technology (Danvers, MA)	3195
Bmi-1	Cell Signaling Technology (Danvers, MA)	5856
β-Actin	Santa Cruz Biotechnology (Dallas, TX)	sc-47778
β-Tubulin	Cell Signaling Technology (Danvers, MA)	2146
Goat Anti-Rabbit conjugated to HRP	Jackson ImmunoResearch Laboratories (West Grove, PA)	111-035-144
Goat Anti-Mouse conjugated to HRP	Jackson ImmunoResearch Laboratories (West Grove, PA)	115-035-003
Goat Anti-Mouse conjugated to Alexa Fluor® 488	Invitrogen (Carlsbad, CA)	A-11001

2.2 Cell Models

2.2.1 NT2/D1 Embryonal Cancer Stem-Like Cells

Embryonal carcinoma cells (ECCs) are the malignant stem cells of teratocarcinomas, which are germ cell tumors that contain undifferentiated pluripotent stem cells and their differentiated derivatives (170). The NT2/D1 cell line is one of the most studied ECC lines and is commonly used as a CSLC model (14,171,172). NT2/D1 is a nude mouse xenograft subclone derived from a testicular teratocarcinoma originally isolated from the metastatic lung site (173). Due to their embryonic origin, NT2/D1 cells express genes that make up an embryonic stem cell (ESC)-like signature (14) such as the pluripotency transcription factors Oct4, Nanog and Sox-2 (14,171,172). This ES signature expression pattern has been associated with poorly differentiated cancers and poor patient prognosis (14). Because of this unique ESC-like cell signature, NT2/D1 cells and similar embryonal carcinoma models have been used in several studies to investigate the regulation of stemness networks in cancer (174-176). The stemness of embryonal CSLCs has been demonstrated *in vivo*, where these pluripotent cells can be successfully transplanted to generate tumors (177,178). In addition to their tumor-initiating ability, embryonal CSLCs can also differentiate into somatic cells of all three germ layers (178). Hence, NT2/D1 embryonal CSLCs represent a useful model for studying the regulation of stemness and differentiation in cancer.

2.2.2 Human Mammary Epithelial Cancer Stem-Like Cell Transition Model

The human mammary epithelial (HMLE)-based CSLC model includes a transition of cells from normal to malignant to CSLCs through the acquisition of specific genes. Primary human mammary epithelial cells (HMECs) were immortalized by ectopic

expression of SV40 large T-antigen and the catalytic subunit of human telomerase reverse transcriptase (hTERT). Expression of SV40 large T-antigen promotes replication by inactivating the cell cycle regulating proteins retinoblastoma (Rb) protein and p53. Expression of hTERT promotes replicative immortality by maintaining the length of chromosome telomeres. This non-tumorigenic immortalized mammary epithelial cell line is termed HMLE and represents a normal cell line with breast epithelial characteristics (32,179). HMLE cells were transformed to tumorigenic cancer cells through ectopic expression of oncogenic H-RASG12V, termed HMLER. Further silencing of E-cadherin (*CDH1*) in HMLER cells (HMLER^{shECad}) was shown to induce epithelial-to-mesenchymal transition (EMT) and generate stem-like cells with significantly increased tumorigenicity (32,179). These HMLER^{shEcad} cells acquired a CD44^{high}/CD24^{low} expression pattern that is associated with breast CSLCs and were proficient at metastatic dissemination, whereas HMLER cells were non-metastatic (32,179). A detailed schematic of the sequential generation of this model is illustrated in Figure 2.1.

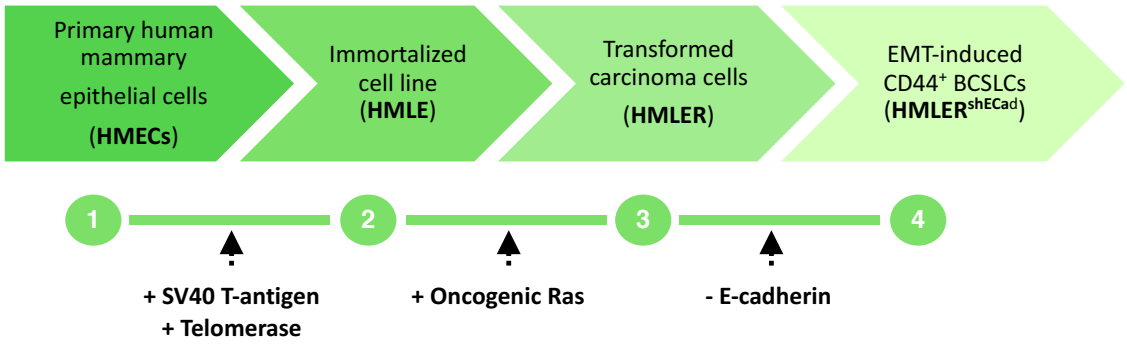

Figure 2.1. *Schematic diagram depicting the generation of a normal breast to breast cancer to breast cancer stem-like cell transition model.* Primary human mammary epithelial cells were immortalized using SV40 T-antigen and telomerase to make an

immortalized non-transformed normal human mammary epithelial cell line (HMLE). HMLE cells were then transformed by inducing oncogenic Ras to make the human breast carcinoma cell line (HMLER). Epithelial-to-mesenchymal transition (EMT) was induced in HMLER cells by silencing of the epithelial marker E-Cadherin to generate $HMLER^{shECad}$ cells. $HMLER^{shECad}$ cells possess breast cancer stem-like cell (BCSLC) properties such as high expression of CD44 and low CD24 expression, and the ability to self-renew and seed tumor formation.

2.2.3 Patient-Derived Glioblastoma Brain Tumor-Initiating Cell Model

Patient-derived brain tumor-initiating cells (BTICs) are identified based on their expression of neural stem cell surface marker CD133. Brain tumor cells expressing high levels of CD133 cells exhibit stem-like cell phenotypes such as a lack of neural differentiation markers, self-renewal capacity, and multi-lineage differentiation potential (180). Xenograft assays injecting as few as 100 BTICs developed differentiated tumors that resembled the original patient tumor (24). For *in vitro* growth, the culturing of BTICs in serum-free conditions has been established to retain their genotypic and stem cell properties after isolation from the patient's primary tumor (24,180).

2.3 Isolation and characterization of patient-derived cells

The patient-derived BTICs were kindly provided by Dr. Sheila Singh (Stem Cell and Cancer Research Institute, McMaster University). Dr. Singh and colleagues performed the following isolation and characterization procedures of patient-derived samples as previously described (181). Human glioblastoma (GBM) samples were obtained from consenting patients, as approved by the Hamilton Health Sciences/McMaster Health Sciences Research Ethics Board. Upon surgical removal, tumor tissues were dissociated in PBS containing 0.2 Wünsch unit/mL Liberase Blendzyme 3 (Roche) and incubated at 37°C in a shaker for 15 min. The dissociated tissue was filtered through a 70μm cell strainer and collected by centrifugation (450g, 3min). Red blood cells were lysed using ammonium

chloride solution (STEMcell Technologies). The cells were washed with PBS and resuspended in NeuroCult™ NS-A Proliferation Medium supplemented with 20 ng/mL EGF, 10 ng/mL bFGF, 2ug/mL of Heparin and 1X Anti-Anti. The cells were then plated on ultra-low attachment plates (Corning) and propagated as tumorspheres.

Tumorspheres were dissociated into single cells and stained with APC-conjugated anti-CD133 or a matched isotype control (Miltenyi) as recommended by the manufacturer and incubated for 15min at room temperature. Samples were run on a MoFlo XDP Cell Sorter (Beckman Coulter). The expression of CD133 was defined as positive or negative based on the analysis regions set on the isotype control. A detailed schematic of the isolation and characterization of these BTICs is illustrated in Figure 2.2.

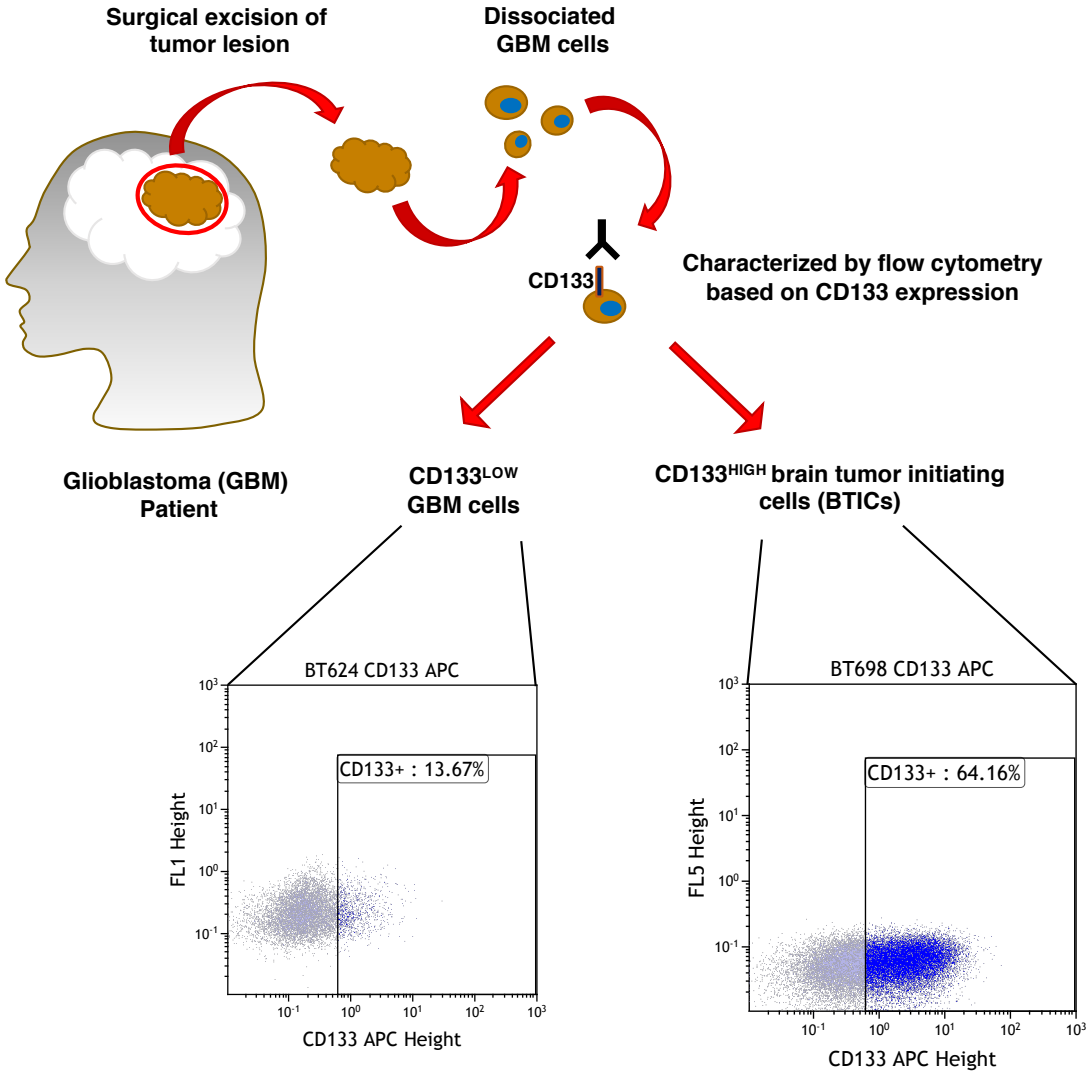

Figure 2.2. *Schematic diagram depicting isolation and characterization of the patient-derived brain tumor-initiating cell model.* Patient glioblastoma (GBM) tumors were surgically excised and the cells were dissociated and characterized using flow cytometry based on the expression of CD133. Dot plots representative of flow cytometry analysis for CD133 expression in patient-derived GBM cells expressing low levels of CD133 (BT624) and high levels of CD133 (BT698) were kindly provided by Dr. Sheila Singh and colleagues.

2.4 Cell culture

2.4.1 Culture of Cell Lines

The NT2/D1 cell line was obtained from the American Type Culture Collection (ATCC®). The human mammary epithelial cell lines, HMLE, HMLER, and HMLER^{shECad}, were generously provided by Dr. Robert Weinberg (Whitehead Institute, MIT).

NT2/D1 cells were maintained in complete DMEM supplemented with 10% (vol/vol) heat-inactivated (56°C for 30 min) FBS, 1X NEAAs, and 1X Anti-Anti. HMLE and HMLER cells were maintained in DMEM/F12 supplemented with 5% FBS, 0.5 µg/ml of hydrocortisone, 20 ng/ml of EGF, 10 of µg/ml of insulin and 1X Anti-Anti. HMLER^{shECad} cells were maintained in HuMEC serum-free media containing HuMEC Supplementation Kit components and 1X Anti-Anti. All cell lines cells were grown in 10 cm tissue culture plates at 37˚C in a humidified incubator containing 5% CO_2. Cells were passaged at 80% confluency using 0.05% trypsin-EDTA.

2.4.2 Culture of patient-derived cells

Patient-derived BTICs were maintained in NeuroCult™ NS-A Proliferation Medium supplemented with 20 ng/mL EGF, 10 ng/mL bFGF 2ug/mL of Heparin and 1X Anti-Anti and propagated as non-adherent tumorspheres. Patient-derived cells were grown in 6 cm tissue culture plates at 37˚C in a humidified incubator containing 5% CO_2. Patient-derived BTIC tumorspheres were passaged by manual dissociation of tumorspheres into single cells through gentle trituration by pipetting.

2.5 Lentivirus production and transduction

Gene silencing was performed using lentiviral plasmids expressing small-hairpin RNA (shRNA) sequences directed against SOD2 or Oct4. Non-silencing (NS) lentiviral

shRNA controls were also used. The oligomer sequences of shRNA clones are present in Table 2.2. shRNA bacterial glycerol stocks were purchased from Dharmacon and the E. coli cultures were grown in 100 mL of LB broth (10 g/L Tryptone, 5 g/L yeast extract, 10g/L NaCl, pH 7.0) supplemented with 100 μg/mL carbenicillin at 37˚C for 16 h. Plasmid DNA was extracted from bacteria using HiPure Plasmid Midiprep Kit according to the manufacturer's protocol.

Following bacterial propagation and plasmid isolation, transfection of HEK293T cells was performed to generate lentivirus using the psPAX2 (packaging) and pMD2.G (envelope) plasmids with PEI as a transfection reagent. The supernatant containing lentiviral particles was collected and filtered 24 h post-transfection.

For transduction, cells were seeded in 6-well plates to be 70% confluent on the day of transduction. Cells were transduced to yield 30-60% infection efficiency by incubating with high titer lentivirus and 8 μg/ml of polybrene for 2 h. Transduced cells were selected with 2 μg/ml puromycin for 24 h.

Table 2.2. *pLKO.1 lentiviral shRNA sequences purchased from GE Dharmacon and used for gene silencing.*

Target	***Clone ID***	***Accession***	***Sequence***
SOD2 clone #1	TRCN0000005939	NM_000636	AAAGAGCTTAACATACTCAGC
SOD2 clone #2	TRCN0000005940	NM_000636	TACTGAAGGTAGTAAGCGTGC
Oct4 clone #1	TRCN0000004879	NM_002701	AATTCCTTCCTTAGTGAATGA
Oct4 clone #2	TRCN0000004881	NM_002701	TACAGTGCAGTGAAGTGAGGG

2.6 ROS analysis by flow cytometry

Reactive oxygen species were measured by detaching cells with 0.5% trypsin-EDTA and incubating in FACS buffer (PBS, pH 7.4 supplemented with 1% FBS and 1 mM EDTA) with 1 μM H2-DCFDA for 30 min at 37˚C. Once in the cell, the non-fluorescent H2-DCFDA is cleaved by intracellular esterases and remains trapped within the cell, where it becomes oxidated and is converted to the highly fluorescent 2',7'-dichlorofluorescein (DCF) (182). Flow cytometry data were collected using a FACSCalibur flow cytometer (BD Bioscience) and analysis was performed using FCS Express (version 6). After live cell gating by FSC and SSC, the mean fluorescence intensity of the FL1 was calculated.

2.7 Trypan blue exclusion cell counting

To monitor cell growth, the trypan blue exclusion assay was used to determine the viability of cells in a suspension. Trypan blue is a dye that does not penetrate the membrane of live cells, and thus live cells appear clear under examination by light microscopy. Meanwhile, non-viable cells have breached membrane integrity and will be permeable to the dye, thus appearing blue and distinguishing them from viable cells (183). 2 x 10^4 NT2/D1 cells were seeded in triplicates in 2 ml of complete DMEM in 6-well plates. Adherent cells were dissociated at the indicated times with 0.05% trypsin-EDTA and then centrifuged into a pellet. The pellet was then re-suspended in PBS. Cells were diluted 1:25 in trypan blue and 10 μl of mixed cell suspension was loaded on a hemacytometer and viewed under a light microscope. The number of viable cells within the grids of the hemacytometer was counted to calculate the number of viable cells per volume of cell suspension, as per the formula: average cells/quadrant x 10^4.

2.8 Tumorsphere formation assay

To assess self-renewal capacity, the well-characterized tumorsphere formation assay was used, where cells are cultivated in ultra-low attachment and specialized serum-free conditions that only support the growth of stem cells (184-186). Under these conditions, only cells with stem-like characteristics will divide and self-renew, producing groups of cells that form spheroid structures, with each spheroid originating from a single self-renewing stem-like cell (184-186). Patient-derived BTICs were dissociated into single cell suspensions through gentle trituration by pipetting and cells were seeded at a low density of $1x10^3$ cells/mL. Cells were plated in ultralow-adherent 6-well plates in NeuroCult™ NS-A Proliferation Medium supplemented with 20 ng/mL EGF, 10 ng/mL bFGF, 2ug/mL of Heparin and 1X Anti-Anti. Images of tumorspheres were taken 5 days after initial seeding using a light microscope from multiple fields of view. Using ImageJ software (National Institutes of Health) for quantification of tumorsphere images, spheres with a diameter equal to or larger than 50 μm were deemed tumorspheres and the average number of tumorspheres was determined from 3 independent experiments (A detailed schematic of the protocol is illustrated in Figure 2.3.

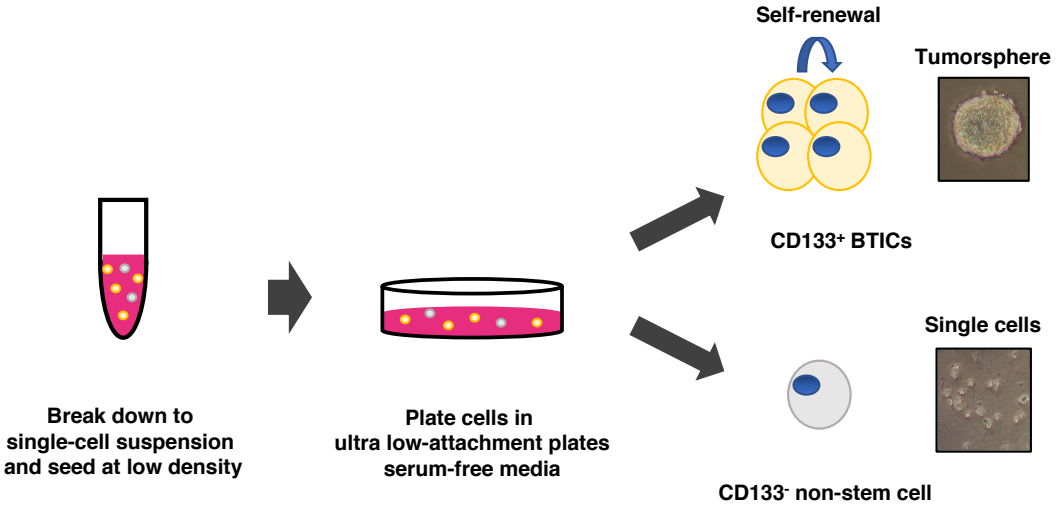

Figure 2.3. *Schematic diagram depicting the protocol for tumorsphere formation assay.* Cells are dissociated into single cells suspension through gentle trituration by pipetting. Cells are seeded at low density and cultivated in ultra-low attachment conditions with serum-free media. Under these conditions, only cells with stem-like characteristics will divide and self-renew, producing groups of cells which form spheroid structures, with each spheroid originating from a single self-renewing stem-like cell. Non-stem cells will be present as single cells in suspension.

2.9 Protein extraction

Cells were scraped in cold 1X PBS at pH 7.4 and centrifuged at 500g for 5 min at 4˚C. Pellets were resuspended in 70 µl of RIPA lysis buffer (25 mM Tris pH 7.6, 150 mM NaCl, 1% NP-40, 1% sodium deoxycholate, 1% SDS) containing 1% PIC and phosphatase inhibitors. Whole cell lysates were incubated on ice for 45 min and then sonicated for 1 min. The samples were centrifuged at 20 000g for 15 min at 4˚C and the supernatants containing the proteins were collected.

2.10 Protein Quantification

Protein concentrations were determined using the colorimetric Micro BCA™ assay kit in a 96-well flat bottom plate. Micro BCA™ solution was prepared according to

manufacturer's instructions by mixing 25 parts of reagent A, to 24 parts of reagent B and 1 part of reagent C. Protein samples were diluted 1:5 in ddH_2O and 5 µl of diluted protein sample was loaded in duplicates to 150 µl of Micro BCA™ solution. Protein standards from 0.2 to 2.0 mg/ml were prepared using BSA to generate a protein standard curve. The plate was covered and incubated with shaking for 45 min before measuring the absorbance at 570 nm using the SpectraMax Microplate Reader. Protein concentrations were calculated using the protein standard curve.

2.11 SDS-PAGE and Western Blotting

SDS-polyacrylamide resolving gels were prepared (8-12% acrylamide [30:1], 0.1% SDS, 375 mM Tris-HCl at pH 8.8, 0.1% APS, TEMED), along with stacking gels (6% acrylamide [30:1], 375 mM Tris-HCl at pH 6.8, 0.1% SDS, 0.1% APS, TEMED). Equivalent quantities of whole cell lysate samples (5-15 µg) were prepared in 5 µl of loading buffer (95% BioRad 2x Laemmli sample buffer, 5% β-mercaptoethanol) and heated at 90˚C for 5 min. Protein samples were loaded and resolved by gel electrophoresis in SDS running buffer (0.1% SDS, 200 mM glycine, 20 mM Tris-HCl) at 120 V for 1 h.

Proteins were transferred from the gel to a nitrocellulose membrane by electrotransfer in transfer buffer (glycine, Tris-HCl, methanol) at 120 V for 1.5 hrs on ice. If Ponceau Stain (Ponceau S) was performed, membranes were coated in Ponceau S dye (0.1%) dissolved in 1% acetic acid and water. The Ponceau S stains all protein bands present on the membrane and images of total protein bands were captured using the ChemiDoc Touch imaging system (BioRad). Proteins of interest were then normalized to the intensity of total protein bands detected by Ponceau S, according to corresponding figure legends. Membranes were then washed in PBST to remove Ponceau S before

blocking. Membranes were blocked in 5% non-fat milk in PBST (PBS, 0.05% Tween 20) for 45 min, then washed in PBST and incubated in the appropriate primary antibody overnight at 4°C with shaking. The primary antibodies were prepared at a 1:1000 dilution in 1% BSA in PBST.

The following day, membranes were washed in PBST before incubating in horseradish peroxidase (HRP)-labeled secondary antibodies against the primary antibodies. The secondary antibody was prepared at a 1:10 000 in 5% non-fat milk in PBST and added to the membranes for 1.5 h at room temperature.

Following secondary antibody incubation, membranes were washed in PBST before they were visualized with electrochemiluminescence (ECL) detection reagent (BioRad) using the ChemiDoc Touch imaging system (BioRad).

To verify that equal amounts of protein were loaded for each sample, membranes were probed for β-Actin or β-tubulin. The intensity of the visualized protein bands was quantified by densitometry using ImageJ software (National Institutes of Health). Protein bands were first normalized by their respective loading controls and then fold changes of samples compared to the first sample were calculated.

2.12 Immunofluorescence

Cells were seeded on coverslips 24 h before fixation at a density to be 70% confluent on the day of fixation. Cells were fixed using 4% paraformaldehyde for 15 min, permeabilized with 0.1% Triton X-100 in PBST. Following fixation, cells were washed in PBST and blocked in 1% BSA in PBST for 30 min at room temperature. After blocking, cells were washed in PBST and incubated with a mouse anti-β3-tubulin antibody diluted 1:250 in 2% BSA in PBST overnight 4°C.

The following day, cells were washed with PBST and incubated in goat anti-mouse conjugated to Alexa Fluor® 488 diluted 1:2000 in 2% BSA in PBST for 1 h at room temperature in the dark. After rinsing, cells were stained for an additional 30 min at room temperature in the dark with the nuclear stain TO-PRO3 diluted at 1:1000 in PBST according to manufacturer's protocol. Cells were then washed with PBST and coverslips were mounted to slides using Dako mounting medium. Imaging was performed using Zeiss LSM 510.

2.13 Punctae formation assay

Autophagosome assembly was assessed using the punctae formation assay by exogenously expressing EGFP-LC3B and monitoring autophagosome-associated punctae formation by confocal microscopy in the presence or absence of the late-stage autophagy inhibitor CQ (44,46). CQ inhibits the fusion of the autophagosome with the lysosome, thereby preventing the degradation of autophagosome-associated proteins (46).

For punctae formation, cells were seeded on coverslips 48 h before fixation at a density to be 70% confluent on the day of fixation. Cells were transfected with 4 μg/ml of EGFP-LC3 plasmid 24 h after seeding. Cells were subsequently treated with 12.5 μM of CQ 6 hours after EGFP-LC3 transfection. Forty-eight h after seeding, cells were fixed using 4% paraformaldehyde. Following fixation, cells were washed in PBST and coverslips were mounted to slides using Dako mounting medium. Imaging was performed using Zeiss LSM 510 and analysis was performed using Image J software.

2.14 Quantitative Real-Time Polymerase Chain Reaction

RNA was extracted from cultured cells using the PureLink ® RNA Mini Kit (ThermoFisher) according to the manufacturers protocol. Similarily, cDNA was

synthesized using enzyme Superscript™ II Reverse Transcriptase (ThermoFisher) according to the manufacturer's protocol. Each sample of cDNA was quantitated and diluted to a similar concentration of 10 ng/mL.

Two ng of cDNA was loaded into a 96 well clear PCR plate (BioRad) mixed with 1μM of forward and reverse primers targeting the gene of interest and 5μL of SsoAdvanced™ Universal SYBR® Green Supermix for a total reaction volume of 10 μL.

The BioRad CFX96 PCR machine was used for the quantitative real-time polymerase chain reaction (qRT-PCR). The qRT-PCR reaction protocol used was as follows: (a) 95°C for 3 min, (b) 95°C for 10 sec, (c) 55°C for 30 sec (d) repeat steps b-c for a total of 39 cycles. Oligonucleotide primer sequences were designed using NCBI Primer-BLAST and purchased from Invitrogen. Primer sequences are presented in Table 2.3. The results were analyzed using the $2^{-\Delta\Delta CT}$ method (187) and expressed as fold change to respective controls. Primer verification was performed using agarose gel electrophoresis of PCR products.

Table 2.3. *Gene-specific human primer sequences utilized for qRT-PCR.*

Target	***Forward Sequence (5'-3')***	***Reverse Sequence (5'-3')***
BMP4	GATCTTTACCGGCTTCAGTCTGGG	ACCTCGTTCTCAGGGATGCTGC
CDX2	CCAGGACGAAAGACAAATATCGA	AACCAGATTTTAACCTGCCTCTC
TUBB3	GGCCTCTTCTCACAAGTACG	CCACTCTGACCAAAGATGA
NES	TGGCTCAGAGGAAGAGTCTGA	TCCCCCATTTACATGCTGTGA
SYN1	AGCTCAACAAATCCCAGTCTCT	CGGATGGTCTCAGCTTTCAC
AHNAK	GTGACCGAGATTCCCGACGA	AGCTCCCGGGTTGTCTCCTC
SPP1	GCCGAGGTGATAGTGTGGTT	TGAGGTGATGTCCTCGTCTG
SNA1	ACCACTATGCCGCGCTCTT	GGTCGTAGGGCTGCTGGAA
VIM	TCTACGAGGAGGAGATGCGG	GGTCAAGACGTGCCAGAGAC
TBXT	TCCCGTCTCCTTCAGCAAAGT	GTGATCTCCTCGTTCTGATAAGC

2.15 Mass Spectrometry-Based Proteomic Analysis

Samples were prepared and subjected to mass spectrometry-based proteomic analysis with the help of Dr. Patrick Murphy (Department of Pathology, Dalhousie University) using the following protocol as previously described (188). Cells were rinsed with PBS and removed from plates by scraping into 2 mL of lysis buffer: 2% SDS, 150 mM NaCl, 50 mM Tris (pH 8.5), 5 mM DTT, and 1 tablet of protease inhibitor (Sigma #11836170001). Lysates were disrupted using an Omni homogenizer (Omni #TH115) with 3 cycles of 12 sec, with cooling on ice between cycles. Samples were incubated at 56°C for 30 min, cooled, then cysteines were alkylated using 14 mM iodoacetamide, followed by methanol-chloroform precipitation. Proteins were resolubilized in 1.5 mL of 8 M urea, 50 mM Tris, pH 8.8 and total protein content was measured using a BCA assay according to the manufacturer's protocol. An aliquot of 100 μg of protein was diluted to 1.5 M urea, digested for 2 h with endoproteinase Lys-C at a ratio of 1:200 Lys-C:protein then overnight

with MS-grade trypsin at a ratio of 1:100 trypsin:protein at 37°C. The pH of the digest was adjusted to < 3 using formic acid and peptides were desalted using 50 mg solid phase C18 extraction cartridges then lyophilized. Dried peptides were resuspended in 100 µL of 100 mM HEPES, 30% acetonitrile and 10 µL of TMT10 reagents pre-aliquoted at a concentration of 20 µg/mL in anhydrous acetonitrile. The reaction was quenched with 0.5% hydroxylamine, mixed equally, desalted using a 200 mg solid phase C18 extraction cartridge, and lyophilized. Peptides were fractionated using an Agilent 300-Extend, 4.6 mm × 250 mm, 5 µm particle size C18 column. A gradient of 5 to 40% acetonitrile (10 mM ammonium formate, pH 8) was applied at a flow rate of 800 µL/min using an Agilent 1100 pump. Fractions were collected every 0.38 min, beginning at 10 min; then, every 12th fraction was combined to a single sample to create 12 fractions, which were then desalted using homemade Stage-tips packed with Empore C18 extraction material (Sigma #66883-U) as previously described (189), then lyophilized and subjected to LC-SPS-MS3.

Each basic reverse phase fraction was resuspended in 0.1% formic acid and analyzed using an Orbitrap Velos Pro mass spectrometer (Thermo Fisher). Peptides were separated on a 75 µm × 30 cm column packed with 0.5 cm of Magic C4 resin and 28 cm of C18 Accucore 120 resin. Peptides were separated at a flow rate of 300 nL/min using a gradient of 8%–26% acetonitrile (0.125% formic acid over 120 min followed by 10 min at 100% acetonitrile). Spectra were acquired using a synchronous precursor selection (SPS)-MS3 method on the mass spectrometer (190). In this method, MS1 scans were acquired over 400–1400 m/z, 120,000 resolution, 2e5 AGC target, 100 msec maximum injection time. The 10 most abundant MS1 ions from charge states 2–6 were selected for fragmentation using an isolation window of 0.5 Th, CID activation at 35% energy, rapid

scan rate, 4000 AGC target, 30 sec dynamic exclusion, and 150 msec maximum injection time. MS3 scans were acquired using SPS of 10 isolation notches, 100–1000 m/z, 60 000 resolution, 5e4 AGC, HCD activation at 55% energy, 250 msec maximum injection time.

MS data files were converted to mzXML using a modified version of ReadW.exe. MS2 spectra were searched against the human Uniprot database (downloaded August, 2011) using Sequest (Ver28) with TMT as a fixed modification (+229.162932) on lysine residues and peptide N-termini, and carbamidomethylation (15.99492) as a fixed modification on cysteine. The allowable precursor mass tolerance was 10 ppm and product ion mass tolerance was 1 Da. All FDR filtering and protein quantitation was performed as previously described (191). The sum of all reporter ion summed signal to noise (S/N) values for peptides matching each protein was used for protein quantitation.

GO-annotation analysis was performed using DAVID Bioinformatics Resources (https://david.ncifcrf.gov/) (192,193) to conduct GO- term analysis for biological processes, molecular functions, and cellular compartment.

2.16 Statistical analysis

Analyses were completed using Microsoft Office Excel and GraphPad Prism software. Error bars represent mean ± standard error mean (SEM) unless otherwise noted. Statistical significance was determined using either; Student's t-test with 95% confidence interval or ANOVA followed by Tukey's multiple comparisons test, as stated in corresponding figure legends. All statistical tests were two-sided. $P < 0.05$ was considered significant.

CHAPTER 3. RESULTS

3.1 SOD2 is required for preventing the accumulation of ROS and maintaining the proliferation of NT2/D1 cancer stem-like cells

To investigate the importance of SOD2 in CSLC biology, silencing of SOD2 was performed in NT2/D1 embryonal carcinoma stem-like cells using two distinct shRNA clones targeting independent sequences of SOD2 and a non-silencing shRNA control vector was used as a control. As the main function of SOD2 is to act as an antioxidant enzyme, the effect of SOD2 silencing on the accumulation of ROS was first determined. For this purpose, NT2/D1 cells with shNS control, shSOD2 clone #1, and shSOD2 clone #2 were treated with H2-DCFDA. Once in the cell, the non-fluorescent H2-DCFDA is cleaved by intracellular esterases and remains trapped within the cell, where it gets oxidized in the presence of ROS and is converted to the highly fluorescent DCF (182). Hence, the measurement of DCF fluorescence by flow cytometry acts as a readout of ROS levels within the cell. The mean fluorescent intensity (MFI) of DCF was significantly higher in NT2/D1 cells with SOD2 silencing using both shRNA clones compared to the control (Fig. 3.1A). These findings indicate that SOD2 is required for preventing the accumulation of ROS in CSLCs and that depletion of SOD2 levels leads to increased levels of ROS. To determine whether loss of SOD2 affects the function of CSLCs, the proliferation of NT2/D1 cells was monitored using a trypan blue-based cell count assay. Trypan blue was used to identify viable cells, which will exclude the dye. Equal numbers of NT2/D1 cells with shNS control, shSOD2 clone #1, and shSOD2 clone #2 were seeded and the number of viable cells were counted at 24, 48 and 72 h. As shown in Figure 3.1B, the number of viable cells was significantly reduced in NT2/D1 cells with SOD2 silencing

compared to control cells. These findings suggest that the proliferation of NT2/D1 cells is hampered by silencing of SOD2 and adds credence to the hypothesis that CSLCs rely on SOD2 expression to maintain their growth and proliferation.

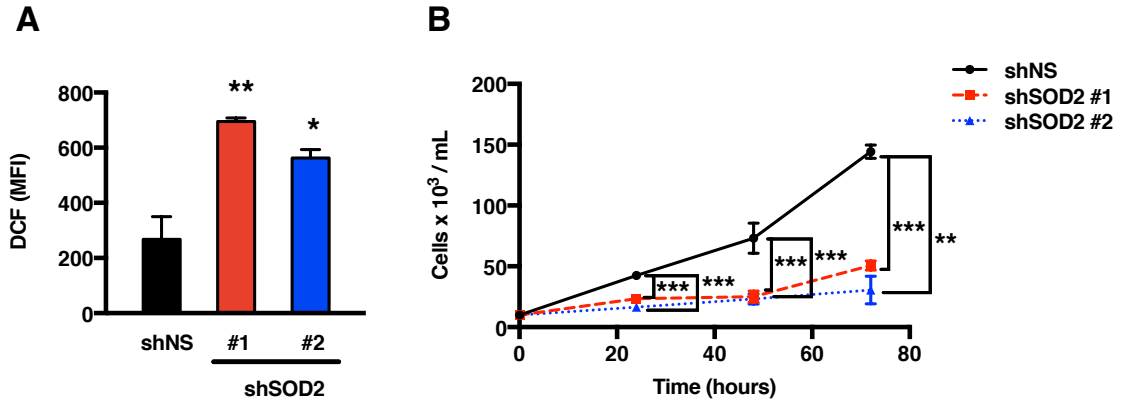

Figure 3.1. *SOD2 is required for preventing the accumulation of ROS and maintaining the proliferation of NT2/D1 cancer stem-like cells*. NT2/D1 CSLCs were transduced with either non-silencing shRNA control, or with 2 distinct shRNA targeting SOD2 (shSOD2). (A) The presence of reactive oxygen species (ROS) was analyzed by flow cytometry using a DCF-based assay and the mean fluorescent intensity (MFI) was measured. Background fluorescence of non-stained cells was subtracted from all values. Statistical analysis was performed using ANOVA followed by Tukey's multiple comparisons test. * $p < 0.05$, ** $p < 0.01$, *** $p < 0.001$, ns = not significant. (B) Cell proliferation was measured by staining cells with trypan blue dye and counting the number of viable cells at the indicated time points. Statistical analysis was performed using ANOVA followed by Tukey's multiple comparisons test. * $p < 0.05$, ** $p < 0.01$, *** $p < 0.001$, ns = not significant.

3.2 Loss of SOD2 expression hampers the expression of pluripotency factors in NT2/D1 cancer stem-like cells

The impairment in the proliferative capacity of NT2/D1 cells following SOD2 depletion suggests a disturbance in their functional capacity. Therefore, the effect of SOD2 silencing on the stemness capacity of NT2/D1 cells was further investigated. Since NT2/D1 cells express all of the major pluripotency factors associated with reprogramming and the ESC-like gene expression signature (Oct4, Nanog, Sox-2, and KLF4) (14,171,172), the

expression of these factors was analyzed by western blot following SOD2 silencing in NT2/D1 cells. SOD2 depletion with both shRNA clones led to a drastic reduction in the expression of the pluripotency factors Oct4, Nanog, Sox-2 and KLF4 in NT2/D1 cells compared to the controls (Fig. 3.2). This decrease in the expression of important stemness-maintaining factors indicates that CSLCs lose their stemness capacity following SOD2 silencing. These findings provide further evidence supporting an important function for SOD2 in CSLC biology.

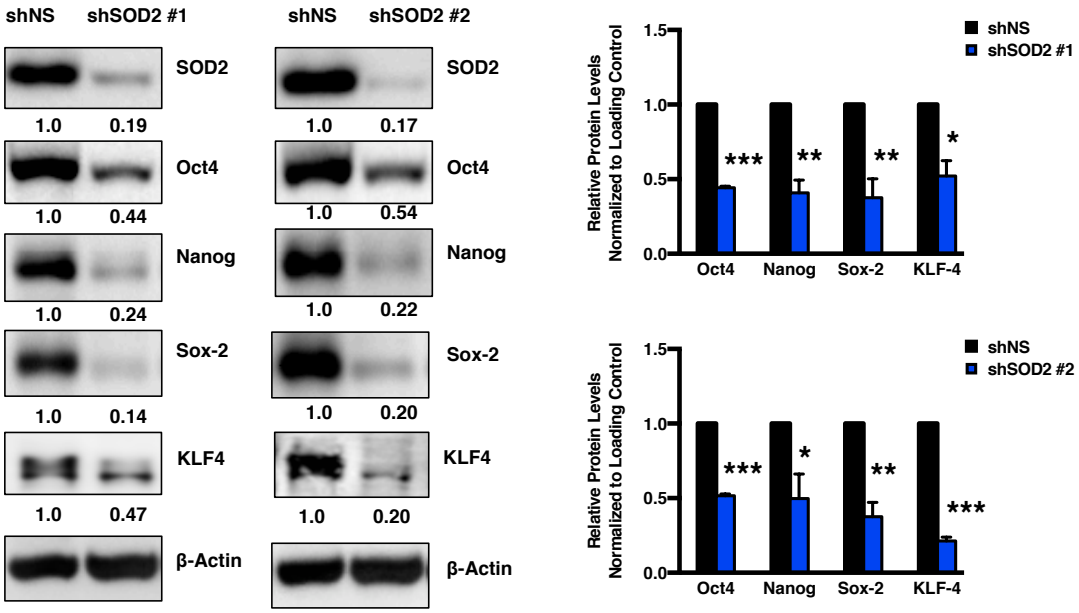

Figure 3.2. *Loss of SOD2 expression hampers the expression of pluripotency factors in NT2/D1 cancer stem-like cells*. NT2/D1 cells with either non-silencing shRNA (shNS) control or shSOD2 (clone #1 and clone #2) were subjected to western blot analysis for Oct4, Nanog, Sox-2 and KLF4. β-Actin was used as a loading control and all proteins were probed on separate blots run in parallel with the same loading volume (5 µg) from the same cell lysate. Blots are representative of three independent experiments and numeric values represent relative protein intensity normalized to β-Actin. Bar graphs represent average densitometry quantification from three independent experiments. Statistical analysis was performed with two-tailed, Student's t-test with 95% confidence interval. * $p < 0.05$, ** $p < 0.01$, *** $p < 0.001$, ns = not significant.

3.3 SOD2 depletion promotes differentiation in NT2/D1 cells

CSLCs which express stemness factors associated with the ESC-like gene signature are typically more aggressive and resistant to therapies as compared to their differentiated counterparts (14). Loss of these stemness features in CSLCs is often associated with an induction of differentiation, which may make them more susceptible to therapeutic modulations (194,195). Since the loss of SOD2 expression in NT2/D1 cells suppressed the expression of stemness-maintaining factors from the ESC-like gene expression signature, the effect of SOD2 silencing on differentiation was evaluated. Observations by light microscopy revealed distinct morphological changes following SOD2 depletion using two different shRNA clones in NT2/D1 cells compared to the control. These morphological changes were characteristic of a more differentiated phenotype, where cells became elongated and larger in size and formed dendritic outgrowths (Fig. 3.3).

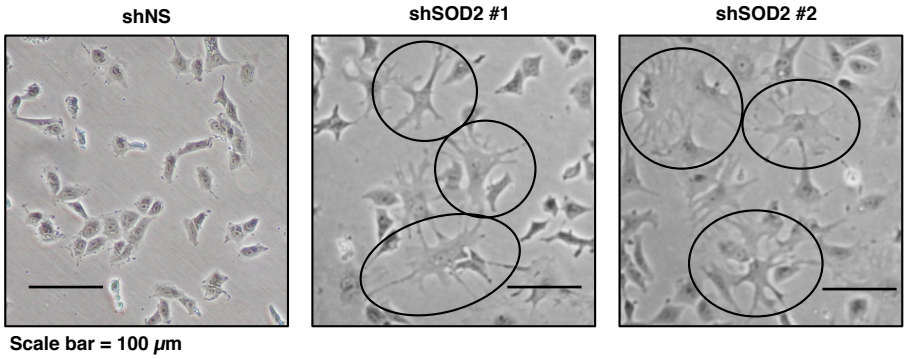

Figure 3.3. *Loss of SOD2 causes morphological changes in NT2/D1 cancer stem-like cells.* NT2/D1 cells with either non-silencing (shNS) control or shSOD2 (clone #1 and clone #2) shRNA were analyzed by light microscopy and micrographs were taken to compare morphology.

The morphological indication that NT2/D1 cells were undergoing differentiation following SOD2 depletion was further corroborated by the observation that SOD2 silencing upregulated the expression of the well-established neuronal differentiation

marker β3-tubulin, as determined by western blot analysis (Fig. 3.4A). Using immunofluorescent labeling of β3-tubulin followed by confocal microscopy analysis, it was revealed that the upregulation of β3-tubulin expression following SOD2 silencing was accompanied by a change in cellular localization, where β3-tubulin moved from nucleus to the cytoplasm and became distributed towards the periphery of the cells, localized in the dendritic structures (Fig. 3.4B). Altogether, these findings indicate that the loss of stemness following the depletion of SOD2 induces differentiation in NT2/D1 cells.

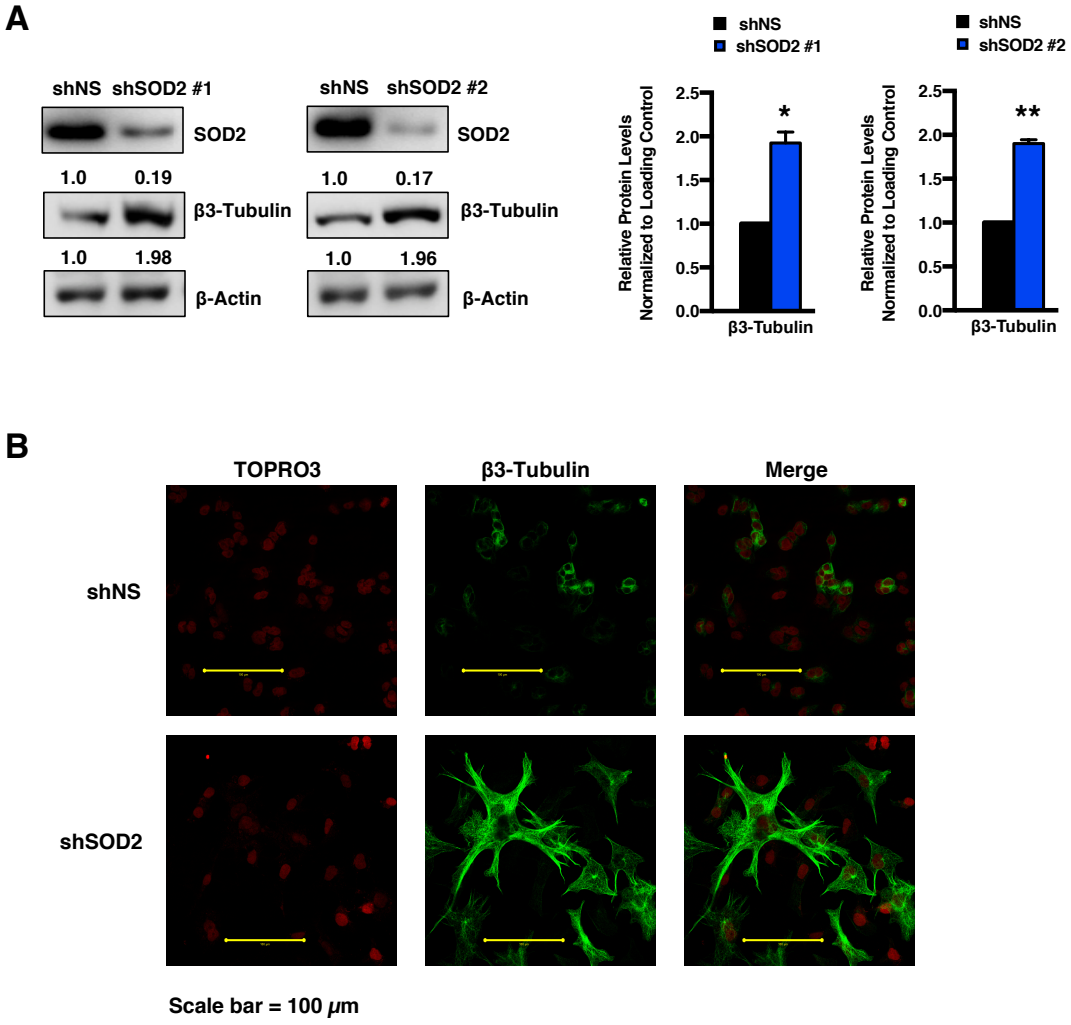

Figure 3.4

Figure 3.4. *Loss of SOD2 increases the expression and changes the distribution of differentiation marker β3-tubulin in NT2/D1 cancer stem-like cells.* (A) NT2/D1 cells with either non-silencing (shNS) control or shSOD2 (clone #1 and clone #2) shRNA were subjected to western blot analysis for the levels of β3-tubulin. β-Actin was used as a loading control and all proteins were probed on the same blot with a loading volume of 5 μg of cell lysate. Blots are representative of three independent experiments and numeric values represent relative protein intensity normalized to β-Actin. Bar graphs represent average densitometry quantification from three independent experiments. Statistical analysis was performed with two-tailed, Student's t-test with 95% confidence interval. * $p < 0.05$, ** $p < 0.01$, *** $p < 0.001$, ns = not significant. (B) NT2/D1 cells with either shNS control or shSOD2 clone #1 were subjected to immunofluorescence analysis for β3-tubulin distribution. Photos are representative of three independent experiments.

3.4 SOD2 deficiency promotes multi-lineage differentiation in NT2/D1 cells

NT2/D1 cells are characterized by their pluripotent ability to differentiate into various somatic cell lineages (174,176,196). To further characterize the type of differentiation induced by SOD2 silencing in NT2/D1 cells, the mRNA levels of a panel of differentiation markers from several distinct lineages were analyzed by qRT-PCR. This panel included markers from; early-stage ectodermal lineage (*BMP4* and *CDX2*), neural progenitor lineage (*TUBB3, SYP, NES, SYN1,* and *AHNAK*), primitive endodermal lineage (*SPP1*), mesenchymal lineage (*SNA1* and *VIM*), and early mesodermal lineage (*TBXT*). As shown in Figure 3.5 silencing of SOD2 significantly upregulated the expression of differentiation markers from multiple lineages (*BMP4, CDX2, TUBB3, SYP, AHNAK, SPP1, VIM*, and *T*/*TBXT*). Taken together, these results demonstrate that silencing of SOD2 leads to a suppression of stemness and shifts CSLCs towards a more differentiated state by promoting multi-lineage differentiation.

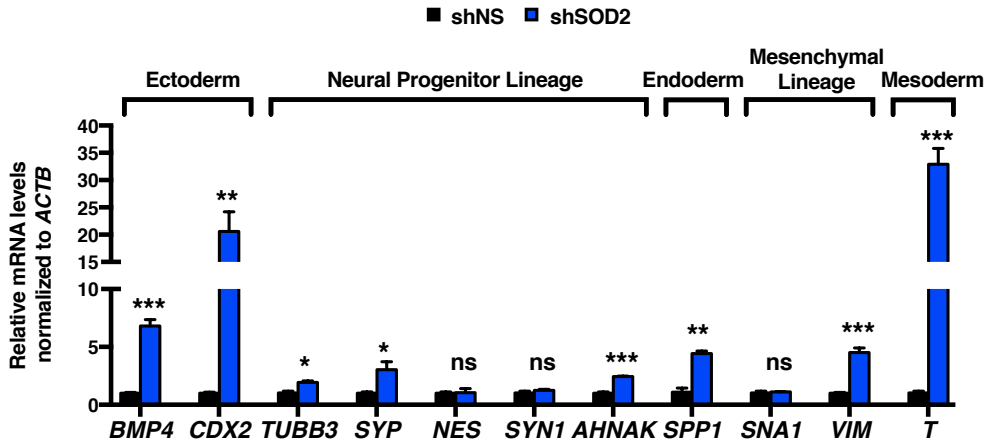

Figure 3.5. *Loss of SOD2 promotes multi-lineage differentiation in NT2/D1 cancer stem-like cells.* NT2/D1 cells with either non-silencing shRNA (shNS) control or shSOD2 were subjected to quantitative real-time PCR (qRT-PCR) analysis for *BMP4, CDX2, TUBB3, SYP, NES, SYN1, AHNAK1, SPP1, SNA1, VIM,* and *T/TBXT*. Statistical analysis was performed with two-tailed, Student's t-test with 95% confidence interval. * $p < 0.05$, ** $p < 0.01$, *** $p < 0.001$, ns = not significant.

3.5 Loss of SOD2 does not promote autophagy

The data thus far demonstrate the importance of SOD2 for maintaining the stemness and proliferation capacity of NT2/D1 CSLCs and preventing differentiation. To further explore the role of SOD2 in supporting CSLC growth and survival, the effect of SOD2 on cell death and survival mechanisms was investigated. As autophagy is an important homeostatic process involved in both cell survival and cell death (48), the role of SOD2 in regulating autophagy was first established. The effect of SOD2 silencing on autophagy flux was assessed by using two different techniques. First, the levels of the autophagosome-associated proteins SQSTM1, LC3A-II, and LC3B-II were measured by flux analysis followed by western blot analysis. In the autophagy flux analysis, the expression of these autophagosome-associated proteins was analyzed following the silencing of SOD2 in the presence or absence of the late-stage autophagy inhibitor chloroquine (CQ). CQ inhibits

the fusion of the autophagosome with the lysosome, thereby preventing the degradation of autophagosome-associated proteins. This assay allows for monitoring of the turnover of autophagy-mediated degradation turnover as opposed to simple changes in the steady-state expression of autophagosome proteins (46). SOD2 silencing in NT2/D1 cells decreased the expression of LC3A-II with no discernable change in the basal levels of LC3B-II or SQSTM1 (Fig. 3.6A). Treatment with 12.5 μM of CQ led to the accumulation of these autophagosome-associated proteins in shNS control NT2/D1 cells, but SOD2 depletion did not enhance the accumulation of SQSTM1, LC3A-II or LC3B-II compared to control, indicating no increase in autophagy flux following SOD2 silencing.

These findings were also validated by using an additional complementary method to examine autophagosome assembly by exogenously expressing EGFP-LC3B and monitoring autophagosome-associated punctae formation in the presence or absence of CQ (44). Treatment with CQ led to a robust accumulation of EGFP-LC3B punctae in control cells, however, NT2/D1 cells with SOD2 silencing failed to accumulate EGFP-LC3B punctae to the same extent as control cells following CQ treatment (Fig. 3.6B). Altogether, these findings indicate that SOD2 depletion does not promote autophagy in CSLCs.

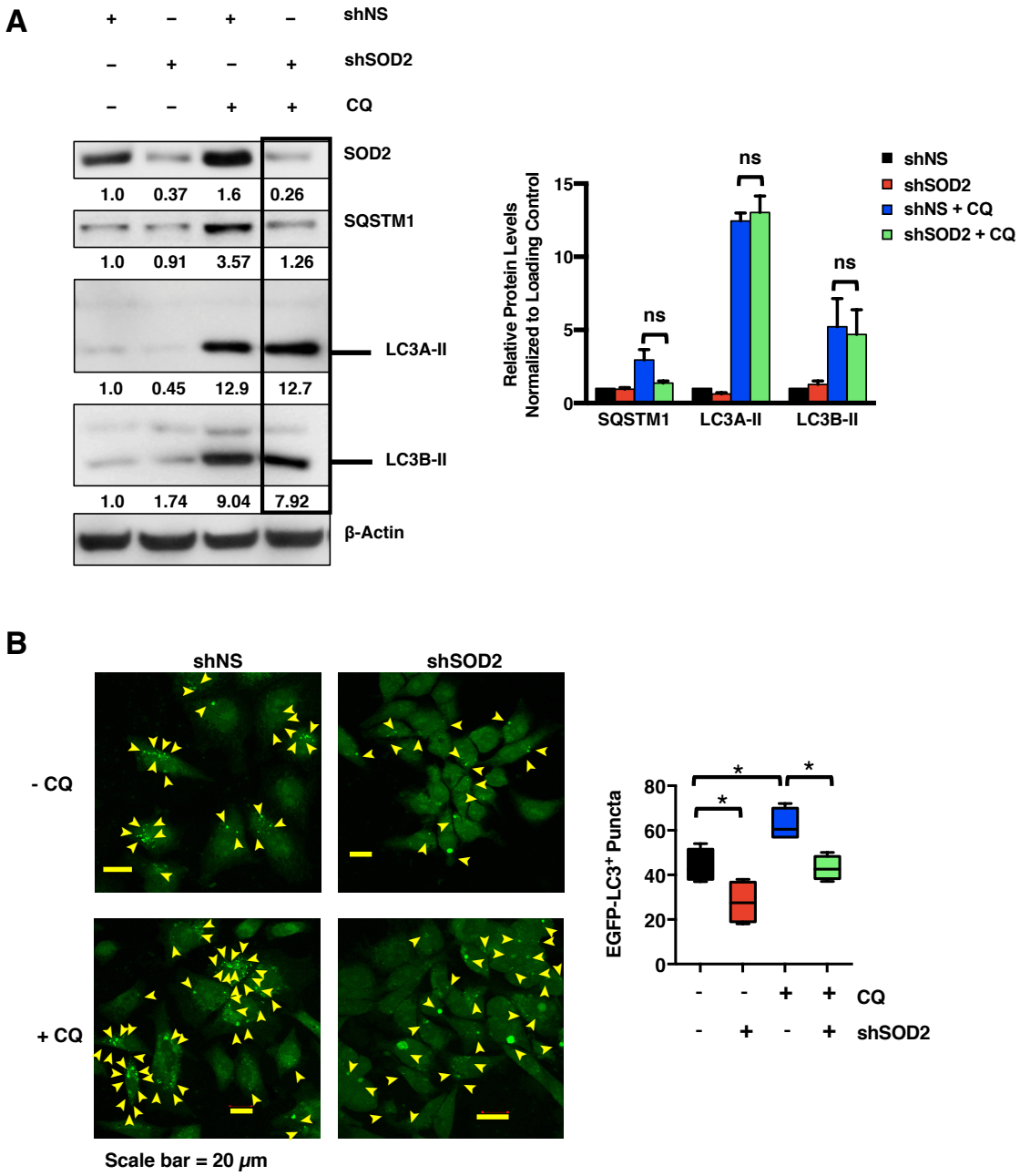
A
shNS
shSOD2
CQ
SOD2
1.0 0.37 1.6 0.26
SQSTM1
1.0 0.91 3.57 1.26
LC3A-II
1.0 0.45 12.9 12.7
LC3B-II
1.0 1.74 9.04 7.92
β-Actin
Relative Protein Levels Normalized to Loading Control
ns
shNS
shSOD2
shNS + CQ
shSOD2 + CQ
SQSTM1
LC3A-II
LC3B-II
B
shNS
shSOD2
- CQ
+ CQ
Scale bar = 20 μm
EGFP-LC3+ Puncta
CQ
shSOD2

Figure 3.6

Figure 3.6. *Loss of SOD2 does not promote autophagy in NT2/D1 cancer stem-like cells.* (A) Autophagy was analyzed following shSOD2 silencing in NT2/D1 cells using the autophagy flux assay where cells were treated with the late-stage autophagy inhibitor chloroquine (CQ) and the expression autophagosome markers SQSTM1, LC3A-II, and LC3B-II were measured by western blot analysis. β-Actin was used as a loading control and all proteins were probed on separate blots run in parallel with the same loading volume (15 μg) from the same cell lysate. Blots are representative of three independent experiments and numeric values represent relative protein intensity normalized to β-Actin. Bar graphs represent average densitometry quantification from three independent experiments. Statistical analysis was performed using ANOVA followed by Tukey's multiple comparisons test. * $p < 0.05$, ** $p < 0.01$, *** $p < 0.001$, ns = not significant.(B) autophagosome assembly was monitored by exogenously expressing EGFP-LC3B and analyzing autophagosome-associated punctae formation in the presence or absence of CQ. Statistical analysis was performed using ANOVA followed by Tukey's multiple comparisons test. * $p < 0.05$, ** $p < 0.01$, *** $p < 0.001$, ns = not significant.

3.6 SOD2 deficiency promotes the activation of upstream inhibitors of autophagy

As it was observed that autophagy flux was not induced following SOD2 silencing in NT2/D1 CSLCs, the activation of negative regulators of autophagy was investigated to determine whether autophagy is being inhibited. For this purpose, the activating phosphorylation sites of the autophagy-inhibiting kinases AKT (Ser473) and MTOR (Ser2448) were analyzed by western blot analysis (36). The activated, phosphorylated forms of AKT and MTOR were found to be increased in SOD2 deficient cells compared to the control, with no discernible change in the total levels of AKT or MTOR, supporting the observation that autophagy is not induced following SOD2 silencing in CSLCs (Fig. 3.7).

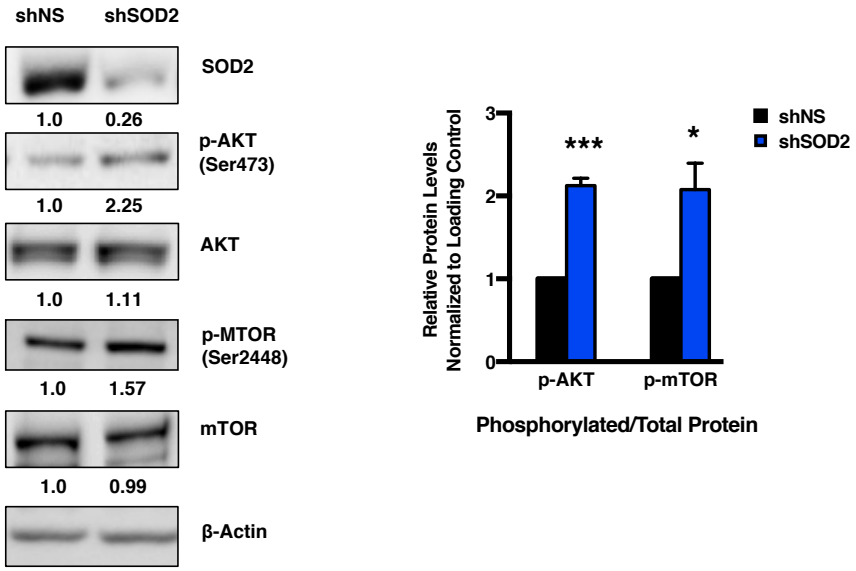

Figure 3.7. *SOD2 silencing increases the activation of autophagy inhibitors AKT and MTOR NT2/D1 cancer stem-like cells.* NT2/D1 cells with either non-silencing shRNA (shNS) control or shSOD2 were subjected to western blot analysis for p-AKT (Ser473) and total AKT along with p-MTOR (Ser2448) and total MTOR. β-Actin was used as a loading control and all proteins were probed on separate blots run in parallel with the same loading volume (5 µg) from the same cell lysate. Blots are representative of three independent experiments and numeric values represent relative protein intensity normalized to β-Actin. Bar graphs represent average densitometry quantification of intensity of phosphorylated proteins normalized to total protein level from three independent experiments. Statistical analysis was performed with two-tailed, Student's t-test with 95% confidence interval. * $p < 0.05$, ** $p < 0.01$, *** $p < 0.001$, ns = not significant.

3.7 SOD2 depletion promotes apoptosis (not necroptosis) in NT2/D1 cells

Since it was found that SOD2 depletion does not promote autophagy in NT2/D1 CLSCs, the effect of SOD2 on other modes of cell death was evaluated. Apoptosis is a mechanism of programmed cell death that is intimately linked with perturbations in mitochondrial integrity. As the cleavage and activation of caspase-3 represents the committed step of the apoptotic pathway, caspase-3 levels were analyzed by western blot analysis as an indication of apoptosis activation. The inactivated form of caspase-3, procaspase-3, was detected as a 35 kDa band, in both control and SOD2 knock-down cells

(Fig. 3.8A). The activated, cleaved form of caspase-3 presents a band of 17 kDa, which could not be detected in the control NT2/D1 cells. Following SOD2 silencing, there was a robust induction of caspase-3 activation, as determined by a strong detection of 17 kDa cleaved caspase-3 by western blot (Fig. 3.8A). The activation of caspase-3 was further confirmed by western blot analysis for cleaved PARP. PARP is an established target of activated caspase-3 protease activity and becomes cleaved when caspase-3 is activated and apoptosis is initiated. SOD2 depletion led to a clear increase in the cleavage of PARP, indicating increased caspase-3 activity and induction of apoptotic cell death (Fig. 3.8A). To comprehensively assess the effect of SOD2 on all potential modes of cell death, the process of necroptosis was also investigated. Necroptosis occurs in response to traumatic cell injury and is a cell death mechanism associated with promoting inflammation. Necroptosis is induced by the formation of the necroptosome complex, which consists of caspase-8, receptor-activating serine/threonine kinase 1 (RIPK1), and receptor-activating serine/threonine kinase 3 (RIPK3). Caspase-8 and RIPK1 also have roles in apoptotic signaling mechanisms, whereas RIPK3 is a unique marker of necroptosis. Therefore, the expression of RIPK3 was analyzed by western blot. Loss of SOD2 in NT2/D1 CSLCs did not increase the levels of RIPK3, indicating that necroptosis is not induced following SOD2 depletion (Fig. 3.8B). Altogether, these findings demonstrate that SOD2 silencing-mediated decrease in cell viability and proliferation of CSLCs is a consequence of apoptosis, independent of autophagy and necroptosis.

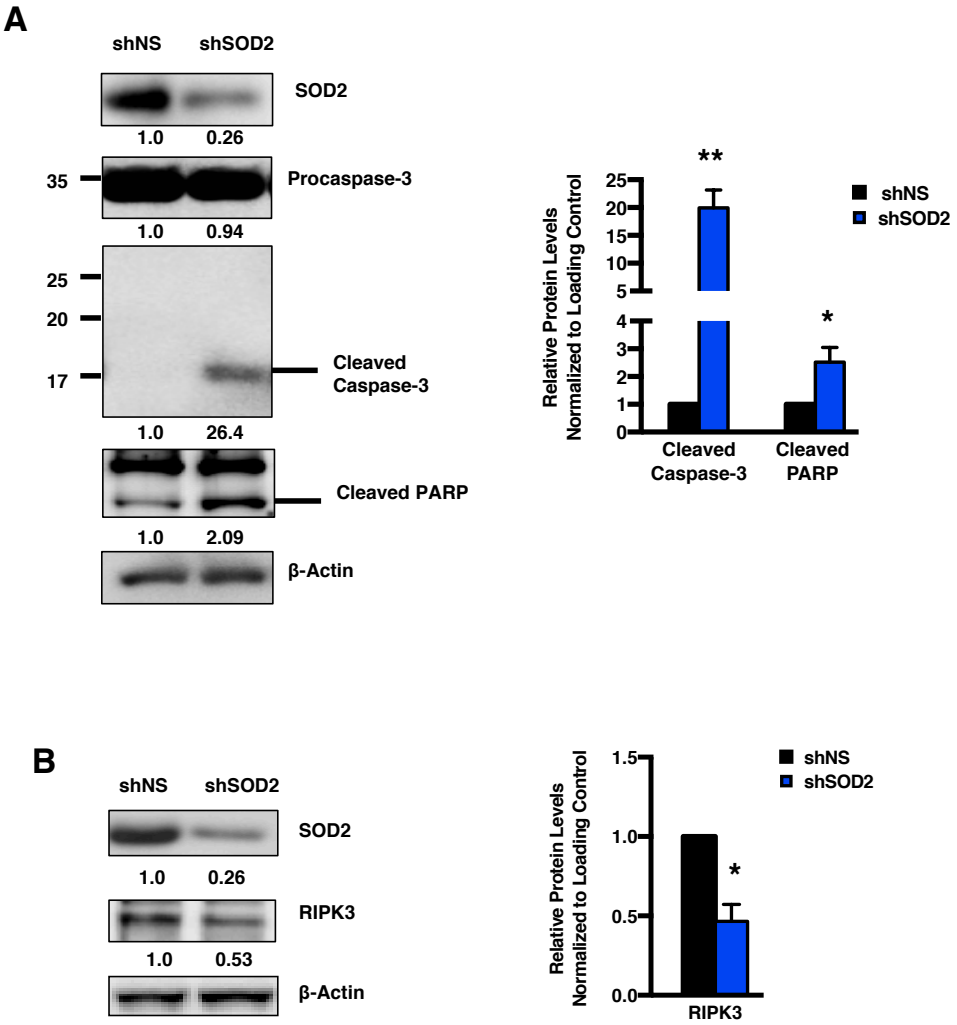

Figure 3.8. *SOD2 depletion promotes apoptosis, not necroptosis in NT2/D1 cancer stem-like cells.* (A) NT2/D1 cells with either non-silencing shRNA (shNS) control or shSOD2 were subjected to western blot analysis for apoptosis-inducing protease caspase-3 and its target PARP. β-Actin was used as a loading control and all proteins were probed on the same blot with a loading volume of 5 µg of cell lysate. Blots are representative of three independent experiments and numeric values represent relative protein intensity normalized to β-Actin. Bar graphs represent average densitometry quantification from three independent experiments. Statistical analysis was performed with two-tailed, Student's t-test with 95% confidence interval. * $p < 0.05$, ** $p < 0.01$, *** $p < 0.001$, ns = not significant. (B) NT2/D1 cells with either shNS control or shSOD2 were subjected to western blot analysis for necroptosis-associated kinase RIPK3. β-Actin was used as a loading control and all proteins were probed on the same blot with a loading volume of 5 µg of cell lysate. Blots are representative of three independent experiments and numeric values represent relative protein intensity normalized to β-Actin. Bar graphs represent average densitometry quantification from three independent experiments. Statistical analysis was performed with two-tailed, Student's t-test with 95% confidence interval. * $p < 0.05$, ** $p < 0.01$, *** $p < 0.001$, ns = not significant.

3.8 Quantitative proteomics reveals SOD2 depletion modifies proteins related to mitochondria, metabolism, differentiation, and apoptosis

After observing that loss of SOD2 in CSLCs lead to several cellular responses such as loss of stemness along with induction of differentiation and apoptosis, the effect of SOD2 silencing on overall cellular processes was evaluated using global proteomics profiling. NT2/D1 cells with shNS control or SOD2 knock-down were processed in duplicates and cells were lysed and proteins were extracted using MeOH/Chloroform precipitation and normalized using a BCA assay. Samples were digested into peptides using MS grade trypsin and labeled with TMT. Samples were pooled and subjected to 2D liquid chromatography (LC)-based mass spectrometry using an MS3 method. Spectra were searched against a Uniprot database. Peptide-spectral matches were filtered to a 1% false discovery rate (FDR) using linear discriminant analysis in combination with the target-decoy method. Proteins were quantified by adding the TMT reporter ion counts together, across all peptide-spectral matches after they were filtered based on isolation specificity. Control and shSOD2 cells were analyzed for differences in protein expression and the proteins that were either upregulated or downregulated following the silencing of SOD2 were identified. When changes in protein expression were analyzed following SOD2 depletion in NT2/D1 CSLCs, there were a considerable number of proteins that were identified to be upregulated or downregulated greater than 1.5-fold as compared to control cells. Out of 3886 total proteins identified, there were 267 proteins that were upregulated greater than 1.5-fold as well as 84 proteins that were downregulated greater than 1.5-fold following SOD2 depletion in NT2/D1 cells (Fig. 3.9). To further characterize the function

of the proteins which were modulated by SOD2 silencing, the list of 352 protein hits was entered into DAVID and grouped into processes and pathways based on Go-Term analysis.

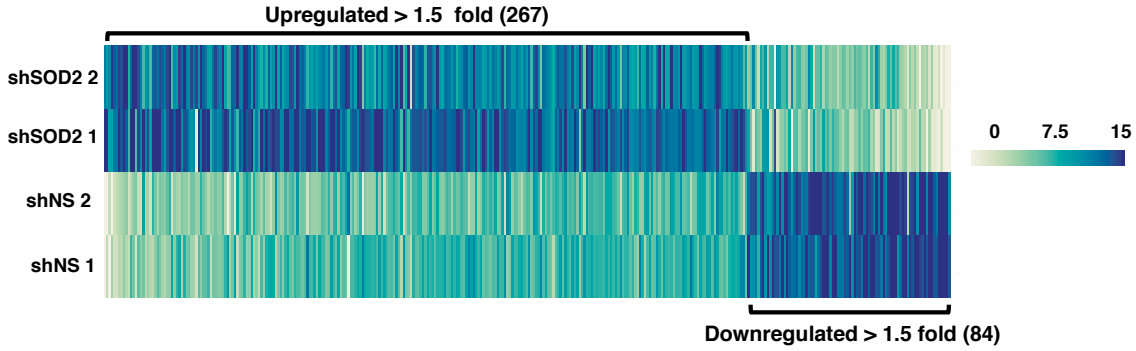

Figure 3.9. *SOD2 depletion reveals unique proteomic phenotype in NT2/D1 cancer stem-like cells.* Two technical replicates of NT2/D1 cells with either non-silencing shRNA (shNS) control or shSOD2 were subjected to quantitative mass spectrometry-based proteomic analysis and the heatmap depicts proteins which were upregulated >1.5 fold (267 proteins) and downregulated > 1.5 fold (84 proteins) following SOD2 silencing.

Using DAVID, it was identified that the major group of proteins which were regulated by SOD2 silencing were proteins related to the mitochondria. This is not surprising since SOD2 is a mitochondrial antioxidant enzyme. Among these proteins, there were several protein components of the mitochondrial electron transport chain that were upregulated following SOD2 silencing, such as: NAD:ubiquinone oxidoreductase subunits (NDUFB4, NDUFB7, and NDUFB5) which are accessory subunits for complex I, Ubiquinol-cytochrome C reductase complex assembly factors (UQCC1 and UQCC2) which are components of complex III, and the mitochondrial ATP synthase subunit d (ATP5PD). It was also noted that several enzymes involved in pathways which can feed in to the mitochondrial TCA cycle were also modified by SOD2 depletion, such as: arginase 2 (ARG2) which is an enzyme in the urea cycle, and proline dehydrogenase 1 (PRODH) which is part of the proline-regulatory axis (Fig. 3.10A). Overall, these findings indicate

that SOD2 depletion in NT2/D1 CSLCs modifies the expression of proteins involved in mitochondrial metabolism.

As mitochondrial function is intimately linked with the regulation of many other metabolic pathways, it is not surprising that one of the other major groups of proteins that was regulated by SOD2 silencing were metabolism-related proteins. In particular, SOD2 depletion led to the upregulation of several enzymes involved in glycolytic metabolism, such as: hexokinase (HK1) which catalyzes the first step of glycolysis and phosphorylates glucose to generate glucose-6-phosphate; enolase isoforms (ENO1 and ENO3) which converts 2-phosphoglycerate to phosphoenolpyruvate; pyruvate kinase (PKM) which converts PEP to pyruvate (Fig. 3.10B). Pyruvate generated from glycolysis can either enter the mitochondria to feed in to the TCA cycle and support oxidative phosphorylation or it can be converted to lactate by the action of lactate dehydrogenase (LDH), which was also upregulated following SOD2 silencing, and this promotes the regeneration of NAD+ to sustain ongoing glycolysis (Fig 3.10B). Altogether, these results suggest that SOD2 depletion may rewire cellular metabolism to enhance glycolysis in CSLCs.

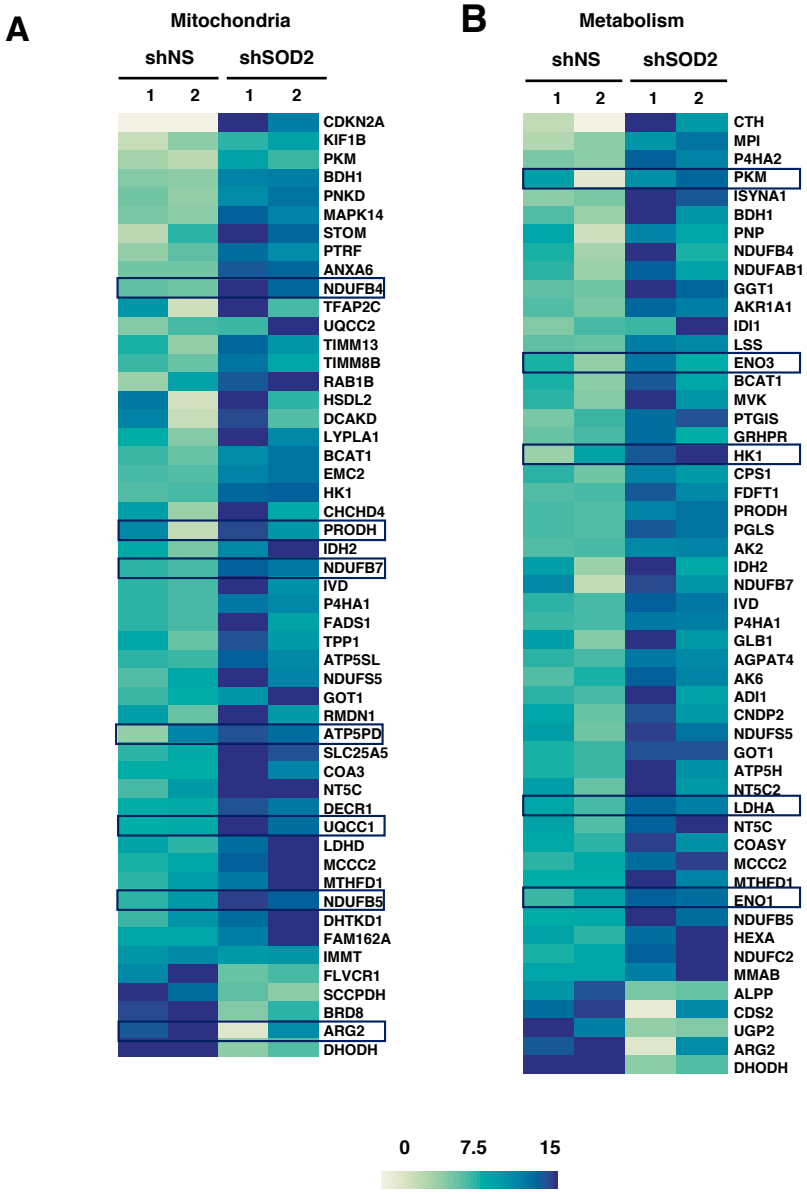

Figure 3.10. *Quantitative proteomics reveals SOD2 depletion modifies proteins related to mitochondria and metabolism.* NT2/D1 cells with either non-silencing shRNA (shNS) control or shSOD2 were subjected to quantitative mass spectrometry-based proteomic analysis and the upregulated and downregulated protein hits were entered into DAVID software and grouped based on Go-Term analysis. Heat maps depict proteins regulated by SOD2 silencing related to (A) mitochondria and (B) metabolism. Selected representative proteins are encircled.

In line with the previous findings which demonstrated that SOD2 depletion promotes multi-lineage differentiation in NT2/D1 CSLCs, the proteomics analysis also

identified various markers associated with differentiation were upregulated following SOD2 silencing, such as: the neuroblast differentiation-associated protein AHNAK which is known to inhibit stemness by regulating the expression of c-myc; laminin subunit alpha 5 (LAMA5) which is an extracellular matrix glycoprotein involved in cell adhesion and neurite outgrowth; collagen type V1 alpha 1 chain (COL6A1) which is an extracellular matrix protein involved in Schwann cell differentiation; and vimentin (VIM) which is a type III intermediate filament protein involved in mesenchymal differentiation (Fig. 3.11A).

Induction of differentiation is often associated with alterations in cell cycle regulation and proliferation. It was previously observed that the loss of SOD2 suppresses the proliferative capacity of NT2/D1 CSLCs. In line with this, proteomics analysis also revealed that SOD2 silencing modulated several proteins involved in cell cycle regulation, such as: upregulation CDKN2A/p16 which is a tumor suppressor and senescence promoting protein and cyclin-dependent kinase 4 (CDK4) which is involved in G1 of the cell cycle, as well as downregulation of CDC20 which is required for the transition in to anaphase as a part of the APC (Fig. 3.11B). These findings indicate that NT2/D1 CSLCs cells may be undergoing cell-cycle arrest or senescence following SOD2 depletion.

The cell cycle is also tightly coupled with the regulation of apoptosis and these two processes are cross-regulated by some of the same proteins. As shown in Figure 3.11C, it was previously demonstrated that SOD2 silencing promotes apoptosis in NT2/D1 CSLCs. This was further confirmed by the proteomics data where it was found that several proteins related to apoptosis were modulated following SOD2 depletion. The proteomics analysis also showed that SOD2 silencing decreased the expression of autophagy-related protein

SQSTM1, which supports previous findings where it was found that autophagy is not induced following the loss of SOD2 (Fig. 3.6 and Fig. 3.7). The observation that SOD2 silencing promotes apoptosis was further supported by the finding that annexin proteins were strongly upregulated in SOD2 depleted cells, including ANAX5 which is a commonly used marker for measuring apoptosis (Fig. 3.11D). Altogether, these data shed light on the breadth of processes that are regulated by SOD2, such as metabolism and cell cycle, and further support our previous findings that SOD2 silencing promotes differentiation and apoptosis in NT2/D1 CSLCs.

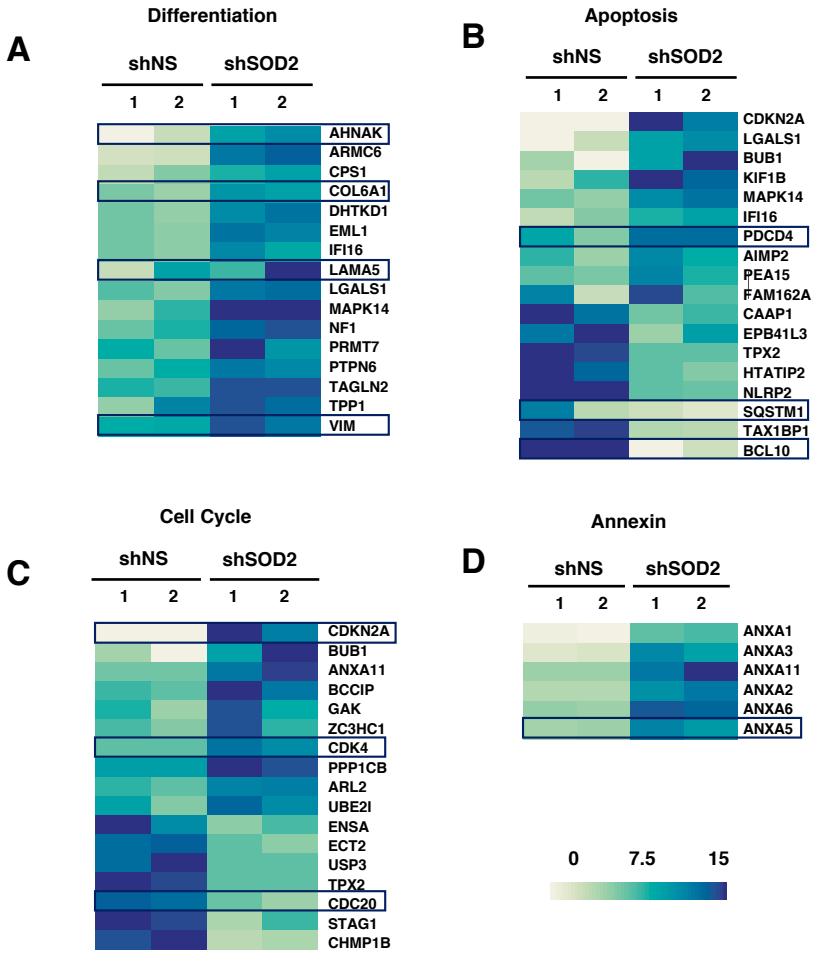

Figure 3.11

Figure 3.11. *Quantitative proteomics reveals SOD2 depletion modifies proteins related to differentiation, apoptosis, cell cycle and annexin.* NT2/D1 cells with either non-silencing shRNA (shNS) control or shSOD2 were subjected to quantitative mass spectrometry-based proteomic analysis and the upregulated and downregulated protein hits were entered into DAVID software and grouped based on Go-Term analysis. Heat maps depict proteins regulated by SOD2 silencing related to (A) differentiation, (B) apoptosis, (C) cell cycle, and (D) annexin. Selected representative proteins are encircled.

3.9 Cancer stem-like cells rely more heavily on SOD2 expression than non-stem-like, differentiated cancer cells

The findings thus far demonstrate the importance of SOD2 expression for maintaining the poorly-differentiated and stem-like state of CSLCs, where the loss of SOD2 suppresses the growth and stemness features of NT2/D1 CSLCs and promotes multi-lineage differentiation and apoptosis. Moving forward, the differential dependence of stem-like versus differentiated cancer cells on SOD2 was investigated. To achieve this, differentiation was induced in NT2/D1 CSLCs through shRNA-mediated silencing of the stemness-maintaining pluripotency factor Oct4. The loss of Oct4 in pluripotent stem-like cells abolishes their stemness capacity and leads to robust induction of differentiation, as demonstrated in various models of stem cells, including NT2/D1 cells (85,197). Induction of differentiation in NT2/D1 cells via the silencing of Oct4 using two distinct shRNA clones led to a reduction in the expression of SOD2 (Fig. 3.12). These findings suggest that once CSLCs lose the expression of pluripotency factors and undergo differentiation, they are less reliant on SOD2.

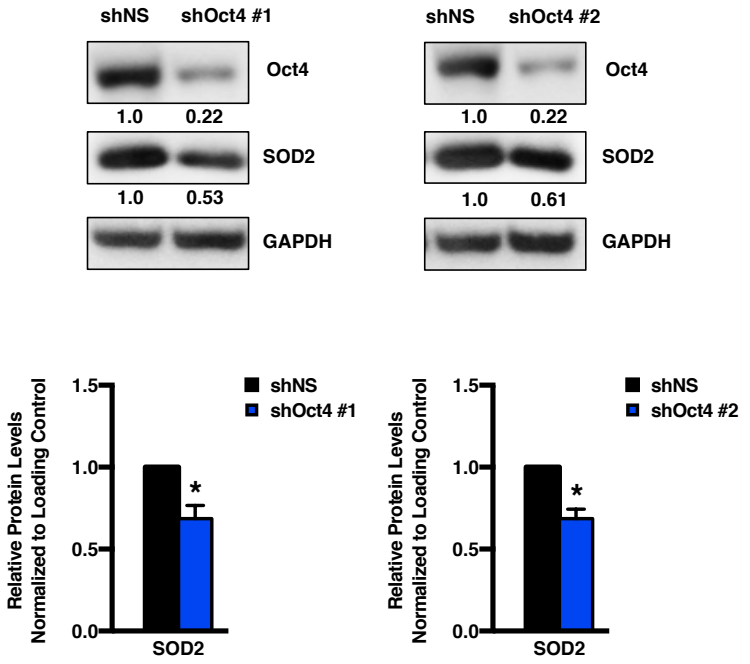

Figure 3.12. *Loss of pluripotency downregulates SOD2 expression in NT2/D1 cancer stem-like cells.* Pluripotency was inhibited in NT2/D1 cells by silencing of the master pluripotency factor, Oct4, using 2 distinct shRNAs. The expression of SOD2 was measured in shOct4 cells by western blot analysis. β-Actin was used as a loading control and all proteins were probed on the same blot with a loading volume of 5 µg of cell lysate. Blots are representative of three independent experiments and numeric values represent relative protein intensity normalized to β-Actin. Bar graphs represent average densitometry quantification from three independent experiments. Statistical analysis was performed with two-tailed, Student's t-test with 95% confidence interval. * $p < 0.05$, ** $p < 0.01$, *** $p < 0.001$, ns = not significant.

3.10 Clinically-relevant cancer stem-like cell models harbor high levels of SOD2

To further explore the hypothesis that CSLCs rely more heavily on SOD2 than their non-stem-like counterparts, the investigation was extended in two additional models of CSLCs which are more clinically relevant. The change in SOD2 expression during the normal-cancer-CSLC transition was monitored using a human breast cancer system that involves the transformation from normal breast epithelial cells to breast carcinoma cells to epithelial-to-mesenchymal transition (EMT)-induced breast cancer stem-like cells

(BCSLCs). Through this system, as illustrated in Figure 2.1, immortalized human mammary epithelial cells (HMLE), were transformed by ectopic expression of oncogenic Ras to produce HMLE-Ras (HMLER) cells, then EMT was induced through shRNA silencing of the epithelial marker E-cadherin/*CDH1*, which produced breast cancer cells with stem-like properties ($HMLER^{shECad}$) (32,179). The levels of SOD2 were found to be drastically higher in $HMLER^{shECad}$ BCSLCs compared to the non-stem-like cancerous (HMLER) and non-transformed (HMLE) counterparts, further supporting the notion that CSLCs require enhanced antioxidant defense mechanisms (Fig. 3.13A). These findings were further validated using primary, patient-derived brain cancer cells. CSLCs from brain cancers are identified based on the high expression of the stemness marker CD133. These $CD133^{High}$ brain cells display CSLCs properties such as the capacity to self-renew and seed tumor formation, hence, these cells are commonly referred to as BTICs (24,180). Tumors from GBM brain cancer patients were resected and the tumor cells were dissociated and characterized based on the expression of CD133 as illustrated in Figure 2.2 and then cultured for *in vitro* analysis. Brain tumor cells with low CD133 expression ($CD133^{Low}$) are defined as non-stem-like GBM cells and $CD133^{High}$ brain tumor cells are defined as stem-like BTICs. The expression of SOD2 was compared between non-stem-like $CD133^{Low}$ GBM cells and $CD133^{High}$ stem-like BTICs by western blot analysis. Patient-derived stem-like $CD133^{High}$ BTICs harbored considerably higher expression of SOD2 compared to non-stem like $CD133^{Low}$ GBM cells (Fig. 3.13B). Altogether, these findings provide strong credence to support the hypothesis that CSLCs are more reliant on the mitochondrial antioxidant enzyme SOD2 compared to non-stem-like and differentiated cancer cells.

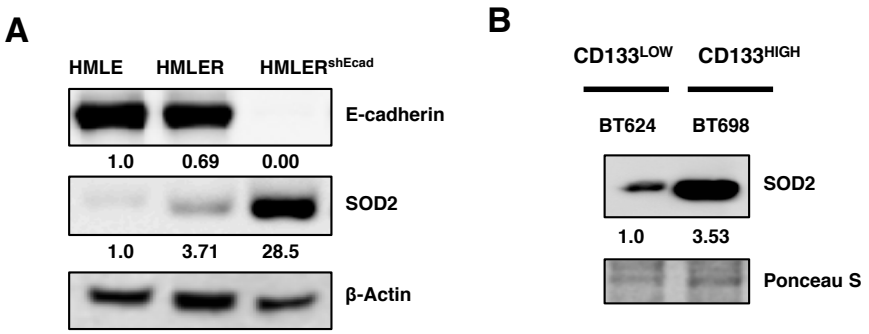

Figure 3.13. *Cancer stem-like cells rely more heavily on SOD2 expression than non-stem-like, differentiated cancer cells*. (A) Comparison of SOD2 levels by western blot analysis in non-transformed immortalized human mammary epithelial cell line (HMLE), the transformed breast carcinoma cell line (HMLER), and the epithelial-to-mesenchymal (EMT)-induced CD44+ breast cancer stem-like cells (BCSLCs), HMLER^{shECad}. β-Actin was used as a loading control and all proteins were probed on the same blot with a loading volume of 5 μg of cell lysate (n=1). Numeric values represent relative protein intensity normalized to β-Actin. (B) The levels of SOD2 were compared in non-stem-like patient-derived glioblastoma (GBM) cells which have low CD133 expression (BT624) or stem-like patient-derived brain tumor-initiating cells (BTICs) which have high CD133 expression (BT698). Ponceau Stain (S) was used as a loading control and all proteins were probed on the same blot with a loading volume of 5 μg of cell lysate (n=1). Numeric values represent relative protein intensity normalized to Ponceau S.

3.11 Targeting SOD2 in breast cancer stem-like cells suppresses stemness and promotes apoptosis

As it was found that HMLER^{shECad} BCSLCs displayed elevated levels of SOD2 compared to non-stem-like breast cancer and non-transformed breast epithelial cells, the importance of this enhanced SOD2 expression in maintaining the stemness and viability of BCSLCs was further determined. For this purpose, SOD2 expression was depleted in HMLER^{shECad} BCSLCs by shRNA-mediated silencing of SOD2 with two different shRNA clones and the effect on the stemness-associated factors Sox-2 and Bmi-1 was assessed by western blot analysis. Depletion of SOD2 in HMLER^{shECad} BCSLCs with both shRNA clones led to a downregulation in the expression of the stemness-maintaining factors Sox-

2 and Bmi-1 (Fig. 3.14). In line with the observations following SOD2 silencing in NT2/D1 CSLCs, these findings in HMLER^{shECad} BCSLCs indicate that loss of SOD2 diminishes the stemness capacity in various models of CSLCs.

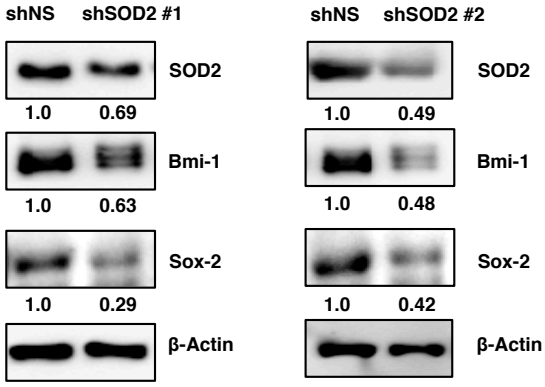

Figure 3.14. *Targeting SOD2 in breast cancer stem-like cells suppresses stemness.* HMLER^{shECad} cells with either non-silencing shRNA (shNS) control or shSOD2 (clone #1 and clone #2) were subjected to western blot analysis for Bmi-1 and Sox-2. β-Actin was used as a loading control and all proteins were probed on separate blots with the same loading volume (5 μg) from the same cell lysate (n=1). Numeric values represent relative protein intensity normalized to β-Actin.

After having established that SOD2 depletion suppresses the expression of stemness factors in NT2/D1 CSLCs and HMLER^{shECad} BCSLCs in a similar manner, it was next determined whether loss of SOD2 regulates cell death in HMLER^{shECad} BCSLCs via the same mechanisms as in NT2/D1 CSLCs. Since it was observed that SOD2 silencing promotes apoptosis, but not autophagy or necroptosis, in NT2/D1 cells, the effect of SOD2 silencing on apoptosis was examined in HMLER^{shECad} BCSLCs. Using western blot analysis, it was found that the depletion of SOD2 using two different shRNA clones increased the amount of activated, cleaved caspase-3 in HMLER^{shECad} BCSLCs as compared to controls, indicating an increase in the induction of apoptosis (Fig. 3.15). Altogether, in conjunction with findings in NT2/D1 cells, these data demonstrate the

therapeutic potential of targeting SOD2 in various types of cancer to suppress the stemness capacity of CSLCs and induce apoptosis to eliminate CSLC populations and prevent cancer relapse.

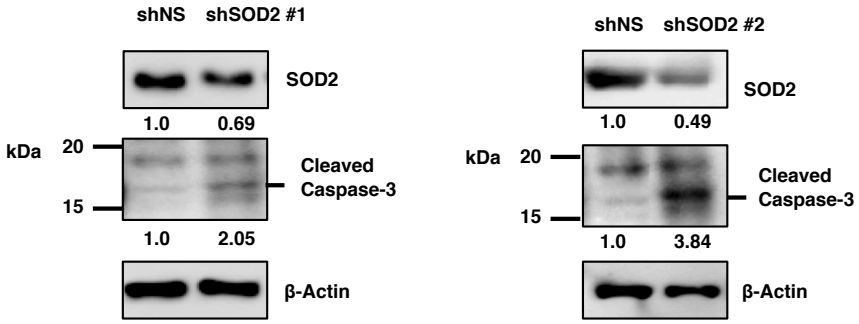

Figure 3.15. *Targeting SOD2 in breast cancer stem-like cells promotes apoptosis*. HMLER^{shECad} cells with either non-silencing shRNA (shNS) control or shSOD2 (clone #1 and clone #2) were subjected to western blot analysis for cleaved caspase-3. β-Actin was used as a loading control and all proteins were probed on separate blots with the same loading volume (5 μg) from the same cell lysate as in Figure 3.14 (n=1). Numeric values represent relative protein intensity normalized to β-Actin.

3.12 Suppression of self-renewal by SOD2 silencing in patient-derived brain-tumor initiating cells can be restored by replenishing mitochondrial antioxidant capacity

Finally, the therapeutic potential of targeting SOD2 in CSLCs was investigated in patient-derived CD133^{High} BTICs. As shown previously in Figure 3.13, stem-like CD133^{High} BTICs possess far higher levels of SOD2 as compared to non-stem-like CD133^{Low} patient-derived GBM cells. Depleting this enhanced expression of SOD2 in CD133^{High} BTICs by shRNA-mediated silencing led to the downregulation of the stemness-maintaining factor Sox-2, similar to findings observed in NT2/D1 CSLCs and HMLER^{shECad} BCSLCs (Fig. 3.16A). The effect of SOD2 on the self-renewal capacity of CD133^{High} BTICs was also investigated. The self-renewal capacity of BTICs is one of their

aggressive stemness properties that helps maintain stem-like cell populations while allowing simultaneous differentiation and recapitulation of tumor formation, leading to cancer recurrence and disease relapse (24,184). To assess the self-renewal capacity of BTICs, the well-characterized tumorsphere formation assay was used, where cells are cultivated in ultra-low attachment and specialized serum-free conditions that only support the growth of stem cells. Under these conditions, only cells with stem-like characteristics will divide and self-renew, producing groups of cells that form spheroid structures, with each spheroid originating from a single self-renewing stem-like cell (180,184-186). As seen in Figure 3.16B, SOD2 silencing in $CD133^{High}$ BTICs drastically impaired their capacity to form tumorspheres as compared to the BTICs with shNS control. These findings further highlight the importance of SOD2 for maintaining the expression of stemness-associated factors in various models of CSLCs, and also demonstrate the reliance of $CD133^{High}$ BTICs on SOD2 expression for maintaining their ability to self-renew.

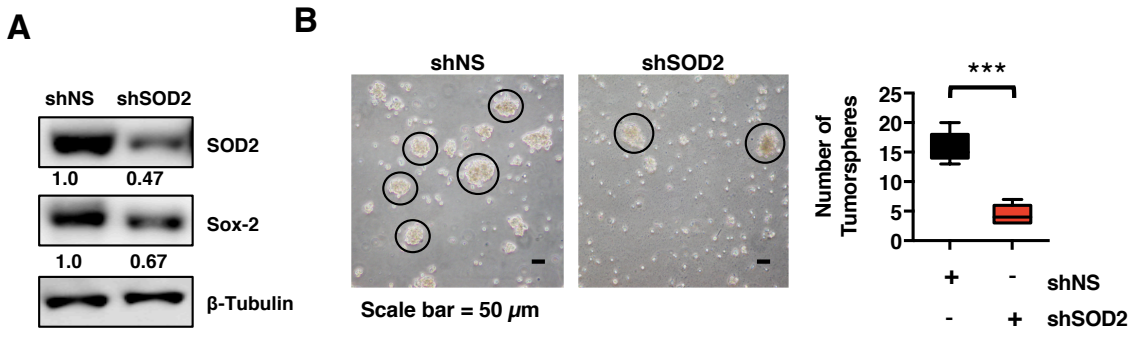

Figure 3.16

Figure 3.16. *Depletion of SOD2 in patient-derived CD133^{High} brain tumor-initiating cells suppresses stemness and self-renewal*. (A) Patient-derived CD133^{High} BTICs (BT698) with either non-silencing shRNA (shNS) control or shSOD2 were subjected to western blot analysis for Sox-2. β-Tubulin was used as a loading control and all proteins were probed on the same blot with a loading volume of 5 μg of cell lysate (n=1). Numeric values represent relative protein intensity normalized to β-Tubulin. (B) The tumorsphere formation ability of patient-derived CD133^{High} BTICs (BT698) was measured in shNS control and shSOD2 cells to assess self-renewal. Box plot represents average number of tumorspheres (>50 μm in diameter) quantified over five distinct fields of view. Statistical analysis was performed with two-tailed, Student's t-test with 95% confidence interval. * $p < 0.05$, ** $p < 0.01$, *** $p < 0.001$, ns = not significant.

The main function of antioxidant enzyme SOD2 is to prevent the accumulation of ROS in the mitochondria. To determine whether the antioxidant function of SOD2 is important for maintaining stemness features in CSLCs, the mitochondrial antioxidant activity was restored in SOD2 silenced CD133^{High} BTICs by exogenous addition of the pharmacological mitochondrial-specific antioxidant, MitoTEMPO, and the effect on self-renewal capacity was assessed. As determined previously, SOD2 depletion suppressed the tumorsphere formation capacity of CD133^{High} BTICs, however, the addition of MitoTEMPO to shNS control CD133^{High} BTICs had no significant effect on their ability to form tumorspheres. When MitoTEMPO was given to SOD2 depleted CD133^{High} BTICs, their tumorsphere formation capacity was restored back to levels similar to control cells (Fig. 3.17). These findings highlight the importance of the mitochondrial antioxidant activity of SOD2 for maintaining the self-renewal capacity of CD133^{High} BTICs, and support the hypothesis that CSLCs require antioxidant defense systems to prevent the accumulation of ROS and maintain their poorly differentiated, stem-like state.

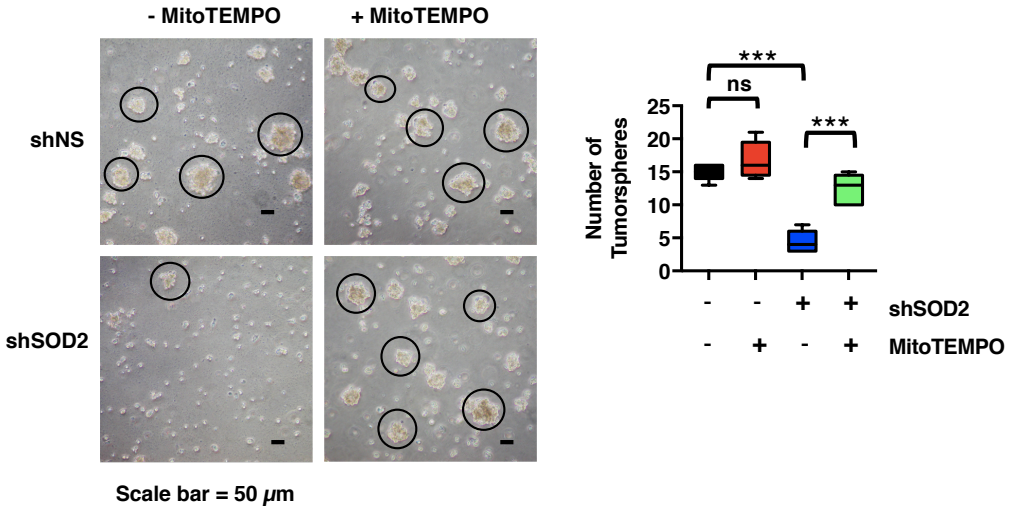

Figure 3.17. *Suppression of self-renewal by SOD2 silencing in patient-derived brain-tumor initiating cells can be restored by replenishing mitochondrial antioxidant capacity.* shNS control and shSOD2 patient-derived CD133^{High} BTICs (BT698) were treated with the mitochondrial antioxidant MitoTEMPO and their tumorsphere formation ability was measured to assess self-renewal capacity. Box plot represents average number of tumorspheres (>50 μm in diameter) quantified over five distinct fields of view. Statistical analysis was performed using ANOVA followed by Tukey's multiple comparisons test. * $p < 0.05$, ** $p < 0.01$, *** $p < 0.001$, ns = not significant.

CHAPTER 4. DISCUSSION

The cancer stem cell hypothesis proposes that small populations of poorly-differentiated cells with stem-like properties are responsible for maintaining the clonal heterogeneity of neoplastic tumor masses (15). This concept has been well-established in hematopoietic malignancies such as leukemia, where perturbances in differentiation can lead to uncontrolled proliferation and accumulation of poorly differentiated progenitor cells (26,29,198). Induction of differentiation in these cells in combination with additional chemotherapeutic agents has been highly successful in curing some hematopoietic neoplasms, such as APL (27-29). Over the past two decades, the cancer stem cell hypothesis has been expanded to encompass solid tumors, and CSLCs have been isolated from almost every tumor type (18,24,26,162-168,180,199-203). The specific markers that are used to define and isolate CSLC populations and the genetic characteristics of these CSLCs can vary based on the tumor type (17,164,200,204,205). Despite the differences in the tissue of origin, all CSLCs possess unique characteristics that define their stem-like phenotype. These characteristics include the capacity to self-renew, the potential to undergo multi-lineage differentiation, and the ability to seed tumor formation at very low cell number (15). Although CSLCs represent a rare minority population within tumor tissue, they have significant clinical implications. CSLCs, due to their unique characteristics, are often highly resistant to various traditional therapeutic interventions (17,20-23). Because these cells are highly tumorigenic, only small proportions of residual CSLCs are required to re-initiate tumor formation following treatment (24,26,165,201,203). Hence, CSLCs play an important role in cancer relapse and disease recurrence (181). As such, patients with tumors that display evidence of CSLCs

populations have a worse prognostic outcome (14,204-206). Despite the extensive evidence demonstrating the existence of CSLCs in solid tumors and their clinical impact, there are currently no therapies being used in clinics to specially target these cell populations in solid tumors. In order to identify CSLC-targeting therapies, the biological differences between CSLCs and non-stem like cancer cells must be elucidated.

SOD2 is a mitochondrial antioxidant enzyme that has a controversial role in cancer development and progression (144). While it has been demonstrated that suppressing SOD2 may enhance oncogenic transformation by increasing ROS-dependent DNA damage that leads to genomic instability and oncogenic mutations, it has also been shown that highly aggressive and metastatic cancers often display increased SOD2 expression (112,133,136,144). Aggressive and metastatic tumors have been shown to possess higher proportions of CSLC populations, however, the role of SOD2 in CSLCs has never been explored (144). Therefore, the purpose of this study was to investigate the role of SOD2 in CSLC biology using multiple models of CSLCs from various biological origins. It was hypothesized that CSLCs will rely more heavily on SOD2 compared to their non-stem-like, differentiated counterparts.

Our collaborator Dr. Sheila Singh led some of the pioneering studies deciphering the characteristics features of CSLCs in solid tumors from the brain. In 2003, Singh and colleagues characterized cells from patient brain tumors by applying a technique designed for the isolation and culture of normal neural stem cells (180). It was found that several patient tumors contained small populations of cells that were capable of propagating in conditions that only permit the growth of stem cells (180). It was determined that these tumor cells express markers that define normal stem cell populations such as Nestin and

CD133, yet, they also exhibit abnormal karyotypes that are characteristic of transformed neoplastic cells (180). Hence, these small populations represent bonafide cancer cells with stem-like characteristics, as opposed to contaminating normal neural stem cells (180). Moreover, these cells were found to contain the ability of self-renewal, a quality that only stem-like cells possess (180). In a subsequent publication, it was demonstrated that these CSLC populations could be defined and isolated based on the expression of CD133 (24). Using magnetic beads, dissociated patient-derived brain tumor cells were fractionated into $CD133^+$ stem-like brain tumor cells and $CD133^-$ non-stem-like brain tumor cells for further functional characterization. It was demonstrated that only the $CD133^+$ cells were capable of initiating brain tumor formation when xenografted into the frontal lobe of immune-compromised mice (24). It was found that as little as 100 $CD133^+$ stem-like cells were sufficient to initiate the formation of brain tumors in mice, whereas $CD133^-$ cells were incapable of forming comparable tumors after injection of $1x10^5$ cells (24). Therefore, it was concluded that a major distinguishing characteristic of stem-like $CD133^+$ brain tumor cells is their aggressive tumor-initiating capacity, whereas non-stem-like $CD133^-$ cells are far less tumorigenic (24). Hence, these $CD133^+$ cell populations are now commonly referred to as BTICs. Not only are $CD133^+$ brain tumor cells capable of initiating tumor formation, but the tumors formed from these cells also recapitulate the clonal heterogeneity of the original patient tumor (24). Furthermore, only a small subpopulation of cells within the newly formed tumor mass were found to be $CD133^+$, indicating that the bulk of $CD133^+$ cells undergo differentiation into $CD133^-$ cells upon transplantation but a small proportion of self-renewing $CD133^+$ stem-like cells is maintained within the tumor, perpetuating the tumor hierarchy (24). In line with their remarkable tumor seeding potential, it was also

demonstrated that $CD133^{+}$ stem-like brain tumor cells possess robust proliferation capacity as compared to non-stem-like $CD133^{-}$ brain tumor cells (24). To determine whether stem-like $CD133^{High}$ BTICs rely more heavily on SOD2 in order to maintain their self-renewal and enhanced proliferation capacity, the expression levels of SOD2 were compared in stem-like $CD133^{High}$ BTICs and non-stem-like $CD133^{Low}$ GBM cells. Stem-like $CD133^{High}$ BTICs were found to have drastically higher expression of SOD2 as compared to non-stem-like $CD133^{Low}$ GBM cells. Furthermore, depletion of SOD2 in $CD133^{High}$ BTICs led to a downregulation in the expression of the stemness-maintaining factor Sox-2 and significantly hampered their ability to form self-renewing tumorspheres, indicating that BTICs rely on SOD2 in order to maintain their stem-like features.

Recent studies have shown that cancer cells with stem-like properties can be generated through certain pathophysiological events that occur during oncogenic transformation. EMT is an important process for the metastasis of tumors of epithelial origin, such as breast cancers. This process involves the dedifferentiation of epithelial-type cancer cells to a more mesenchymal phenotype, which allows cells to detach from the basement membranes at the tissue of origin and disseminate to distant sites (207). In two subsequent studies from the research group led by Dr. Robert Weinberg, it was demonstrated that induction of EMT in breast cancer cells through ectopic expression of the mesenchymal-associated transcription factors Twist or Snail or by silencing of the epithelial differentiation marker E-cadherin (*CDH1*), breast cancer cells became dedifferentiated into a more mesenchymal phenotype and gained stem-like properties (32,179). These EMT-induced BCSLCs developed the expression of phenotypic markers used to identify BCSLC populations, $CD44^{High}/CD24^{Low}$ (32,179). Moreover, these EMT-

induced BCSLCs gained the ability to self-renew and seed tumor formation from only 1000 cells, whereas non-stem like breast cancer cells were unable to form comparable tumors following injection of up to $1x10^6$ cells (32,179). To determine whether CSLCs from breast cancer also have a unique reliance on SOD2 as compared to non-stem-like breast epithelial cells, the expression of SOD2 was compared between non-malignant human mammary epithelial cells (HMLE), breast carcinoma cells (HMLER), and EMT-induced BCSLCs ($HMLER^{shECad}$). It was found that EMT-induced BCSLCs harbor considerably higher levels of SOD2 compared to non-stem-like differentiated breast cancer cells and normal breast epithelial cells, further supporting the hypothesis that CSLCs rely more on SOD2 compared to their differentiated counterparts. These findings are in line with previous reports which have shown that SOD2 expression is increased following induction of EMT in breast cancer and that this may be important for cancer cells to cope with the oxidative stress associated with matrix detachment and dissemination (132,208). The findings from this study further demonstrate that this enhanced expression of SOD2 is important for maintaining the stemness capacity of BCSLC populations enriched following EMT induction, where the loss of SOD2 hampers the stemness capacity and induces apoptosis in $HMLER^{shECad}$ BCSLCs. These findings highlight a potential therapeutic opportunity to target a unique characteristic CSLCs for cancer treatment.

To maintain their enhanced proliferation and self-renewal capacity, CSCLs must undergo metabolic adaptation. The Warburg effect is a well-documented phenomenon of cancer cell metabolism, where, unlike normal cells that rely primarily on oxidative phosphorylation for energy production under aerobic conditions, cancer cells preferentially utilize glycolysis to sustain energy production and macromolecule synthesis, even in the

presence of oxygen (145-147,150). Glycolysis is a far less efficient mechanism for producing energy, as only 2 ATP molecules are produced per molecule of glucose, as compared to oxidative phosphorylation, which can produce up to 32 molecules of ATP (108,109). The possible reason that cancer cells typically enhance glycolysis is that it allows them to subvert glycolytic and TCA cycle intermediates for macromolecule synthesis to produce nucleotides and proteins required for cell growth (150,151). To compensate for the less efficient means of energy production, cancer cells will often upregulate glucose and glutamine uptake receptors to provide more fuel for glycolysis and other energy-producing pathways (145,148). The Warburg effect was the dominating central dogma of cancer cell metabolism for decades, and the hypothesis proposed by Dr. Warburg stipulated that mitochondria are dispensable for cancer cells (153). However, it is now accepted that mitochondrial metabolism is important for many types of cancers (153). Recent evidence has highlighted the complexities of cancer cell metabolism and the heterogeneous metabolic phenotypes of cancer cells from different types of cancers (108). Moreover, accumulating evidence has demonstrated that different populations of cancer cells within heterogeneous tumor masses display differential metabolic dependencies (158,160,161).

Due to their high proliferative capacity, tumorigenic potential and drug-resistant properties, it was originally speculated that CSLCs should rely heavily on glycolysis to maintain the macromolecule demands associated with rapid proliferation. This theory was strengthened by the existing knowledge that normal stem cells display a highly glycolytic phenotype and that switching from oxidative phosphorylation to glycolysis is a hallmark of successful reprogramming of induced pluripotent stem cells (iPSCs) (209,210). The

concept that CSLCs favor glycolysis more than differentiated cancer cells has been supported by several studies in hepatocellular carcinoma, glioblastoma, breast cancer, and osteosarcoma (211-214). However, other studies in glioblastoma, ovarian cancer, breast cancer, lung cancer, and leukemia, have demonstrated that CSLCs prefer to utilize oxidative phosphorylation as their primary means of energy production (155-158,160). Examination of CSLCs derived from patient glioma and ovarian tumors have also advocated that CSLCs rely on oxidative phosphorylation (157,160). These discrepancies could be attributed to a higher degree of metabolic plasticity within CSLCs, where some studies have demonstrated that CSLCs can readily switch between glycolysis and oxidative phosphorylation for energy productions depending on the environmental circumstances (154,159). Studies have demonstrated that cells undergoing EMT also undergo metabolic reprogramming and that breast cancer cells may require more metabolic plasticity during EMT to adapt to stress and therefore rely on both glycolysis and oxidative phosphorylation (215,216). Metabolic plasticity in cancer cells is attributed to increased aggressiveness and confers a growth advantage for cancer cells under conditions of metabolic or hypoxic stress. Metabolic plasticity may also play a role in the chemoresistant nature of CSLCs (154,159).

Because of the enhanced proliferation potential and unique metabolic requirements of CSLCs compared to non-stem-like differentiated cancer cells, it is highly likely that CSLCs are more reliant on antioxidant defense systems for removal of ROS waste generated by increased metabolic activity. In support of this hypothesis, it was observed that CSLCs from GBM and breast cancer models express higher levels of the mitochondrial antioxidant enzyme SOD2 as compared to non-stem-like differentiated cancer cells. To

determine whether this characteristic of CSLCs could be exploited as a therapeutic vulnerability, the effect of targeting SOD2 in CSLCs was explored. Indeed, it was found that the depletion of SOD2 in embryonal CSLCs led to a significant increase in the levels of ROS, indicating that CSLCs rely on the antioxidant function of SOD2 to prevent the accumulation of ROS. Furthermore, it was found that replenishing the mitochondrial antioxidant capacity in SOD2-deficient $CD133^{High}$ GBM BTICs through exogenous supplementation with the mitochondrial antioxidant MitoTEMPO significantly restored their self-renewal capacity, further indicating that the mitochondrial antioxidant function of SOD2 is important for maintaining the stemness capacity of CSLCs.

Differentiation therapy in combination with other chemotherapeutic strategies has been very successful in clinics for targeting stem-like progenitor cell populations in hematopoietic malignancies (29). Recent studies have also highlighted the potential for pursuing differentiation-inducing therapies to target CSLCs from solid tumors (30,33), although this strategy has yet to be pursued in clinics. High levels of ROS are also known to induce differentiation in normal stem cells (169), therefore, it is reasonable to postulate that inhibition of the antioxidant enzyme SOD2 may represent a valid therapeutic strategy to induce differentiation and inhibit the stemness capacity of CSLCs. To explore the role of SOD2 in the differentiation of CSLCs, the NT2/D1 embryonal CSLC line was utilized. NT2/D1 cells possess all of the traditional stem cell properties such as the ability to self-renew and maintain an undifferentiated state (174-176,217). These cells express all of the major reprogramming pluripotency factors (Oct4, Nanog, Sox-2 and KLF4) (218) and have a similar gene expression signature to ESCs, which has been associated with cancers that are poorly differentiated and more aggressive (14). These cells also have the potential to

differentiate into many different downstream derivatives from ectoderm, mesoderm, and endodermal lineages and are commonly used to study neuroendothelial differentiation. Thus, NT2/D1 cells represent a useful model for studying the role of SOD2 in regulating stemness and differentiation in CSLCs (196,219,220). It was observed that silencing SOD2 drastically hampered the proliferation of NT2/D1 CSLCs and suppressed the expression of pluripotency factors (Oct4, Nanog, Sox-2, and KLF-4) involved in stemness maintenance. These findings indicate that CSLCs are sensitive to targeting SOD2 and that depletion of SOD2 abrogates their proliferation and stemness capacity. Interestingly, this suppression of proliferation and stemness following SOD2 silencing in NT2/D1 CSLCs was accompanied by induction of multi-lineage differentiation as determined by western blot and immunofluorescence analysis of differentiation marker β3-tubulin and as well qRT-PCR analysis of differentiation markers from several distinct lineages (Ectoderm: *BMP4, CDX2;* Neural Progenitor: *TUBB3, SYP, AHNAK;* Endoderm: *SPP1;* Mesenchymal: *VIM*; and Mesoderm: *TBXT*). The hypothesis that CSLCs rely more heavily on SOD2 than differentiated cancer cells was further confirmed in NT2/D1 CSLCs, where it was found that induction of differentiation by suppressing the expression of pluripotency-maintaining factor Oct4, led to a downregulation in the expression of SOD2. These findings indicate that once CSLCs lose their pluripotent capacity and undergo differentiation, they do not require enhanced SOD2 expression. These findings highlight the potential of targeting SOD2 in CSLCs to suppress their stemness capacity and promote differentiation, which may render them more susceptible to subsequent therapeutic interventions.

Recent studies have highlighted the importance of the metabolism-responsive process of autophagy in maintaining the stemness of both normal and CSLCs (83-85,221).

It has been demonstrated that any deviation in the homeostatic balance of autophagy, either through upregulation or downregulation, is sufficient to hamper stemness and induce differentiation (85). Since it was observed that loss of SOD2 suppresses stemness and promotes differentiation in CSLCs, the effect on autophagy was monitored. Using two different assays to asses autophagy flux and puncta formation, it was determined that SOD2 silencing does not promote autophagy in CSLCs. The upregulation of autophagy has been shown to act as an adaptive resistance mechanism in response to therapeutic stress (74). In two recent independent studies, it was found that inhibition of mutant Ras or downstream ERK/MEK signaling in pancreatic ductal adenocarcinoma (PDAC) cells leads to robust activation of autophagy which confers resistance (222,223). Using patient-derived xenograft models, Bryant et al. and Kinsey et al. both found that concomitant treatment of PDAC tumors with ERK/MEK inhibitors and autophagy inhibitors leads to a synergistic suppression of tumor growth and represents a viable combination strategy to target mutant RAS-driven cancers (222,223). Since it was observed that SOD2 inhibition hampers growth and promotes differentiation of CSLCs without inducing autophagy, these findings indicate that targeting SOD2 may represent an ideal strategy to inhibit CSLCs without activating resistance-associated mechanisms. Further mechanistic analysis determined that SOD2 depletion leads to activation of p-AKT and p-MTOR, two upstream negative regulators of autophagy. P-MTOR acts as a major regulator of autophagy in response to metabolic stress (36). Since it was observed that p-MTOR is activated, this indicates that CSLCs are not deprived of nutrients or energy following SOD2 inhibition. Subsequent proteomic analysis revealed that many proteins related to mitochondria and metabolism are modulated following SOD2 suppression in CSLCs. In particular, several enzymes involved

in the glycolytic pathway are upregulated following SOD2 depletion. These findings indicate that CSLCs may rewire their metabolism towards glycolysis following the loss of SOD2, possibly as a means to maintain energy production while limiting the amount of mitochondrial ROS generated by oxidative phosphorylation. Hence, energy deprivation may not be a mechanism-of-action associated with targeting SOD2 in CSLCs, which could explain why autophagy is not activated in response to SOD2 silencing.

Induction of cancer cell death is a desirable therapeutic response to cancer-targeting interventions (224). However, resistance to apoptosis-inducing stimuli is a well-established hallmark of cancer (5). Therapeutic strategies that overcome this resistance and promote apoptotic cell death in cancer cells are typically effective anti-cancer agents. Despite this, CSLCs often display increased resistance to chemotherapeutic agents that otherwise kill non-stem-like differentiated cancer cells (23). Therefore, it is important to identify novel targets that are able to eliminate CSLC populations by promoting apoptosis. It was found that silencing of SOD2 led to a strong induction of apoptotic cell death in CSLCs as indicated by activation of the executioner caspase-3 and evidence of proteolytic cleavage of its target substrates. Moreover, proteomic analysis identified several proteins related to apoptosis which were upregulated following the loss of SOD2. It was also found that SOD2 does not induce the activation of necroptosis, an apoptosis-independent mechanism of traumatic cell death. Unlike apoptosis, necroptosis is typically associated with the activation of inflammatory responses following cell death. It has been postulated that the induction of necroptosis may be desirable for cancer therapy, as activation of anti-tumor immune responses can help eliminate tumor cells and prevent cancer recurrence (225). However, pro-inflammatory responses associated with necroptosis have also been

associated with facilitating the invasion and metastasis of cancer cells (225). Therefore, targeting SOD2 may be ideal for selectively inducing apoptotic cell death of cancer cells without promoting pro-tumor inflammatory responses. These findings further highlight the potential of targeting SOD2 as a therapeutic strategy for the effective elimination of CSLC populations.

4.1 Limitations of the study and future directions

The results of this study propose SOD2 as a novel therapeutic target to inhibit CSLCs. It was observed that SOD2 depletion effectively suppresses the stemness capacity of various CSLC models and has the ability to promote the differentiation and elimination of CSLCs via apoptotic cell death. There are several findings from this investigation that could be expanded upon in future studies to gain a more comprehensive understanding of the mechanisms associated with targeting SOD2 and the efficacy of inhibiting SOD2 as a therapeutic strategy. Potential future experiments that could be pursued are described below.

4.1.1 Understanding how SOD2 depletion regulates the expression of stemness factors

It was observed that silencing of SOD2 suppresses the stemness features of NT2/D1 CSLCs, HMLER^{shECad} BCSLCs, and patient-derived CD133^{High} BTICs. Moving forward, it will important to characterize the molecular mechanisms by which SOD2 regulates stemness. The downregulation of stemness-maintaining transcription factors following SOD2 depletion was a key finding observed in all three CSLC models. Therefore, it would be interesting to determine the mechanisms by which these stemness factors are decreased following SOD2 silencing. For this purpose, the post-translational stability of stemness factors could be explored. The proteasome inhibitor MG132 (also known as Bortezomib)

could be used in SOD2 silenced CSLCs to determine whether the downregulated expression of stemness factors can be rescued following inhibition of proteasomal degradation. Since the loss of the antioxidant enzyme SOD2 leads to the accumulation of ROS in CSLCs, it is possible that this promotes the oxidation of cysteine residues on important stemness-maintaining factors. It has been demonstrated in human ESCs that the accumulation of ROS under glutamine and GSH deficiency leads to oxidation of the pluripotency factor Oct4 (226). This increase in oxidation abrogates the DNA binding activity of Oct4 and promotes its degradation. This loss in Oct4 activity and expression suppresses stemness and promotes the differentiation of ESCs (226). It is likely that the mechanism by which SOD2 depletion regulates stemness is dependent on the accumulation of ROS, as it was found that restoration of mitochondrial antioxidant activity by exogenous administration of MitoTEMPO effectively rescued the self-renewal capacity of patient-derived $CD133^{High}$ BTICs. Identification and characterization of the downstream molecular targets mediating the response of SOD2 silencing could lead to the development of combinatorial strategies to be pursued to enhance therapeutic efficacy.

4.1.2 Exploring the mechanisms associated with SOD2 depletion-mediated induction of apoptosis

It was found that SOD2 silencing leads to the induction of apoptosis in CSLCs. Future investigations ought to explore the mechanisms associated with SOD2 depletion-mediated apoptosis. Since SOD2 is located in the mitochondria, it is likely that mitochondrial apoptotic signaling is affected by the loss of SOD2 expression. It would be of interest to analyze the effect of SOD2 depletion on the expression or phosphorylation of mitochondrial associated anti-apoptotic proteins such as Bcl-2 and pro-apoptotic proteins

such as Bax and Bak (59). One common mechanism leveraged by cancer cells to evade apoptotic stimuli is through the overexpression of inhibitors of apoptosis (IAP) proteins, which will directly bind and inhibit the function of caspase proteases and prevent apoptotic cell death (227,228). Naturally occurring antagonists of IAPs have been identified, which have the ability to interact directly with IAP proteins and allow the release and activation of caspases (229-231). Some common IAP-antagonists include SMAC, Diablo and ARTS (a pro-apoptotic splice variant of the Septin4 gene, Sept4_i2) (230-232). Often, cancer cells will suppress the expression of IAP-antagonists as a means of protecting IAP-mediated resistance to apoptosis (233). Because IAP antagonists possess the ability to potently inhibit IAPs and activate apoptosis, small peptides that mimic the function of naturally occurring antagonists of IAPs, such as SMAC and ARTS, have been developed and are currently under clinical evaluation (234-237). It would be of interest to explore the effect of SOD2 silencing on the expression and activation of IAP-antagonists and investigate whether the combination of SOD2 inhibition along with administration of IAP-antagonist mimetic peptides could be utilized to enhance the therapeutic efficacy of SOD2-depletion mediated apoptosis.

4.1.3 Characterization of the metabolic phenotype of SOD2-deficient cancer stem-like cells

The findings from this investigation suggest that silencing of SOD2 does not lead to energy-deprivation or induction of autophagy in CSLCs. Proteomics analysis indicates that CSLCs may upregulate glycolytic metabolism as a mechanism of maintaining energy production and minimizing mitochondrial ROS production. Further studies should aim to validate these observations using molecular techniques such as western blot and qRT-PCR

for the expression of glycolytic enzymes. Further metabolic analysis could be performed using a Seahorse© extracellular flux (XF) analyzer to measure the mitochondrial oxygen consumption rate (OCR) and the extracellular acidification rate (ECAR) to assess changes in OXPHOS and glycolytic activity, respectively. MS-based metabolomics techniques could also determine whether these changes in the expression of glycolytic enzymes modulates the overall metabolic activity of CSLCs. If glycolytic activity is indeed enhanced following SOD2 silencing in CSLCs, then it would be reasonable to explore whether concomitant suppression of glycolytic activity by treatment with glycolysis inhibitors such as 2-deoxyglucose (2-DG) and Bromopyruvic Acid (BrPA) in combination with targeting SOD2 could lead to synergistic suppression of CSLC growth.

4.1.4 Investigation of the effect of SOD2 silencing in cancer stem-like cells on other enzymes and non-enzymatic components of the antioxidant defense system

Following SOD2 depletion in CSLCs, it was found that the levels of ROS were increased, indicating that SOD2 is critical for preventing the accumulation of ROS in CSLCs. This suggests that other components of the antioxidant defense system are not able to fully compensate and maintain low ROS levels following the loss of SOD2 in CSLCs. However, it would be of interest to explore the effect of SOD2 silencing on the levels and activity of other antioxidant enzymes and non-enzymatic antioxidants such as SOD1, Catalase, and GSH. It is possible that the expression or activity of these antioxidants may be enhanced in CSLCs following SOD2 depletion which may prevent the accumulation of ROS to lethal levels. Targeting other components of the antioxidant defense system along with SOD2 (e.g. through SOD1 inhibition or glutamine deprivation to suppress GSH) may

have an additive effect for suppressing the growth and viability of CSLCs and could be explored as a potential therapeutic combination strategy.

4.1.5 Exploring the potential toxic side effects of SOD2 inhibition in non-malignant cells

The findings from this study demonstrate that SOD2 inhibition represents an effective strategy to suppress the proliferation and stemness capacity of CSLCs and promote their elimination through apoptotic cell death. However, an ideal anti-cancer therapy must also display minimal toxicity in normal, non-malignant cells in order to mitigate detrimental side-effects in patients. Therefore, the effect of SOD2 depletion should also be investigated in several non-transformed cell models from various origins such as fibroblasts and epithelial cells. Ideally, inhibition of SOD2 in normal cells will not affect the growth or viability of these cells and will not induce apoptosis. The findings presented here showing the comparison of SOD2 levels in the breast cancer transition model (HMLE-HMLER-HMLER^{shECad} cells) demonstrate that non-malignant HMLE mammary epithelial cells possess much lower expression of SOD2 compared to HMLER^{shECad} BCSLCs, which indicates that these cells may not rely as heavily on SOD2 expression and may be less sensitive to SOD2 inhibition. However, the HMLE cell line may not be the best representation of normal breast epithelial tissue, as these cells have been immortalized using SV40 T antigen, which inactivates the tumor suppressors Rb and p53. Therefore, it would also be important to investigate the expression of SOD2 in normal, primary tissues that have not been genetically manipulated.

4.1.6 Development of specific SOD2 inhibiting drugs and assessment of the therapeutic efficacy of targeting of SOD2 in vivo

Utilizing shRNA-mediated silencing techniques, the findings from this study provide *in vitro* evidence that the specific targeting of SOD2 can effectively suppress the proliferation and stemness capacity of CSLCs and promote apoptotic cell death. The effect of SOD2 silencing on the tumorigenic potential of CSLCs could be explored *in vivo* using limiting dilution tumorigenicity assays of CSLC models and patient-derived xenografts (PDXs). However, RNA-mediated silencing is not a viable option to use for therapeutic inhibition of SOD2 in developed tumors *in vivo* or in patients, as the effective delivery of small RNAs to tumors and efficient uptake and processing by cancer cells *in vivo* and in patients remains a problem. Therefore, it would be important to pursue the development of potent and specific drug inhibitors of SOD2 to evaluate the *in vivo* therapeutic efficacy of targeting SOD2 for cancer treatment.

4.2 Conclusions

Altogether, from the findings of this work we conclude that CSLCs, as compared to their non-stem-like differentiated counterparts, have enhanced expression of SOD2 and are sensitive to manipulations that suppress SOD2 expression. These observations highlight the important role of the antioxidant defense system in maintaining the poorly differentiated physiology of CSLCs and also identify SOD2 as a potential clinically-relevant therapeutic target for cancer treatment.

REFERENCES

1. Bray F, Ferlay J, Soerjomataram I, Siegel RL, Torre LA, Jemal A. Global cancer statistics 2018: GLOBOCAN estimates of incidence and mortality worldwide for 36 cancers in 185 countries. CA Cancer J Clin **2018**;68(6):394-424 doi 10.3322/caac.21492.

2. Canadian Cancer Statistics 2018. Toronto, ON: Canadian Cancer Society; 2018.

3. Lichtenstein P, Holm NV, Verkasalo PK, Iliadou A, Kaprio J, Koskenvuo M*, et al.* Environmental and heritable factors in the causation of cancer--analyses of cohorts of twins from Sweden, Denmark, and Finland. N Engl J Med **2000**;343(2):78-85 doi 10.1056/NEJM200007133430201.

4. Salk JJ, Fox EJ, Loeb LA. Mutational heterogeneity in human cancers: origin and consequences. Annu Rev Pathol **2010**;5:51-75 doi 10.1146/annurev-pathol-121808-102113.

5. Hanahan D, Weinberg RA. The hallmarks of cancer. Cell **2000**;100(1):57-70.

6. Hanahan D, Weinberg RA. Hallmarks of cancer: the next generation. Cell **2011**;144(5):646-74 doi 10.1016/j.cell.2011.02.013.

7. Coyle KM, Boudreau JE, Marcato P. Genetic Mutations and Epigenetic Modifications: Driving Cancer and Informing Precision Medicine. Biomed Res Int **2017**;2017:9620870 doi 10.1155/2017/9620870.

8. Steinherz LJ, Steinherz PG, Tan CT, Heller G, Murphy ML. Cardiac toxicity 4 to 20 years after completing anthracycline therapy. JAMA **1991**;266(12):1672-7.

9. Timmerman R, McGarry R, Yiannoutsos C, Papiez L, Tudor K, DeLuca J*, et al.* Excessive toxicity when treating central tumors in a phase II study of stereotactic body radiation therapy for medically inoperable early-stage lung cancer. J Clin Oncol **2006**;24(30):4833-9 doi 10.1200/JCO.2006.07.5937.

10. Willers H, Azzoli CG, Santivasi WL, Xia F. Basic mechanisms of therapeutic resistance to radiation and chemotherapy in lung cancer. Cancer J **2013**;19(3):200-7 doi 10.1097/PPO.0b013e318292e4e3.

11. Doyle LA, Yang W, Abruzzo LV, Krogmann T, Gao Y, Rishi AK*, et al.* A multidrug resistance transporter from human MCF-7 breast cancer cells. Proc Natl Acad Sci U S A **1998**;95(26):15665-70 doi 10.1073/pnas.95.26.15665.

12. McGranahan N, Swanton C. Clonal Heterogeneity and Tumor Evolution: Past, Present, and the Future. Cell **2017**;168(4):613-28 doi 10.1016/j.cell.2017.01.018.

13. Stingl J, Caldas C. Molecular heterogeneity of breast carcinomas and the cancer stem cell hypothesis. Nat Rev Cancer **2007**;7(10):791-9 doi 10.1038/nrc2212.

14. Ben-Porath I, Thomson MW, Carey VJ, Ge R, Bell GW, Regev A*, et al.* An embryonic stem cell-like gene expression signature in poorly differentiated aggressive human tumors. Nat Genet **2008**;40(5):499-507 doi 10.1038/ng.127.

15. Reya T, Morrison SJ, Clarke MF, Weissman IL. Stem cells, cancer, and cancer stem cells. Nature **2001**;414(6859):105-11 doi 10.1038/35102167.

16. Lobo NA, Shimono Y, Qian D, Clarke MF. The biology of cancer stem cells. Annu Rev Cell Dev Biol **2007**;23:675-99 doi 10.1146/annurev.cellbio.22.010305.104154.

17. Liu G, Yuan X, Zeng Z, Tunici P, Ng H, Abdulkadir IR*, et al.* Analysis of gene expression and chemoresistance of CD133+ cancer stem cells in glioblastoma. Mol Cancer **2006**;5:67 doi 10.1186/1476-4598-5-67.

18. Bertolini G, Roz L, Perego P, Tortoreto M, Fontanella E, Gatti L*, et al.* Highly tumorigenic lung cancer CD133+ cells display stem-like features and are spared by cisplatin treatment. Proc Natl Acad Sci U S A **2009**;106(38):16281-6 doi 10.1073/pnas.0905653106.

19. Sarvi S, Mackinnon AC, Avlonitis N, Bradley M, Rintoul RC, Rassl DM*, et al.* CD133+ cancer stem-like cells in small cell lung cancer are highly tumorigenic and chemoresistant but sensitive to a novel neuropeptide antagonist. Cancer Res **2014**;74(5):1554-65 doi 10.1158/0008-5472.CAN-13-1541.

20. Eramo A, Ricci-Vitiani L, Zeuner A, Pallini R, Lotti F, Sette G*, et al.* Chemotherapy resistance of glioblastoma stem cells. Cell Death Differ **2006**;13(7):1238-41 doi 10.1038/sj.cdd.4401872.

21. Tanei T, Morimoto K, Shimazu K, Kim SJ, Tanji Y, Taguchi T*, et al.* Association of breast cancer stem cells identified by aldehyde dehydrogenase 1 expression with resistance to sequential Paclitaxel and epirubicin-based chemotherapy for breast cancers. Clin Cancer Res **2009**;15(12):4234-41 doi 10.1158/1078-0432.CCR-08-1479.

22. Bao S, Wu Q, McLendon RE, Hao Y, Shi Q, Hjelmeland AB*, et al.* Glioma stem cells promote radioresistance by preferential activation of the DNA damage response. Nature **2006**;444(7120):756-60 doi 10.1038/nature05236.

23. Abdullah LN, Chow EK. Mechanisms of chemoresistance in cancer stem cells. Clin Transl Med **2013**;2(1):3 doi 10.1186/2001-1326-2-3.

24. Singh SK, Hawkins C, Clarke ID, Squire JA, Bayani J, Hide T*, et al.* Identification of human brain tumour initiating cells. Nature **2004**;432(7015):396-401 doi 10.1038/nature03128.

25. Quintana E, Shackleton M, Sabel MS, Fullen DR, Johnson TM, Morrison SJ. Efficient tumour formation by single human melanoma cells. Nature **2008**;456(7222):593-8 doi 10.1038/nature07567.

26. Lapidot T, Sirard C, Vormoor J, Murdoch B, Hoang T, Caceres-Cortes J*, et al.* A cell initiating human acute myeloid leukaemia after transplantation into SCID mice. Nature **1994**;367(6464):645-8 doi 10.1038/367645a0.

27. Huang ME, Ye YC, Chen SR, Chai JR, Lu JX, Zhoa L*, et al.* Use of all-trans retinoic acid in the treatment of acute promyelocytic leukemia. Blood **1988**;72(2):567-72.

28. Castaigne S, Chomienne C, Daniel MT, Ballerini P, Berger R, Fenaux P*, et al.* All-trans retinoic acid as a differentiation therapy for acute promyelocytic leukemia. I. Clinical results. Blood **1990**;76(9):1704-9.

29. de The H, Chen Z. Acute promyelocytic leukaemia: novel insights into the mechanisms of cure. Nat Rev Cancer **2010**;10(11):775-83 doi 10.1038/nrc2943.

30. Campos B, Wan F, Farhadi M, Ernst A, Zeppernick F, Tagscherer KE*, et al.* Differentiation therapy exerts antitumor effects on stem-like glioma cells. Clin Cancer Res **2010**;16(10):2715-28 doi 10.1158/1078-0432.CCR-09-1800.

31. Caren H, Stricker SH, Bulstrode H, Gagrica S, Johnstone E, Bartlett TE*, et al.* Glioblastoma Stem Cells Respond to Differentiation Cues but Fail to Undergo Commitment and Terminal Cell-Cycle Arrest. Stem Cell Reports **2015**;5(5):829-42 doi 10.1016/j.stemcr.2015.09.014.

32. Gupta PB, Onder TT, Jiang G, Tao K, Kuperwasser C, Weinberg RA*, et al.* Identification of selective inhibitors of cancer stem cells by high-throughput screening. Cell **2009**;138(4):645-59 doi 10.1016/j.cell.2009.06.034.

33. Beug H. Breast cancer stem cells: eradication by differentiation therapy? Cell **2009**;138(4):623-5 doi 10.1016/j.cell.2009.08.007.

34. Mizushima N. Autophagy: process and function. Genes Dev **2007**;21(22):2861-73 doi 10.1101/gad.1599207.

35. Mizushima N, Yamamoto A, Matsui M, Yoshimori T, Ohsumi Y. In vivo analysis of autophagy in response to nutrient starvation using transgenic mice expressing a fluorescent autophagosome marker. Mol Biol Cell **2004**;15(3):1101-11 doi 10.1091/mbc.e03-09-0704.

36. Jung CH, Ro SH, Cao J, Otto NM, Kim DH. mTOR regulation of autophagy. FEBS Lett **2010**;584(7):1287-95 doi 10.1016/j.febslet.2010.01.017.

37. Manning BD, Tee AR, Logsdon MN, Blenis J, Cantley LC. Identification of the tuberous sclerosis complex-2 tumor suppressor gene product tuberin as a target of the phosphoinositide 3-kinase/akt pathway. Mol Cell **2002**;10(1):151-62.

38. Nave BT, Ouwens M, Withers DJ, Alessi DR, Shepherd PR. Mammalian target of rapamycin is a direct target for protein kinase B: identification of a convergence point for opposing effects of insulin and amino-acid deficiency on protein translation. Biochem J **1999**;344 Pt 2:427-31.

39. Inoki K, Li Y, Zhu T, Wu J, Guan KL. TSC2 is phosphorylated and inhibited by Akt and suppresses mTOR signalling. Nat Cell Biol **2002**;4(9):648-57 doi 10.1038/ncb839.

40. Inoki K, Li Y, Xu T, Guan KL. Rheb GTPase is a direct target of TSC2 GAP activity and regulates mTOR signaling. Genes Dev **2003**;17(15):1829-34 doi 10.1101/gad.1110003.

41. Long X, Lin Y, Ortiz-Vega S, Yonezawa K, Avruch J. Rheb binds and regulates the mTOR kinase. Curr Biol **2005**;15(8):702-13 doi 10.1016/j.cub.2005.02.053.

42. Hay N, Sonenberg N. Upstream and downstream of mTOR. Genes Dev **2004**;18(16):1926-45 doi 10.1101/gad.1212704.

43. Pyo JO, Nah J, Jung YK. Molecules and their functions in autophagy. Exp Mol Med **2012**;44(2):73-80 doi 10.3858/emm.2012.44.2.029.

44. Kabeya Y, Mizushima N, Ueno T, Yamamoto A, Kirisako T, Noda T*, et al.* LC3, a mammalian homologue of yeast Apg8p, is localized in autophagosome membranes after processing. EMBO J **2000**;19(21):5720-8 doi 10.1093/emboj/19.21.5720.

45. Johansen T, Lamark T. Selective autophagy mediated by autophagic adapter proteins. Autophagy **2011**;7(3):279-96.

46. Klionsky DJ, Abdelmohsen K, Abe A, Abedin MJ, Abeliovich H, Acevedo Arozena A*, et al.* Guidelines for the use and interpretation of assays for monitoring autophagy (3rd edition). Autophagy **2016**;12(1):1-222 doi 10.1080/15548627.2015.1100356.

47. Huang J, Klionsky DJ. Autophagy and human disease. Cell Cycle **2007**;6(15):1837-49.

48. Mathew R, Karantza-Wadsworth V, White E. Role of autophagy in cancer. Nat Rev Cancer **2007**;7(12):961-7 doi 10.1038/nrc2254.

49. Degenhardt K, Mathew R, Beaudoin B, Bray K, Anderson D, Chen G*, et al.* Autophagy promotes tumor cell survival and restricts necrosis, inflammation, and tumorigenesis. Cancer Cell **2006**;10(1):51-64 doi 10.1016/j.ccr.2006.06.001.

50. Karantza-Wadsworth V, Patel S, Kravchuk O, Chen G, Mathew R, Jin S*, et al.* Autophagy mitigates metabolic stress and genome damage in mammary tumorigenesis. Genes Dev **2007**;21(13):1621-35 doi 10.1101/gad.1565707.

51. Lum JJ, Bauer DE, Kong M, Harris MH, Li C, Lindsten T*, et al.* Growth factor regulation of autophagy and cell survival in the absence of apoptosis. Cell **2005**;120(2):237-48 doi 10.1016/j.cell.2004.11.046.

52. Karsli-Uzunbas G, Guo JY, Price S, Teng X, Laddha SV, Khor S*, et al.* Autophagy is required for glucose homeostasis and lung tumor maintenance. Cancer Discov **2014**;4(8):914-27 doi 10.1158/2159-8290.CD-14-0363.

53. Fuchs Y, Steller H. Live to die another way: modes of programmed cell death and the signals emanating from dying cells. Nat Rev Mol Cell Biol **2015**;16(6):329-44 doi 10.1038/nrm3999.

54. Maiuri MC, Zalckvar E, Kimchi A, Kroemer G. Self-eating and self-killing: crosstalk between autophagy and apoptosis. Nat Rev Mol Cell Biol **2007**;8(9):741-52 doi 10.1038/nrm2239.

55. Wei MC, Zong WX, Cheng EH, Lindsten T, Panoutsakopoulou V, Ross AJ*, et al.* Proapoptotic BAX and BAK: a requisite gateway to mitochondrial dysfunction and death. Science **2001**;292(5517):727-30 doi 10.1126/science.1059108.

56. Zou H, Li Y, Liu X, Wang X. An APAF-1.cytochrome c multimeric complex is a functional apoptosome that activates procaspase-9. J Biol Chem **1999**;274(17):11549-56 doi 10.1074/jbc.274.17.11549.

57. Kim HE, Du F, Fang M, Wang X. Formation of apoptosome is initiated by cytochrome c-induced dATP hydrolysis and subsequent nucleotide exchange on Apaf-1. Proc Natl Acad Sci U S A **2005**;102(49):17545-50 doi 10.1073/pnas.0507900102.

58. Jiang X, Wang X. Cytochrome c promotes caspase-9 activation by inducing nucleotide binding to Apaf-1. J Biol Chem **2000**;275(40):31199-203 doi 10.1074/jbc.C000405200.

59. Elmore S. Apoptosis: a review of programmed cell death. Toxicol Pathol **2007**;35(4):495-516 doi 10.1080/01926230701320337.

60. Woo M, Hakem R, Soengas MS, Duncan GS, Shahinian A, Kagi D*, et al.* Essential contribution of caspase 3/CPP32 to apoptosis and its associated nuclear changes. Genes Dev **1998**;12(6):806-19.

61. Slee EA, Adrain C, Martin SJ. Executioner caspase-3, -6, and -7 perform distinct, non-redundant roles during the demolition phase of apoptosis. J Biol Chem **2001**;276(10):7320-6 doi 10.1074/jbc.M008363200.

62. Lazebnik YA, Kaufmann SH, Desnoyers S, Poirier GG, Earnshaw WC. Cleavage of poly(ADP-ribose) polymerase by a proteinase with properties like ICE. Nature **1994**;371(6495):346-7 doi 10.1038/371346a0.

63. Enari M, Sakahira H, Yokoyama H, Okawa K, Iwamatsu A, Nagata S. A caspase-activated DNase that degrades DNA during apoptosis, and its inhibitor ICAD. Nature **1998**;391(6662):43-50 doi 10.1038/34112.

64. Wolf BB, Schuler M, Echeverri F, Green DR. Caspase-3 is the primary activator of apoptotic DNA fragmentation via DNA fragmentation factor-45/inhibitor of caspase-activated DNase inactivation. J Biol Chem **1999**;274(43):30651-6 doi 10.1074/jbc.274.43.30651.

65. Okamoto K, Kondo-Okamoto N, Ohsumi Y. Mitochondria-anchored receptor Atg32 mediates degradation of mitochondria via selective autophagy. Dev Cell **2009**;17(1):87-97 doi 10.1016/j.devcel.2009.06.013.

66. Narendra D, Tanaka A, Suen DF, Youle RJ. Parkin is recruited selectively to impaired mitochondria and promotes their autophagy. J Cell Biol **2008**;183(5):795-803 doi 10.1083/jcb.200809125.

67. Pattingre S, Tassa A, Qu X, Garuti R, Liang XH, Mizushima N*, et al.* Bcl-2 antiapoptotic proteins inhibit Beclin 1-dependent autophagy. Cell **2005**;122(6):927-39 doi 10.1016/j.cell.2005.07.002.

68. Shimizu S, Kanaseki T, Mizushima N, Mizuta T, Arakawa-Kobayashi S, Thompson CB*, et al.* Role of Bcl-2 family proteins in a non-apoptotic programmed cell death dependent on autophagy genes. Nat Cell Biol **2004**;6(12):1221-8 doi 10.1038/ncb1192.

69. Fernandez AF, Sebti S, Wei Y, Zou Z, Shi M, McMillan KL*, et al.* Disruption of the beclin 1-BCL2 autophagy regulatory complex promotes longevity in mice. Nature **2018**;558(7708):136-40 doi 10.1038/s41586-018-0162-7.

70. Kim M, Jung JY, Choi S, Lee H, Morales LD, Koh JT*, et al.* GFRA1 promotes cisplatin-induced chemoresistance in osteosarcoma by inducing autophagy. Autophagy **2017**;13(1):149-68 doi 10.1080/15548627.2016.1239676.

71. Song J, Qu Z, Guo X, Zhao Q, Zhao X, Gao L*, et al.* Hypoxia-induced autophagy contributes to the chemoresistance of hepatocellular carcinoma cells. Autophagy **2009**;5(8):1131-44.

72. Wang F, Xia X, Yang C, Shen J, Mai J, Kim HC*, et al.* SMAD4 Gene Mutation Renders Pancreatic Cancer Resistance to Radiotherapy through Promotion of Autophagy. Clin Cancer Res **2018**;24(13):3176-85 doi 10.1158/1078-0432.CCR-17-3435.

73. Amaravadi RK, Yu D, Lum JJ, Bui T, Christophorou MA, Evan GI*, et al.* Autophagy inhibition enhances therapy-induced apoptosis in a Myc-induced model of lymphoma. J Clin Invest **2007**;117(2):326-36 doi 10.1172/JCI28833.

74. Sui X, Chen R, Wang Z, Huang Z, Kong N, Zhang M*, et al.* Autophagy and chemotherapy resistance: a promising therapeutic target for cancer treatment. Cell Death Dis **2013**;4:e838 doi 10.1038/cddis.2013.350.

75. Manic G, Obrist F, Kroemer G, Vitale I, Galluzzi L. Chloroquine and hydroxychloroquine for cancer therapy. Mol Cell Oncol **2014**;1(1):e29911 doi 10.4161/mco.29911.

76. Rosenfeld MR, Ye X, Supko JG, Desideri S, Grossman SA, Brem S*, et al.* A phase I/II trial of hydroxychloroquine in conjunction with radiation therapy and concurrent and adjuvant temozolomide in patients with newly diagnosed glioblastoma multiforme. Autophagy **2014**;10(8):1359-68 doi 10.4161/auto.28984.

77. Sotelo J, Briceno E, Lopez-Gonzalez MA. Adding chloroquine to conventional treatment for glioblastoma multiforme: a randomized, double-blind, placebo-controlled trial. Ann Intern Med **2006**;144(5):337-43.

78. Rangwala R, Leone R, Chang YC, Fecher LA, Schuchter LM, Kramer A*, et al.* Phase I trial of hydroxychloroquine with dose-intense temozolomide in patients with advanced solid tumors and melanoma. Autophagy **2014**;10(8):1369-79 doi 10.4161/auto.29118.

79. Mahalingam D, Mita M, Sarantopoulos J, Wood L, Amaravadi RK, Davis LE*, et al.* Combined autophagy and HDAC inhibition: a phase I safety, tolerability, pharmacokinetic, and pharmacodynamic analysis of hydroxychloroquine in combination with the HDAC inhibitor vorinostat in patients with advanced solid tumors. Autophagy **2014**;10(8):1403-14 doi 10.4161/auto.29231.

80. Yue Z, Jin S, Yang C, Levine AJ, Heintz N. Beclin 1, an autophagy gene essential for early embryonic development, is a haploinsufficient tumor suppressor. Proc Natl Acad Sci U S A **2003**;100(25):15077-82 doi 10.1073/pnas.2436255100.

81. Qu X, Yu J, Bhagat G, Furuya N, Hibshoosh H, Troxel A*, et al.* Promotion of tumorigenesis by heterozygous disruption of the beclin 1 autophagy gene. J Clin Invest **2003**;112(12):1809-20 doi 10.1172/JCI20039.

82. Lebovitz CB, Robertson AG, Goya R, Jones SJ, Morin RD, Marra MA*, et al.* Cross-cancer profiling of molecular alterations within the human autophagy interaction network. Autophagy **2015**;11(9):1668-87 doi 10.1080/15548627.2015.1067362.

83. Garcia-Prat L, Martinez-Vicente M, Perdiguero E, Ortet L, Rodriguez-Ubreva J, Rebollo E*, et al.* Autophagy maintains stemness by preventing senescence. Nature **2016**;529(7584):37-42 doi 10.1038/nature16187.

84. Ho TT, Warr MR, Adelman ER, Lansinger OM, Flach J, Verovskaya EV*, et al.* Autophagy maintains the metabolism and function of young and old stem cells. Nature **2017**;543(7644):205-10 doi 10.1038/nature21388.

85. Sharif T, Martell E, Dai C, Kennedy BE, Murphy P, Clements DR*, et al.* Autophagic homeostasis is required for the pluripotency of cancer stem cells. Autophagy **2017**;13(2):264-84 doi 10.1080/15548627.2016.1260808.

86. Sharif T, Martell E, Dai C, Ghassemi-Rad MS, Hanes MR, Murphy PJ*, et al.* HDAC6 differentially regulates autophagy in stem-like versus differentiated cancer cells. Autophagy **2019**;15(4):686-706 doi 10.1080/15548627.2018.1548547.

87. Dimski DS. Ammonia metabolism and the urea cycle: function and clinical implications. J Vet Intern Med **1994**;8(2):73-8.

88. DeBerardinis RJ, Thompson CB. Cellular metabolism and disease: what do metabolic outliers teach us? Cell **2012**;148(6):1132-44 doi 10.1016/j.cell.2012.02.032.

89. Chen JL, Lucas JE, Schroeder T, Mori S, Wu J, Nevins J*, et al.* The genomic analysis of lactic acidosis and acidosis response in human cancers. PLoS Genet **2008**;4(12):e1000293 doi 10.1371/journal.pgen.1000293.

90. Liou GY, Storz P. Reactive oxygen species in cancer. Free Radic Res **2010**;44(5):479-96 doi 10.3109/10715761003667554.

91. Dickinson BC, Chang CJ. Chemistry and biology of reactive oxygen species in signaling or stress responses. Nat Chem Biol **2011**;7(8):504-11 doi 10.1038/nchembio.607.

92. Bergamini CM, Gambetti S, Dondi A, Cervellati C. Oxygen, reactive oxygen species and tissue damage. Curr Pharm Des **2004**;10(14):1611-26.

93. Ames BN, Shigenaga MK, Hagen TM. Oxidants, antioxidants, and the degenerative diseases of aging. Proc Natl Acad Sci U S A **1993**;90(17):7915-22 doi 10.1073/pnas.90.17.7915.

94. Dizdaroglu M, Jaruga P, Birincioglu M, Rodriguez H. Free radical-induced damage to DNA: mechanisms and measurement. Free Radic Biol Med **2002**;32(11):1102-15.

95. Maynard S, Schurman SH, Harboe C, de Souza-Pinto NC, Bohr VA. Base excision repair of oxidative DNA damage and association with cancer and aging. Carcinogenesis **2009**;30(1):2-10 doi 10.1093/carcin/bgn250.

96. Birben E, Sahiner UM, Sackesen C, Erzurum S, Kalayci O. Oxidative stress and antioxidant defense. World Allergy Organ J **2012**;5(1):9-19 doi 10.1097/WOX.0b013e3182439613.

97. Zelko IN, Mariani TJ, Folz RJ. Superoxide dismutase multigene family: a comparison of the CuZn-SOD (SOD1), Mn-SOD (SOD2), and EC-SOD (SOD3) gene structures, evolution, and expression. Free Radic Biol Med **2002**;33(3):337-49.

98. Mueller S, Riedel HD, Stremmel W. Direct evidence for catalase as the predominant H2O2 -removing enzyme in human erythrocytes. Blood **1997**;90(12):4973-8.

99. Arthur JR. The glutathione peroxidases. Cell Mol Life Sci **2000**;57(13-14):1825-35.

100. Stahl W, Sies H. Antioxidant defense: vitamins E and C and carotenoids. Diabetes **1997**;46 Suppl 2:S14-8.

101. Jones DP. Redox potential of GSH/GSSG couple: assay and biological significance. Methods Enzymol **2002**;348:93-112.

102. Fang FC. Antimicrobial reactive oxygen and nitrogen species: concepts and controversies. Nat Rev Microbiol **2004**;2(10):820-32 doi 10.1038/nrmicro1004.

103. Ray PD, Huang BW, Tsuji Y. Reactive oxygen species (ROS) homeostasis and redox regulation in cellular signaling. Cell Signal **2012**;24(5):981-90 doi 10.1016/j.cellsig.2012.01.008.

104. Irani K, Xia Y, Zweier JL, Sollott SJ, Der CJ, Fearon ER*, et al.* Mitogenic signaling mediated by oxidants in Ras-transformed fibroblasts. Science **1997**;275(5306):1649-52.

105. Storz P. Reactive oxygen species in tumor progression. Front Biosci **2005**;10:1881-96.

106. Valavanidis A, Vlachogianni T, Fiotakis K. Tobacco smoke: involvement of reactive oxygen species and stable free radicals in mechanisms of oxidative damage, carcinogenesis and synergistic effects with other respirable particles. Int J Environ Res Public Health **2009**;6(2):445-62 doi 10.3390/ijerph6020445.

107. Weisburger JH. Nutritional approach to cancer prevention with emphasis on vitamins, antioxidants, and carotenoids. Am J Clin Nutr **1991**;53(1 Suppl):226S-37S doi 10.1093/ajcn/53.1.226S.

108. Zheng J. Energy metabolism of cancer: Glycolysis versus oxidative phosphorylation (Review). Oncol Lett **2012**;4(6):1151-7 doi 10.3892/ol.2012.928.

109. Balaban RS. Regulation of oxidative phosphorylation in the mammalian cell. Am J Physiol **1990**;258(3 Pt 1):C377-89 doi 10.1152/ajpcell.1990.258.3.C377.

110. Liu Y, Fiskum G, Schubert D. Generation of reactive oxygen species by the mitochondrial electron transport chain. J Neurochem **2002**;80(5):780-7.

111. Kokoszka JE, Coskun P, Esposito LA, Wallace DC. Increased mitochondrial oxidative stress in the Sod2 (+/-) mouse results in the age-related decline of mitochondrial function culminating in increased apoptosis. Proc Natl Acad Sci U S A **2001**;98(5):2278-83 doi 10.1073/pnas.051627098.

112. Van Remmen H, Ikeno Y, Hamilton M, Pahlavani M, Wolf N, Thorpe SR*, et al.* Life-long reduction in MnSOD activity results in increased DNA damage and higher incidence of cancer but does not accelerate aging. Physiol Genomics **2003**;16(1):29-37 doi 10.1152/physiolgenomics.00122.2003.

113. van de Wetering CI, Coleman MC, Spitz DR, Smith BJ, Knudson CM. Manganese superoxide dismutase gene dosage affects chromosomal instability and tumor onset in a mouse model of T cell lymphoma. Free Radic Biol Med **2008**;44(8):1677-86 doi 10.1016/j.freeradbiomed.2008.01.022.

114. Oberley LW, Buettner GR. Role of superoxide dismutase in cancer: a review. Cancer Res **1979**;39(4):1141-9.

115. Zhong W, Oberley LW, Oberley TD, Clair DKS. Suppression of the malignant phenotype of human glioma cells by overexpression of manganese superoxide dismutase. Oncogene **1997**;14(4):481-90 doi 10.1038/sj.onc.1200852.

116. Weydert C, Roling B, Liu J, Hinkhouse MM, Ritchie JM, Oberley LW*, et al.* Suppression of the Malignant Phenotype in Human Pancreatic Cancer Cells by the Overexpression of Manganese Superoxide Dismutase. Molecular Cancer Therapeutics **2003**;2(4):361.

117. Bravard A, Sabatier L, Hoffschir F, Ricoul M, Luccioni C, Dutrillaux B. SOD2: a new type of tumor-suppressor gene? Int J Cancer **1992**;51(3):476-80.

118. Zhao Y, Xue Y, Oberley TD, Kiningham KK, Lin SM, Yen HC*, et al.* Overexpression of manganese superoxide dismutase suppresses tumor formation by modulation of activator protein-1 signaling in a multistage skin carcinogenesis model. Cancer Res **2001**;61(16):6082-8.

119. Tsai SM, Hou MF, Wu SH, Hu BW, Yang SF, Chen WT*, et al.* Expression of manganese superoxide dismutase in patients with breast cancer. Kaohsiung J Med Sci **2011**;27(5):167-72 doi 10.1016/j.kjms.2010.11.003.

120. Hodge DR, Peng B, Pompeia C, Thomas S, Cho E, Clausen PA*, et al.* Epigenetic silencing of manganese superoxide dismutase (SOD-2) in KAS 6/1 human multiple myeloma cells increases cell proliferation. Cancer Biol Ther **2005**;4(5):585-92.

121. Hurt EM, Thomas SB, Peng B, Farrar WL. Integrated molecular profiling of SOD2 expression in multiple myeloma. Blood **2007**;109(9):3953-62 doi 10.1182/blood-2006-07-035162.

122. Huang Y, He T, Domann FE. Decreased expression of manganese superoxide dismutase in transformed cells is associated with increased cytosine methylation of the SOD2 gene. DNA Cell Biol **1999**;18(8):643-52 doi 10.1089/104454999315051.

123. Martin RC, Liu Q, Wo JM, Ray MB, Li Y. Chemoprevention of carcinogenic progression to esophageal adenocarcinoma by the manganese superoxide dismutase supplementation. Clin Cancer Res **2007**;13(17):5176-82 doi 10.1158/1078-0432.CCR-07-1152.

124. Liu G, Zhou W, Park S, Wang LI, Miller DP, Wain JC*, et al.* The SOD2 Val/Val genotype enhances the risk of nonsmall cell lung carcinoma by p53 and XRCC1 polymorphisms. Cancer **2004**;101(12):2802-8 doi 10.1002/cncr.20716.

125. Wheatley-Price P, Asomaning K, Reid A, Zhai R, Su L, Zhou W*, et al.* Myeloperoxidase and superoxide dismutase polymorphisms are associated with an increased risk of developing pancreatic adenocarcinoma. Cancer **2008**;112(5):1037-42 doi 10.1002/cncr.23267.

126. Dhar SK, Tangpong J, Chaiswing L, Oberley TD, St Clair DK. Manganese superoxide dismutase is a p53-regulated gene that switches cancers between early and advanced stages. Cancer Res **2011**;71(21):6684-95 doi 10.1158/0008-5472.CAN-11-1233.

127. Drane P, Bravard A, Bouvard V, May E. Reciprocal down-regulation of p53 and SOD2 gene expression-implication in p53 mediated apoptosis. Oncogene **2001**;20(4):430-9 doi 10.1038/sj.onc.1204101.

128. Dhar SK, Xu Y, Chen Y, St Clair DK. Specificity protein 1-dependent p53-mediated suppression of human manganese superoxide dismutase gene expression. J Biol Chem **2006**;281(31):21698-709 doi 10.1074/jbc.M601083200.

129. Woodson K, Tangrea JA, Lehman TA, Modali R, Taylor KM, Snyder K*, et al.* Manganese superoxide dismutase (MnSOD) polymorphism, alpha-tocopherol supplementation and prostate cancer risk in the alpha-tocopherol, beta-carotene cancer prevention study (Finland). Cancer Causes Control **2003**;14(6):513-8.

130. Olson SH, Carlson MD, Ostrer H, Harlap S, Stone A, Winters M*, et al.* Genetic variants in SOD2, MPO, and NQO1, and risk of ovarian cancer. Gynecol Oncol **2004**;93(3):615-20 doi 10.1016/j.ygyno.2004.03.027.

131. Berto MD, Bica CG, de Sa GP, Barbisan F, Azzolin VF, Rogalski F*, et al.* The effect of superoxide anion and hydrogen peroxide imbalance on prostate cancer: an integrative in vivo and in vitro analysis. Med Oncol **2015**;32(11):251 doi 10.1007/s12032-015-0700-1.

132. Kamarajugadda S, Cai Q, Chen H, Nayak S, Zhu J, He M*, et al.* Manganese superoxide dismutase promotes anoikis resistance and tumor metastasis. Cell Death Dis **2013**;4:e504 doi 10.1038/cddis.2013.20.

133. Hempel N, Ye H, Abessi B, Mian B, Melendez JA. Altered redox status accompanies progression to metastatic human bladder cancer. Free Radic Biol Med **2009**;46(1):42-50 doi 10.1016/j.freeradbiomed.2008.09.020.

134. Miar A, Hevia D, Munoz-Cimadevilla H, Astudillo A, Velasco J, Sainz RM*, et al.* Manganese superoxide dismutase (SOD2/MnSOD)/catalase and SOD2/GPx1 ratios as biomarkers for tumor progression and metastasis in prostate, colon, and lung cancer. Free Radic Biol Med **2015**;85:45-55 doi 10.1016/j.freeradbiomed.2015.04.001.

135. Salzman R, Kankova K, Pacal L, Tomandl J, Horakova Z, Kostrica R. Increased activity of superoxide dismutase in advanced stages of head and neck squamous cell carcinoma with locoregional metastases. Neoplasma **2007**;54(4):321-5.

136. Lewis A, Du J, Liu J, Ritchie JM, Oberley LW, Cullen JJ. Metastatic progression of pancreatic cancer: changes in antioxidant enzymes and cell growth. Clin Exp Metastasis **2005**;22(7):523-32 doi 10.1007/s10585-005-4919-7.

137. Malafa M, Margenthaler J, Webb B, Neitzel L, Christophersen M. MnSOD expression is increased in metastatic gastric cancer. J Surg Res **2000**;88(2):130-4 doi 10.1006/jsre.1999.5773.

138. Nozoe T, Honda M, Inutsuka S, Yasuda M, Korenaga D. Significance of immunohistochemical expression of manganese superoxide dismutase as a marker of malignant potential in colorectal carcinoma. Oncol Rep **2003**;10(1):39-43.

139. Ye H, Wang A, Lee BS, Yu T, Sheng S, Peng T*, et al.* Proteomic based identification of manganese superoxide dismutase 2 (SOD2) as a metastasis marker for oral squamous cell carcinoma. Cancer Genomics Proteomics **2008**;5(2):85-94.

140. Quiros I, Sainz RM, Hevia D, Garcia-Suarez O, Astudillo A, Rivas M*, et al.* Upregulation of manganese superoxide dismutase (SOD2) is a common pathway for neuroendocrine differentiation in prostate cancer cells. Int J Cancer **2009**;125(7):1497-504 doi 10.1002/ijc.24501.

141. Chung-man Ho J, Zheng S, Comhair SA, Farver C, Erzurum SC. Differential expression of manganese superoxide dismutase and catalase in lung cancer. Cancer Res **2001**;61(23):8578-85.

142. Liu Z, Li S, Cai Y, Wang A, He Q, Zheng C*, et al.* Manganese superoxide dismutase induces migration and invasion of tongue squamous cell carcinoma via H2O2-dependent Snail signaling. Free Radic Biol Med **2012**;53(1):44-50 doi 10.1016/j.freeradbiomed.2012.04.031.

143. Connor KM, Hempel N, Nelson KK, Dabiri G, Gamarra A, Belarmino J*, et al.* Manganese superoxide dismutase enhances the invasive and migratory activity of tumor cells. Cancer Res **2007**;67(21):10260-7 doi 10.1158/0008-5472.CAN-07-1204.

144. Kim YS, Gupta Vallur P, Phaeton R, Mythreye K, Hempel N. Insights into the Dichotomous Regulation of SOD2 in Cancer. Antioxidants (Basel) **2017**;6(4) doi 10.3390/antiox6040086.

145. Ward PS, Thompson CB. Metabolic reprogramming: a cancer hallmark even warburg did not anticipate. Cancer Cell **2012**;21(3):297-308 doi 10.1016/j.ccr.2012.02.014.

146. Hsu PP, Sabatini DM. Cancer cell metabolism: Warburg and beyond. Cell **2008**;134(5):703-7 doi 10.1016/j.cell.2008.08.021.

147. Warburg O. On the origin of cancer cells. Science **1956**;123(3191):309-14.

148. Szablewski L. Expression of glucose transporters in cancers. Biochim Biophys Acta **2013**;1835(2):164-9 doi 10.1016/j.bbcan.2012.12.004.

149. Sharif T, Martell E, Dai C, Ghassemi-Rad MS, Kennedy BE, Lee PWK*, et al.* Regulation of Cancer and Cancer-Related Genes via NAD(+). Antioxid Redox Signal **2019**;30(6):906-23 doi 10.1089/ars.2017.7478.

150. Liberti MV, Locasale JW. The Warburg Effect: How Does it Benefit Cancer Cells? Trends Biochem Sci **2016**;41(3):211-8 doi 10.1016/j.tibs.2015.12.001.

151. Amelio I, Cutruzzola F, Antonov A, Agostini M, Melino G. Serine and glycine metabolism in cancer. Trends Biochem Sci **2014**;39(4):191-8 doi 10.1016/j.tibs.2014.02.004.

152. Serkova NJ, Glunde K. Metabolomics of cancer. Methods Mol Biol **2009**;520:273-95 doi 10.1007/978-1-60327-811-9_20.

153. Zong WX, Rabinowitz JD, White E. Mitochondria and Cancer. Mol Cell **2016**;61(5):667-76 doi 10.1016/j.molcel.2016.02.011.

154. Andrzejewski S, Klimcakova E, Johnson RM, Tabaries S, Annis MG, McGuirk S*, et al.* PGC-1alpha Promotes Breast Cancer Metastasis and Confers Bioenergetic Flexibility against Metabolic Drugs. Cell Metab **2017**;26(5):778-87 e5 doi 10.1016/j.cmet.2017.09.006.

155. Kuntz EM, Baquero P, Michie AM, Dunn K, Tardito S, Holyoake TL*, et al.* Targeting mitochondrial oxidative phosphorylation eradicates therapy-resistant chronic myeloid leukemia stem cells. Nat Med **2017**;23(10):1234-40 doi 10.1038/nm.4399.

156. Lagadinou ED, Sach A, Callahan K, Rossi RM, Neering SJ, Minhajuddin M*, et al.* BCL-2 inhibition targets oxidative phosphorylation and selectively eradicates quiescent human leukemia stem cells. Cell Stem Cell **2013**;12(3):329-41 doi 10.1016/j.stem.2012.12.013.

157. Janiszewska M, Suva ML, Riggi N, Houtkooper RH, Auwerx J, Clement-Schatlo V*, et al.* Imp2 controls oxidative phosphorylation and is crucial for preserving glioblastoma cancer stem cells. Genes Dev **2012**;26(17):1926-44 doi 10.1101/gad.188292.112.

158. Vlashi E, Lagadec C, Vergnes L, Reue K, Frohnen P, Chan M*, et al.* Metabolic differences in breast cancer stem cells and differentiated progeny. Breast Cancer Res Treat **2014**;146(3):525-34 doi 10.1007/s10549-014-3051-2.

159. Sancho P, Burgos-Ramos E, Tavera A, Bou Kheir T, Jagust P, Schoenhals M*, et al.* MYC/PGC-1alpha Balance Determines the Metabolic Phenotype and Plasticity of Pancreatic Cancer Stem Cells. Cell Metab **2015**;22(4):590-605 doi 10.1016/j.cmet.2015.08.015.

160. Pasto A, Bellio C, Pilotto G, Ciminale V, Silic-Benussi M, Guzzo G*, et al.* Cancer stem cells from epithelial ovarian cancer patients privilege oxidative phosphorylation, and resist glucose deprivation. Oncotarget **2014**;5(12):4305-19 doi 10.18632/oncotarget.2010.

161. Robertson-Tessi M, Gillies RJ, Gatenby RA, Anderson AR. Impact of metabolic heterogeneity on tumor growth, invasion, and treatment outcomes. Cancer Res **2015**;75(8):1567-79 doi 10.1158/0008-5472.CAN-14-1428.

162. Hermann PC, Huber SL, Herrler T, Aicher A, Ellwart JW, Guba M*, et al.* Distinct populations of cancer stem cells determine tumor growth and metastatic activity in human pancreatic cancer. Cell Stem Cell **2007**;1(3):313-23 doi 10.1016/j.stem.2007.06.002.

163. Collins AT, Berry PA, Hyde C, Stower MJ, Maitland NJ. Prospective identification of tumorigenic prostate cancer stem cells. Cancer Res **2005**;65(23):10946-51 doi 10.1158/0008-5472.CAN-05-2018.

164. Al-Hajj M, Wicha MS, Benito-Hernandez A, Morrison SJ, Clarke MF. Prospective identification of tumorigenic breast cancer cells. Proc Natl Acad Sci U S A **2003**;100(7):3983-8 doi 10.1073/pnas.0530291100.

165. Ricci-Vitiani L, Lombardi DG, Pilozzi E, Biffoni M, Todaro M, Peschle C*, et al.* Identification and expansion of human colon-cancer-initiating cells. Nature **2007**;445(7123):111-5 doi 10.1038/nature05384.

166. Ma S, Chan KW, Hu L, Lee TK, Wo JY, Ng IO*, et al.* Identification and characterization of tumorigenic liver cancer stem/progenitor cells. Gastroenterology **2007**;132(7):2542-56 doi 10.1053/j.gastro.2007.04.025.

167. Eramo A, Lotti F, Sette G, Pilozzi E, Biffoni M, Di Virgilio A*, et al.* Identification and expansion of the tumorigenic lung cancer stem cell population. Cell Death Differ **2008**;15(3):504-14 doi 10.1038/sj.cdd.4402283.

168. Fang D, Nguyen TK, Leishear K, Finko R, Kulp AN, Hotz S*, et al.* A tumorigenic subpopulation with stem cell properties in melanomas. Cancer Res **2005**;65(20):9328-37 doi 10.1158/0008-5472.CAN-05-1343.

169. Chaudhari P, Ye Z, Jang YY. Roles of reactive oxygen species in the fate of stem cells. Antioxid Redox Signal **2014**;20(12):1881-90 doi 10.1089/ars.2012.4963.

170. Damjanov I, Andrews PW. The terminology of teratocarcinomas and teratomas. Nat Biotechnol **2007**;25(11):1212; discussion doi 10.1038/nbt1107-1212a.

171. Gidekel S, Pizov G, Bergman Y, Pikarsky E. Oct-3/4 is a dose-dependent oncogenic fate determinant. Cancer Cell **2003**;4(5):361-70.

172. Santagata S, Ligon KL, Hornick JL. Embryonic stem cell transcription factor signatures in the diagnosis of primary and metastatic germ cell tumors. Am J Surg Pathol **2007**;31(6):836-45 doi 10.1097/PAS.0b013e31802e708a.

173. Andrews PW. Retinoic acid induces neuronal differentiation of a cloned human embryonal carcinoma cell line in vitro. Dev Biol **1984**;103(2):285-93.

174. Tripathi R, Samadder T, Gupta S, Surolia A, Shaha C. Anticancer activity of a combination of cisplatin and fisetin in embryonal carcinoma cells and xenograft tumors. Mol Cancer Ther **2011**;10(2):255-68 doi 10.1158/1535-7163.MCT-10-0606.

175. Lin Y, Yang Y, Li W, Chen Q, Li J, Pan X*, et al.* Reciprocal regulation of Akt and Oct4 promotes the self-renewal and survival of embryonal carcinoma cells. Mol Cell **2012**;48(4):627-40 doi 10.1016/j.molcel.2012.08.030.

176. Emhemmed F, Ali Azouaou S, Thuaud F, Schini-Kerth V, Desaubry L, Muller CD*, et al.* Selective anticancer effects of a synthetic flavagline on human Oct4-expressing cancer stem-like cells via a p38 MAPK-dependent caspase-3-dependent pathway. Biochem Pharmacol **2014**;89(2):185-96 doi 10.1016/j.bcp.2014.02.020.

177. Kleinsmith LJ, Pierce GB, Jr. Multipotentiality of Single Embryonal Carcinoma Cells. Cancer Res **1964**;24:1544-51.

178. Illmensee K, Mintz B. Totipotency and normal differentiation of single teratocarcinoma cells cloned by injection into blastocysts. Proc Natl Acad Sci U S A **1976**;73(2):549-53 doi 10.1073/pnas.73.2.549.

179. Mani SA, Guo W, Liao MJ, Eaton EN, Ayyanan A, Zhou AY*, et al.* The epithelial-mesenchymal transition generates cells with properties of stem cells. Cell **2008**;133(4):704-15 doi 10.1016/j.cell.2008.03.027.

180. Singh SK, Clarke ID, Terasaki M, Bonn VE, Hawkins C, Squire J*, et al.* Identification of a cancer stem cell in human brain tumors. Cancer Res **2003**;63(18):5821-8.

181. Qazi MA, Vora P, Venugopal C, Adams J, Singh M, Hu A*, et al.* Cotargeting Ephrin Receptor Tyrosine Kinases A2 and A3 in Cancer Stem Cells Reduces Growth of Recurrent Glioblastoma. Cancer Res **2018**;78(17):5023-37 doi 10.1158/0008-5472.CAN-18-0267.

182. Kalyanaraman B, Darley-Usmar V, Davies KJ, Dennery PA, Forman HJ, Grisham MB*, et al.* Measuring reactive oxygen and nitrogen species with fluorescent probes: challenges and limitations. Free Radic Biol Med **2012**;52(1):1-6 doi 10.1016/j.freeradbiomed.2011.09.030.

183. Strober W. Trypan blue exclusion test of cell viability. Curr Protoc Immunol **2001**;Appendix 3:Appendix 3B doi 10.1002/0471142735.ima03bs21.

184. Zhu Z, Khan MA, Weiler M, Blaes J, Jestaedt L, Geibert M*, et al.* Targeting self-renewal in high-grade brain tumors leads to loss of brain tumor stem cells and prolonged survival. Cell Stem Cell **2014**;15(2):185-98 doi 10.1016/j.stem.2014.04.007.

185. Liu JC, Deng T, Lehal RS, Kim J, Zacksenhaus E. Identification of tumorsphere- and tumor-initiating cells in HER2/Neu-induced mammary tumors. Cancer Res **2007**;67(18):8671-81 doi 10.1158/0008-5472.CAN-07-1486.

186. Johnson S, Chen H, Lo PK. In vitro Tumorsphere Formation Assays. Bio Protoc **2013**;3(3).

187. Livak KJ, Schmittgen TD. Analysis of relative gene expression data using real-time quantitative PCR and the 2(-Delta Delta C(T)) Method. Methods **2001**;25(4):402-8 doi 10.1006/meth.2001.1262.

188. Murphy JP, Giacomantonio MA, Paulo JA, Everley RA, Kennedy BE, Pathak GP*, et al.* The NAD(+) Salvage Pathway Supports PHGDH-Driven Serine Biosynthesis. Cell Rep **2018**;24(9):2381-91 e5 doi 10.1016/j.celrep.2018.07.086.

189. Rappsilber J, Ishihama Y, Mann M. Stop and go extraction tips for matrix-assisted laser desorption/ionization, nanoelectrospray, and LC/MS sample pretreatment in proteomics. Anal Chem **2003**;75(3):663-70.

190. Ting L, Rad R, Gygi SP, Haas W. MS3 eliminates ratio distortion in isobaric multiplexed quantitative proteomics. Nat Methods **2011**;8(11):937-40 doi 10.1038/nmeth.1714.

191. Murphy JP, Stepanova E, Everley RA, Paulo JA, Gygi SP. Comprehensive Temporal Protein Dynamics during the Diauxic Shift in Saccharomyces cerevisiae. Mol Cell Proteomics **2015**;14(9):2454-65 doi 10.1074/mcp.M114.045849.

192. Huang da W, Sherman BT, Lempicki RA. Systematic and integrative analysis of large gene lists using DAVID bioinformatics resources. Nat Protoc **2009**;4(1):44-57 doi 10.1038/nprot.2008.211.

193. Huang da W, Sherman BT, Lempicki RA. Bioinformatics enrichment tools: paths toward the comprehensive functional analysis of large gene lists. Nucleic Acids Res **2009**;37(1):1-13 doi 10.1093/nar/gkn923.

194. Herreros-Villanueva M, Zhang JS, Koenig A, Abel EV, Smyrk TC, Bamlet WR*, et al.* SOX2 promotes dedifferentiation and imparts stem cell-like features to pancreatic cancer cells. Oncogenesis **2013**;2:e61 doi 10.1038/oncsis.2013.23.

195. Chiou SH, Wang ML, Chou YT, Chen CJ, Hong CF, Hsieh WJ*, et al.* Coexpression of Oct4 and Nanog enhances malignancy in lung adenocarcinoma by inducing cancer stem cell-like properties and epithelial-mesenchymal transdifferentiation. Cancer Res **2010**;70(24):10433-44 doi 10.1158/0008-5472.CAN-10-2638.

196. Looijenga LH, Stoop H, de Leeuw HP, de Gouveia Brazao CA, Gillis AJ, van Roozendaal KE*, et al.* POU5F1 (OCT3/4) identifies cells with pluripotent potential in human germ cell tumors. Cancer Res **2003**;63(9):2244-50.

197. Niwa H, Miyazaki J, Smith AG. Quantitative expression of Oct-3/4 defines differentiation, dedifferentiation or self-renewal of ES cells. Nat Genet **2000**;24(4):372-6 doi 10.1038/74199.

198. Bonnet D, Dick JE. Human acute myeloid leukemia is organized as a hierarchy that originates from a primitive hematopoietic cell. Nat Med **1997**;3(7):730-7.

199. Li C, Heidt DG, Dalerba P, Burant CF, Zhang L, Adsay V*, et al.* Identification of pancreatic cancer stem cells. Cancer Res **2007**;67(3):1030-7 doi 10.1158/0008-5472.CAN-06-2030.

200. Matsui W, Huff CA, Wang Q, Malehorn MT, Barber J, Tanhehco Y*, et al.* Characterization of clonogenic multiple myeloma cells. Blood **2004**;103(6):2332-6 doi 10.1182/blood-2003-09-3064.

201. O'Brien CA, Pollett A, Gallinger S, Dick JE. A human colon cancer cell capable of initiating tumour growth in immunodeficient mice. Nature **2007**;445(7123):106-10 doi 10.1038/nature05372.

202. Prince ME, Sivanandan R, Kaczorowski A, Wolf GT, Kaplan MJ, Dalerba P*, et al.* Identification of a subpopulation of cells with cancer stem cell properties in head and neck squamous cell carcinoma. Proc Natl Acad Sci U S A **2007**;104(3):973-8 doi 10.1073/pnas.0610117104.

203. Zhang S, Balch C, Chan MW, Lai HC, Matei D, Schilder JM*, et al.* Identification and characterization of ovarian cancer-initiating cells from primary human tumors. Cancer Res **2008**;68(11):4311-20 doi 10.1158/0008-5472.CAN-08-0364.

204. Ginestier C, Hur MH, Charafe-Jauffret E, Monville F, Dutcher J, Brown M*, et al.* ALDH1 is a marker of normal and malignant human mammary stem cells and a predictor of poor clinical outcome. Cell Stem Cell **2007**;1(5):555-67 doi 10.1016/j.stem.2007.08.014.

205. Zeppernick F, Ahmadi R, Campos B, Dictus C, Helmke BM, Becker N*, et al.* Stem cell marker CD133 affects clinical outcome in glioma patients. Clin Cancer Res **2008**;14(1):123-9 doi 10.1158/1078-0432.CCR-07-0932.

206. Chiou SH, Yu CC, Huang CY, Lin SC, Liu CJ, Tsai TH*, et al.* Positive correlations of Oct-4 and Nanog in oral cancer stem-like cells and high-grade oral squamous cell carcinoma. Clin Cancer Res **2008**;14(13):4085-95 doi 10.1158/1078-0432.CCR-07-4404.

207. Kalluri R, Weinberg RA. The basics of epithelial-mesenchymal transition. J Clin Invest **2009**;119(6):1420-8 doi 10.1172/JCI39104.

208. Kinugasa H, Whelan KA, Tanaka K, Natsuizaka M, Long A, Guo A*, et al.* Mitochondrial SOD2 regulates epithelial-mesenchymal transition and cell populations defined by differential CD44 expression. Oncogene **2015**;34(41):5229-39 doi 10.1038/onc.2014.449.

209. Intlekofer AM, Finley LWS. Metabolic signatures of cancer cells and stem cells. Nature Metabolism **2019**;1(2):177-88 doi 10.1038/s42255-019-0032-0.

210. Panopoulos AD, Yanes O, Ruiz S, Kida YS, Diep D, Tautenhahn R*, et al.* The metabolome of induced pluripotent stem cells reveals metabolic changes occurring in somatic cell reprogramming. Cell Res **2012**;22(1):168-77 doi 10.1038/cr.2011.177.

211. Dong C, Yuan T, Wu Y, Wang Y, Fan TW, Miriyala S*, et al.* Loss of FBP1 by Snail-mediated repression provides metabolic advantages in basal-like breast cancer. Cancer Cell **2013**;23(3):316-31 doi 10.1016/j.ccr.2013.01.022.

212. Chen CL, Uthaya Kumar DB, Punj V, Xu J, Sher L, Tahara SM*, et al.* NANOG Metabolically Reprograms Tumor-Initiating Stem-like Cells through Tumorigenic Changes in Oxidative Phosphorylation and Fatty Acid Metabolism. Cell Metab **2016**;23(1):206-19 doi 10.1016/j.cmet.2015.12.004.

213. Zhou Y, Zhou Y, Shingu T, Feng L, Chen Z, Ogasawara M*, et al.* Metabolic alterations in highly tumorigenic glioblastoma cells: preference for hypoxia and high dependency on glycolysis. J Biol Chem **2011**;286(37):32843-53 doi 10.1074/jbc.M111.260935.

214. Palorini R, Votta G, Balestrieri C, Monestiroli A, Olivieri S, Vento R*, et al.* Energy metabolism characterization of a novel cancer stem cell-like line 3AB-OS. J Cell Biochem **2014**;115(2):368-79 doi 10.1002/jcb.24671.

215. Morandi A, Taddei ML, Chiarugi P, Giannoni E. Targeting the Metabolic Reprogramming That Controls Epithelial-to-Mesenchymal Transition in Aggressive Tumors. Front Oncol **2017**;7:40 doi 10.3389/fonc.2017.00040.

216. Sciacovelli M, Frezza C. Metabolic reprogramming and epithelial-to-mesenchymal transition in cancer. FEBS J **2017**;284(19):3132-44 doi 10.1111/febs.14090.

217. Kim BS, Lee CH, Chang GE, Cheong E, Shin I. A potent and selective small molecule inhibitor of sirtuin 1 promotes differentiation of pluripotent P19 cells into functional neurons. Sci Rep **2016**;6:34324 doi 10.1038/srep34324.

218. Sperger JM, Chen X, Draper JS, Antosiewicz JE, Chon CH, Jones SB*, et al.* Gene expression patterns in human embryonic stem cells and human pluripotent germ cell tumors. Proc Natl Acad Sci U S A **2003**;100(23):13350-5 doi 10.1073/pnas.2235735100.

219. Pal R, Ravindran G. Assessment of pluripotency and multilineage differentiation potential of NTERA-2 cells as a model for studying human embryonic stem cells. Cell Prolif **2006**;39(6):585-98 doi 10.1111/j.1365-2184.2006.00400.x.

220. Marchal-Victorion S, Deleyrolle L, De Weille J, Saunier M, Dromard C, Sandillon F*, et al.* The human NTERA2 neural cell line generates neurons on growth under neural stem cell conditions and exhibits characteristics of radial glial cells. Mol Cell Neurosci **2003**;24(1):198-213.

221. Peng Q, Qin J, Zhang Y, Cheng X, Wang X, Lu W*, et al.* Autophagy maintains the stemness of ovarian cancer stem cells by FOXA2. J Exp Clin Cancer Res **2017**;36(1):171 doi 10.1186/s13046-017-0644-8.

222. Kinsey CG, Camolotto SA, Boespflug AM, Guillen KP, Foth M, Truong A*, et al.* Protective autophagy elicited by RAF-->MEK-->ERK inhibition suggests a treatment strategy for RAS-driven cancers. Nat Med **2019**;25(4):620-7 doi 10.1038/s41591-019-0367-9.

223. Bryant KL, Stalnecker CA, Zeitouni D, Klomp JE, Peng S, Tikunov AP*, et al.* Combination of ERK and autophagy inhibition as a treatment approach for pancreatic cancer. Nat Med **2019**;25(4):628-40 doi 10.1038/s41591-019-0368-8.

224. Reed JC. Apoptosis-targeted therapies for cancer. Cancer Cell **2003**;3(1):17-22.

225. Najafov A, Chen H, Yuan J. Necroptosis and Cancer. Trends Cancer **2017**;3(4):294-301 doi 10.1016/j.trecan.2017.03.002.

226. Marsboom G, Zhang GF, Pohl-Avila N, Zhang Y, Yuan Y, Kang H*, et al.* Glutamine Metabolism Regulates the Pluripotency Transcription Factor OCT4. Cell Rep **2016**;16(2):323-32 doi 10.1016/j.celrep.2016.05.089.

227. Shi Y. Mechanisms of caspase activation and inhibition during apoptosis. Mol Cell **2002**;9(3):459-70.

228. Ekert PG, Silke J, Vaux DL. Caspase inhibitors. Cell Death Differ **1999**;6(11):1081-6 doi 10.1038/sj.cdd.4400594.

229. Bornstein B, Gottfried Y, Edison N, Shekhtman A, Lev T, Glaser F*, et al.* ARTS binds to a distinct domain in XIAP-BIR3 and promotes apoptosis by a mechanism that is different from other IAP-antagonists. Apoptosis **2011**;16(9):869-81 doi 10.1007/s10495-011-0622-0.

230. Gottfried Y, Rotem A, Lotan R, Steller H, Larisch S. The mitochondrial ARTS protein promotes apoptosis through targeting XIAP. EMBO J **2004**;23(7):1627-35 doi 10.1038/sj.emboj.7600155.

231. Liu Z, Sun C, Olejniczak ET, Meadows RP, Betz SF, Oost T*, et al.* Structural basis for binding of Smac/DIABLO to the XIAP BIR3 domain. Nature **2000**;408(6815):1004-8 doi 10.1038/35050006.

232. Du C, Fang M, Li Y, Li L, Wang X. Smac, a mitochondrial protein that promotes cytochrome c-dependent caspase activation by eliminating IAP inhibition. Cell **2000**;102(1):33-42.

233. Elhasid R, Sahar D, Merling A, Zivony Y, Rotem A, Ben-Arush M*, et al.* Mitochondrial pro-apoptotic ARTS protein is lost in the majority of acute lymphoblastic leukemia patients. Oncogene **2004**;23(32):5468-75 doi 10.1038/sj.onc.1207725.

234. Fulda S. Promises and Challenges of Smac Mimetics as Cancer Therapeutics. Clin Cancer Res **2015**;21(22):5030-6 doi 10.1158/1078-0432.CCR-15-0365.

235. Petersen SL, Peyton M, Minna JD, Wang X. Overcoming cancer cell resistance to Smac mimetic induced apoptosis by modulating cIAP-2 expression. Proc Natl Acad Sci U S A **2010**;107(26):11936-41 doi 10.1073/pnas.1005667107.

236. Sun H, Nikolovska-Coleska Z, Lu J, Meagher JL, Yang CY, Qiu S*, et al.* Design, synthesis, and characterization of a potent, nonpeptide, cell-permeable, bivalent Smac mimetic that concurrently targets both the BIR2 and BIR3 domains in XIAP. J Am Chem Soc **2007**;129(49):15279-94 doi 10.1021/ja074725f.

237. Edison N, Reingewertz TH, Gottfried Y, Lev T, Zuri D, Maniv I*, et al.* Peptides mimicking the unique ARTS-XIAP binding site promote apoptotic cell death in cultured cancer cells. Clin Cancer Res **2012**;18(9):2569-78 doi 10.1158/1078-0432.CCR-11-1430.